

# DISSERTATION

## **Capillary GC-EI-MS and low energy tandem MS of base oils and additives in lubricants and fuels**

ausgeführt zum Zwecke der Erlangung des akademischen Grades  
einer Doktorin der Naturwissenschaften unter der Leitung von

Univ. Prof. Mag. Dr. Günter Allmaier

E164

Institut für Chemische Technologien und Analytik

eingereicht an der Technischen Universität Wien

Fakultät für Technische Chemie

von

Marcella Frauscher, Msc. Bsc.

0600459

Wien, 25. November 2019

# Acknowledgements

First, I want to thank **Univ.-Prof. Mag. Dr. Günter Allmaier** for the supervision of my thesis, his valuable scientific input, his time and efforts, and his personal advice.

I am very grateful for the opportunity to carry out my experimental research work at **AC<sup>2</sup>T research GmbH** (Austrian Excellence Center of Tribology), and for the possibilities offered regarding project management.

In this context, my special gratitude goes to **DI Dr. Nicole Dörr**, scientific leader and my scientific supervisor at AC<sup>2</sup>T. I want to thank her for her technical guidance and her efforts in the revision of my publications. Moreover, I am thankful for her being my mentor in terms of contact with clients, presentation skills, project management and many other things I was able to learn during the past years. In addition, I want to express my appreciation for the interesting tasks I was able to take over because of her trust.

Moreover, I want to thank all my co-workers, the present and the former ones, of the research group “Lubricants and Lubrication”, who created a joyful and inspiring working atmosphere. Among many others, I would like to emphasise especially **Dr. Charlotte Besser, Dr. Andjelka Ristic** and **Ing. Michael Adler**, who supported me not only in my professional life, but also in personal issues. Special thanks to **Josef Brenner and DI Michael Schandl**, who introduced me to GC-MS and shared hours of joy and anger with our analytic devices. Furthermore, I want to express my gratitude to **Adam Agocs, Bsc.** for his experimental support and all the little things he did to make my life and work easier.

Finally, my greatest thanks go to **my husband, my family and friends**, who were irreplaceable support not only during the last years of my PhD studies, but throughout my whole life. Thanks for you all being there whenever I needed a person to listen, a person to show trust in me or a person to share joy with.

This work was funded by the "Austrian COMET-Program" (project XTribology, no. 849109) via the Austrian Research Promotion Agency (FFG) and the Province of Niederösterreich, Vorarlberg and Wien and has been carried out within the “Excellence Centre of Tribology” (AC<sup>2</sup>T research GmbH) and the Vienna University of Technology.

## Abstract (Deutsch)

Sowohl während der Lagerung als auch während des Einsatzes sind Schmier- und Kraftstoffe verschiedenen Belastungen, wie beispielsweise dem Angriff von Sauerstoff, hohen Temperaturen oder Kontaminationseintrag, ausgesetzt. Dies resultiert in Ab- und Umbau der ursprünglichen chemischen Strukturen, wodurch das Erfüllen der geforderten Aufgaben und somit die Leistungsfähigkeit abnehmen. Um den Zustand von Schmier- und Kraftstoffen zu überwachen, gibt es im Bereich der petrochemischen Analytik und Industrie eine Vielzahl von Methoden zur Bestimmung relevanter Parameter wie etwa Oxidation oder Versäuerung. Die meisten dieser Methoden bestimmen einen Summenparameter wodurch weder die Alterung noch die Oxidationsprodukte aufgeklärt werden können. Durch den zunehmenden Einsatz von umweltfreundlicheren oder bio-basierenden Schmier- und Kraftstoffen ist jener Aspekt von immer größer werdender Bedeutung. Typischerweise beinhalten jene Komponenten eine große Anzahl an Sauerstoffatomen in ihren Strukturen, die am Oxidationsprozess beteiligt sein können.

Ziel dieser Arbeit war die Aufklärung der wichtigsten Wege des oxidativen Abbaus und der dabei involvierten Moleküle, sowie der Darstellung der Abbauprodukte im Zeitverlauf. Zu diesem Zweck wurde ein Alterungskonzept entwickelt, der die Elemente der künstlichen Alterung, der Markierung mit stabilen Isotopen und der Kapillargaschromatographie gekoppelt mit Elektronenstoßionisations-Massenspektrometrie (GC-EI-MS) verbindet. Dieses Konzept wurde auf umweltfreundliche Ester-Basisöle, auf Fettsäuremethylester (FAME) sowie auf phenolische Antioxidantien angewendet.

Die entstandenen Oxidationsprodukte wurden mittels GC-EI-MS identifiziert. Durch gezielte Probenahmen, wie beispielsweise nach dem vollständigen Verbrauch des Antioxidans, konnte eine zeitaufgelöste Reihe von Alterungsprodukten ermittelt werden. Da Additive üblicherweise in sehr geringen Konzentrationen eingesetzt werden, wurde eine Tandem-MS Methode zur Quantifizierung des phenolischen Antioxidans Butylhydroxytoluol (BHT) sowie dessen Oxidationsprodukten entwickelt. Dadurch wurde, trotz der komplexen Kraftstoffmatrix, eine Bestimmungsgrenze von unter einem ppb für alle Komponenten erreicht. Die zeitverzögerte Bildung und Abnahme der Alterungsprodukte ermöglichte die Aufklärung der Wirkungsweise von BHT. Durch die Isotopenmarkierung mit  $^{18}\text{O}$  konnten bevorzugte Stellen für den oxidativen Angriff, sowie die Rolle der Sauerstoffatome in der Veränderung der Ausgangsmoleküle aufgeklärt werden. Dieses Wissen ist ein wichtiges Fundament für Modifikationen und Verbesserungen von Schmierstoff- und Kraftstoffkomponenten.

## Abstract (English)

During operation as well as storage, lubricants and fuels undergo degradation as a result of various stressing conditions such as air exposure, high temperature or transfer of contaminations. Consequently, the required functions and the performance decline over time. In order to monitor the condition of a lubricant or fuel a wide range of analytic methods to determine parameters such as oxidation or acidification are known in petrochemical laboratories and industries. However, most of these methods provide only sum parameters, which do not elucidate alteration or distinct oxidation products. These aspects are of increasing importance due to the rising application of eco-friendly or bio-based lubricants and fuels. Typically, these components are containing a high degree of oxygen atoms, which can participate in the oxygen process.

This work aimed at the comprehensive elucidation of the main pathways and involved molecules of oxidative degradation and the formation of oxidative degradation products over time. For this purpose, a combined approach using artificial alteration, stable isotopic tracers and capillary gas chromatography coupled with electron impact ionization mass spectrometry (GC-EI-MS) was developed. This approach was applied to an eco-friendly ester-base oil, to fatty acid methyl esters (FAME) and to phenolic antioxidants.

The obtained oxidation products were identified by means of GC-EI-MS. Sampling at point of interests, e.g., after complete antioxidant consumption enabled a time-resolved mapping of degradation products. As additives are typically present in low levels a tandem-MS based method was developed to quantify not only the phenolic antioxidant butylated hydroxytoluene (BHT), but also oxidation products of interest. The method enabled limits of quantification below one ppb for all components in the complex fuel matrix. A time series of the formation and depletion of the products provided insight to the mode of operation of BHT. Isotope labelling with  $^{18}\text{O}$  revealed the preferential sites of oxidative attack, and the role of the oxygen atoms incorporated in the initial molecules. This knowledge is an important pillow for modifications and enhancement of lubricant and fuel components.

# Table of contents

|  |    |
|--|----|
| <b>PART A: Introduction</b> .....                                      | 8  |
| 1 Lubricants .....   | 8  |
| 1.1 Tasks of the lubricant .....                                       | 8  |
| 1.2 Lubricant base oil types .....                                     | 10 |
| 1.2.1 Mineral oils .....   | 12 |
| 1.2.2 Synthetic base oils .....  | 12 |
| 1.2.3 Ester base oils .....  | 13 |
| 1.3 Lubricant additives .....  | 15 |
| 1.3.1 Antioxidants .....   | 17 |
| 1.3.2 Detergents.....  | 18 |
| 1.3.3 Dispersants .....  | 18 |
| 1.3.4 Antiwear and extreme pressure additives.....                     | 19 |
| 1.3.5 Viscosity modifiers .....  | 20 |
| 1.3.6 Pour point depressants.....                                      | 20 |
| 1.3.7 Foam inhibitors .....  | 21 |
| 2 Liquid fuels .....   | 21 |
| 2.1 Gasoline .....   | 22 |
| 2.1.1 EN 228.....  | 22 |
| 2.1.2 Biocomponents.....   | 23 |
| 2.2 Diesel fuels .....   | 24 |
| 2.2.1 EN 590.....  | 24 |
| 2.2.2 Biodiesel components .....                                       | 25 |
| 2.3 Kerosene .....   | 26 |
| 2.3.1 Specifications for Jet-A-1 fuels according to ASTM D1655-19..... | 26 |
| 2.4 Fuel additives.....  | 28 |

|   |  |           |
|---|--|-----------|
| 2.4.1   | Antioxidants .....   | 31        |
| 2.4.2   | Octane and cetane improvers .....  | 32        |
| 2.4.3   | Lubricity additives.....   | 33        |
| 2.4.4   | Antistatic additives .....   | 34        |
| 3   | Stability assessment.....  | 34        |
| 3.1   | Thermo-oxidative alteration methods.....   | 36        |
| 3.1.1   | Standardized thermo-oxidative methods for lubricants.....                            | 36        |
| 3.1.2   | Standardized thermo-oxidative methods for fuels.....                                 | 41        |
| 3.1.3   | RPVOT and modifications .....  | 43        |
| 3.2   | Oxidative oil degradation mechanisms.....  | 44        |
| 3.2.1   | Chain initiation.....  | 44        |
| 3.2.2   | Chain propagation .....  | 44        |
| 3.2.3   | Chain branching .....  | 45        |
| 3.2.4   | Chain termination.....   | 45        |
| 3.3   | Conventional analytical methods for condition monitoring .....                       | 45        |
| 3.3.1   | Dynamic and kinematic viscosity .....  | 46        |
| 3.3.2   | Neutralization number (NN) and acidification number (AN).....                        | 47        |
| 3.3.3   | Total base number (TBN) .....  | 47        |
| 3.3.4   | Water content .....  | 48        |
| 3.3.5   | FT-IR spectroscopy .....   | 48        |
| 3.4   | Gas chromatography mass spectrometry (GC-MS) for advanced condition monitoring ..... | 50        |
| 3.4.1   | Capillary gas chromatography.....  | 50        |
| 3.4.2   | Mass spectrometry.....   | 60        |
| <b>PART B: Aims, resulting publications and conclusion.....</b> |  | <b>76</b> |
| 1   | Aims of the thesis .....   | 76        |
| 2   | Publications .....   | 77        |

2.1 Publication 1 - Oxidation products of ester-based oils with and without antioxidants identified by stable isotope labelling and mass spectrometry ..... 77

2.2 Publication 2 - Elucidation of oxidation and degradation products of oxygen containing fuel components by combined use of a stable isotopic tracer and mass spectrometry ..... 96

2.3 Publication 3 - Time-resolved quantification of phenolic antioxidants and oxidation products in a model fuel by GC-EI-MS/MS ..... 111

3 Conclusions ..... 136

4 CV ..... 138

References ..... 142

# PART A: Introduction

## 1 Lubricants

### 1.1 Tasks of the lubricant

Lubricants are used in various applications to ensure proper lubrication of moving parts. Although the tasks of a lubricant may differ depending on the field of operation, the main functions are universal: lubrication, heat transfer, cleaning and protection. Within this section, focus is laid on engine lubrication and subordinated hydraulic applications. In the following, the main requirements specific to engine and hydraulic oils are given [1], [2], [3]:

1. Reduction of friction

The energy consumption of lubricated systems is decreased when the friction is reduced, which is particularly important in engines. Simultaneously, this results in lower local heat production during the running time of a machine.

2. Reduction of wear

In order to safeguard an efficient and smooth running of the entire machine over the operating time, the emerging wear must be kept at a minimum. Sufficient lubrication significantly contributes to the required lifetime of the machine components.

3. Transfer of heat – provision of cooling

Caused by combustion, certain parts of the engine are exposed to higher temperatures e.g., pistons and cylinder liners. The engine oil operates as transfer media for heat from these affected part to cooler regions such as the oil sump cooling jacket, where heat dissipation can take place. As to other machine parts without combustion, the heat induced by mechanical work of moving parts, i.e. friction, is transmitted by the lubricant to avoid local overheating, which may result in severe machine damage.

4. Protection against corrosion

Acidic products are built as a result of oil degradation. These compounds may induce corrosion on metallic surfaces of machines. Humid environment and long standstill of machines cause rusting of ferrous machine parts. In engines, these effects may be enhanced by combustion and hence the formation of strong acids, e.g., sulfuric acid, from sulfur-containing fuel compounds. All these effects shall be inhibited and reduced by using a lubricant containing suitable lubricant additives.

## 5. Cleanliness

Solid carbon, varnish, sludge, and combustion deposits are built due to oil degradation and can accumulate on mechanical parts. These residues on the surface may cause fouling or even blocking of oil passages, piston rings get stuck, and severe engine damages can occur. Hence, the lubricant's task is to prevent these deposits, disperse contaminations and preserve the cleanliness of lubricated systems, in particular the engine.

## 6. Sealing

For a proper operation of the combustion engine, the contact between piston and piston rings as well as between piston rings and cylinder liner walls is one of the crucial issues. The sealing between those parts is improved by the lubricant, as it contributes to the decrease of blow-by gas and hence loss of power.

There are several characteristics that indicate if a lubricating oil can fulfil the above described requirements, which are especially important for proper engine operation [1], [2]:

### 1. Suitable temperature-viscosity-behavior

The higher the viscosity index (VI) the lower is the dependence of the viscosity on the temperature. Keeping viscosity in a certain range is important, as the oil has to be sufficiently viscous to prevent wear of the machine parts caused by metal-to-metal contact. However, it has to be thin enough to prevent engine start issues at lower temperatures and to minimize power losses.

### 2. Low volatility

The more volatile the oil, the higher is the loss of oil due to evaporation and therefore more oil consumption. Moreover, as the light oil components tend to evaporate, the viscosity of the remaining oil increases.

### 3. High thermo-oxidative stability

In the engine, the lubricant is exposed to elevated temperatures in the presence of oxygen. In addition, contaminants and degradation products, e.g., acidic compounds amplify the need of highly stable lubricants towards oxidation, temperature, and chemical attack.

### 4. Low deposit forming tendency

In the combustion chamber or the ring zone the metal parts reach high temperatures, and oxidation products are built on them by oil decomposition. Eventually, varnish and similar deposits are formed by polymerization, which can further carbonize to solid

carbon. These deposits prevent machine parts from being able to move freely and cause severe damage as well as undesired pre-ignition when located in the combustion chamber. Hence, the tendency towards deposit formation has to be as low as possible and is a crucial selection criterion.

5. Low foam building tendency

In order to prevent loss of the cooling and lubricating properties by excessive foam this tendency has to be kept on a low level.

6. No harm to engine parts

The emission system components, coating, sealing materials or catalytic converters must not be influenced or harmed by lubricant degradation products or an unsuitable additive selection or the lubricant itself. This makes compatibility of all lubricant components with the machine parts an important requirement.

Moreover, there are some properties which are not related to the lubricant performance but cannot be neglected from an economical, ecological or health aspects. A minimum toxicity for humans and the environment is an indispensable issue for the application of oils. Besides the fresh oil ingredients, also potential degradation products should exhibit preferentially no or low impact on the environment or human health. This aspect has gained more and more importance during the last decades, and many innovations are driven by this fact. At the same time, a considerable pricing pressure on lubricant suppliers is an imported limiting factor for the application of advanced lubricants and new high-performance and eco-friendly technologies.

## 1.2 Lubricant base oil types

Lubricants are composed of base oils equipped with additives. In the case of greases, a thickener is added to generate paste-like consistency to the lubricant. Base oils are classified in 5 groups according to the “Appendix E – API (American Petroleum Institute) base oil interchangeability guidelines for passenger car motor oils and diesel engines”. These groups differ mainly in their method of manufacturing, in their sulfur and saturates content, and in their VI. *Table 1* provides an overview of all 5 groups, and they are described in the following [4].

Table 1: Classification of base oils from group I to V according to API.

| Class of base oil | Method of manufacturing | Sulfur content [%]                       | Saturates content [%] | Viscosity Index [-] |
|-------------------|-------------------------|--|-----------------------|---------------------|
| Group I           | solvent refined         | > 0.03                                   | < 90                  | 80 - 120            |
| Group II          | hydrotreated            | ≤ 0.03                                   | ≥ 90                  | 80 - 120            |
| Group III         | hydrocracked            | ≤ 0.03                                   | ≥ 90                  | ≥ 120               |
| Group IV          | synthetic               | polyalphaolefines                        |                       |                     |
| Group V           | diverse                 | all others not assigned to group I to IV |                       |                     |

Group I base oils contain less than 90 % of saturates and/or have a sulfur content higher than 0.03 %. The VI range has to be in the range between 80 and 120. Base oils of this group are refined mainly by solvent extraction of crude oil distillates to remove undesirable compounds such as waxes and aromates. Due to this simple method, they can be provided at a quite low price but have a minor quality [5], [6].

Base oils of group II contain at least 90 % of saturates and/or a maximum of 0.03 % of sulfur, while the VI is between 80 and 120. Hydroprocessing is used for their production, which results in higher prices compared to group I base oils, but also higher quality, e.g., group II base oils show a better oxidative stability due to higher degree of saturation. This base oil class is the most commonly used for commercially available engine oils [5], [6].

Group III base oils have equal thresholds for the content of sulfur and saturates, but a minimum VI of 120 has to be guaranteed. These oils can be considered as the highest level refined from crude mineral oil, which is achieved by hydrocracking where the molecules are significantly rearranged to provide a high molecular uniformity and stability. For high-performance applications, these base oils are blended with additive packages and distributed as semi-synthetic or even synthetic lubricants [5], [6].

According to Appendix E, group IV base oils are defined as polyalphaolefines (PAOs) and do not have additional qualification besides the manufacturer's specifications [4]. PAOs are produced by oligomerization of alpha-olefins and possess remarkable high purity, molecular uniformity and stability. Combined with the respective additives, they are used in demanding applications whenever high-performance is intended [5], [6].

Group V is the umbrella term for all base stocks not assigned to group I to IV. These are alkylated naphthalenes, esters, polyalkylene glycols, silicones, polybutenes, and biolubes, to

name just some of them. Typically, these oils show high quality parameters, and are mainly used in specific industrial applications or as engine oil additives to improve certain properties, e.g., seal-swelling [5], [6], [7].

### 1.2.1 Mineral oils

As mentioned above, base oils of group I to III are refined from crude oil to mineral oil fractions with distinct properties. A precise characterization of mineral oils is a challenging task as they do not consist of one component with an exact structure but of a variety of chemical compounds. Hence, it is more suitable to identify or quantify groups of certain components with high chemical similarity. In doing so, the determination of hydrocarbons according to their chemical bonds is a crucial element. The hydrocarbon distribution is given in aromatic, naphthenic (i.e. cycloalkanes), and paraffinic (i.e. saturated alkanes) content. These values can be evaluated either by physicochemical data, e.g., refractive index, density, or viscosity at different temperatures or advanced chemical methods such as separation of saturated and aromatic fractions according to the boiling point by gas chromatography (GC; ASTM D 2786-91 [8], ASTM D 3239-91 [9]) [1].

### 1.2.2 Synthetic base oils

In 1962, a pioneering book discussing tailor-made synthetic lubricants was edited by Gunderson and Hart [10], and these lubricants were categorized by certain classes. Since then, a range of new synthetic lubricants was designed, new classes were added, others were dropped or changed [11]. Nowadays, there are numerous synthetic lubricant solutions for high-demanding applications, e.g., at high temperatures and pressures [12]. However, their use on a large scale for standard applications is still limited by the considerably higher prices for these lubricants [1], [7], [11].

To name just a few of the commercially available synthetic lubricants, there are

- synthetic hydrocarbons, among others PAOs and polybutenes,
- alkylated aromates,
- halogenated hydrocarbons,
- polyalkylene glycols (PAGs) and polyethers,
- synthetic esters comprise, among others (di)carboxylic acid esters, polyol esters, complex esters, and fluorinated carboxylic esters (see chapter 1.2.3),
- silicones,
- organic phosphates, and
- perfluorinated polyethers.

In general, synthetic lubricants are either classified according to their production process or, preferably, according to their chemical composition [1].

The oils are tailor-made by reactions based on few defined chemical compounds and are characterized, compared to refined mineral base oils, by a minor distribution of components. A large number of synthetic lubricants are synthesized from ethylene as initial component emphasizing the importance of synthetic lubricant components. A simplified depiction of the synthesis route is given in *Figure 1*. However, the chemical purity may be a drawback when it comes to additive compatibility and response, which is especially observed for saturated hydrocarbons such as PAOs [1].

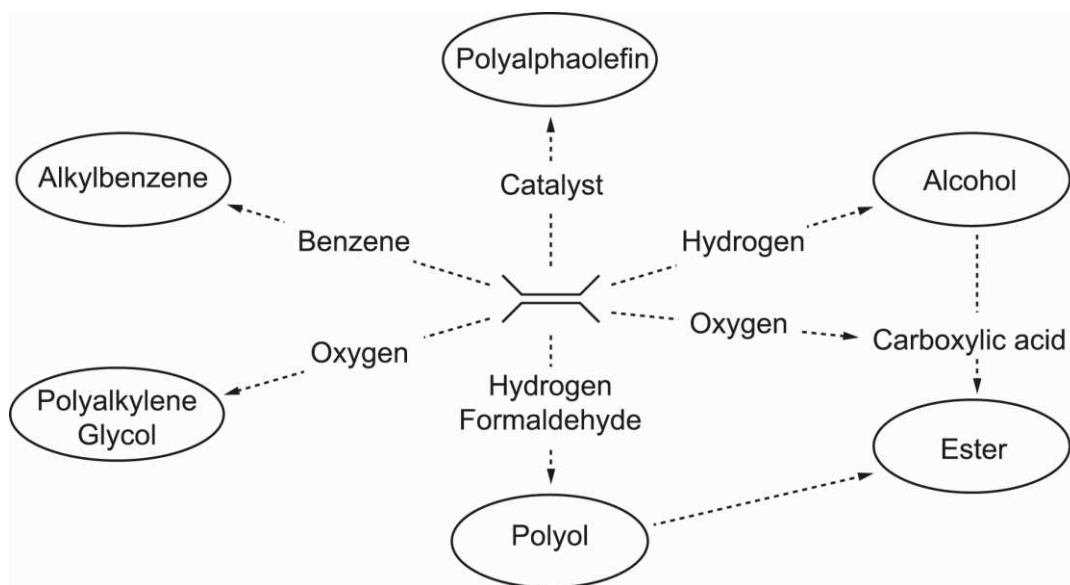


*Figure 1: Simplified synthesis route for various synthetic lubricants based on ethylene [1].*

### 1.2.3 Ester base oils

Ester-based oils are widespread in various application fields ranging from automotive engine oils, hydraulic fluids, compressor and gear oils to grease formulations. This diversity of usage may be explained by the unique set of properties. Besides a good performance in intrinsic lubrication and a stability towards high temperatures, these base oils are characterized by a low toxicity and excellent biodegradability [7], [11], [13]. Some of the most advantageous properties of carboxyl esters can be explained by the polarity of the ester molecule.

In the following, the specific performance characteristics are explained [1], [7], [11], [14]:

1. Low vapor pressure, low volatility and high flashpoints

The strong dipole moment of the carboxylic group in ester molecules affects the

attraction to other ester molecules and polar species. For the transfer of a lubricant molecule from the liquid to the gaseous state, a higher energy input is required to overcome these forces of attachment. These properties make esters highly suitable for vacuum pump lubricants.

## 2. High thermal stability

Caused by the dipole moment as explained above, carboxylic esters show an increased thermal stability compared to other base oils, which makes them suitable for high-temperature applications.

## 3. High solvency

The high polarity ensures a good miscibility with the mostly polar additive components.

## 4. Lubricity

The higher polarity promotes the attraction to metal surfaces. This makes them good boundary lubricants and friction modifiers.

However, the polar ester bond also attracts water molecules, and leads to hygroscopy as well as a limited hydrolytic stability.

In general, one can distinguish between three main types of esters:

- The first type are monoesters, diesters, phthalates, dimerates, and trimellitates that are examples for acid or anhydride centered esters.
- The second type are the alcohol centered molecules, e.g., polyols.
- The third type are so-called complex esters, which contain either or a combination of diols, polyalkylene glycols, mono and dicarboxylic acids, and monofunctional alcohols. This complexity results in a higher molecular weight and viscosity compared to the first two types.

Mono- and diesters are discussed hereafter [7]. The reaction of a monofunctional acid and a (monofunctional) alcohol, typically with a chain length of C1 up to C22, results in a monoester. These molecules have comparably low viscosities, whilst having high VI values ranging from approximately 200 to 250. One of their most important commercial implementations is in metalworking applications. Glycerol monooleates (GMO) may be applied as friction modifiers as well [7].

For the use as a lubricant, diester molecules consisting of a) branched primary alcohols with straight dicarboxylic acids or of b) straight primary alcohols with branched dicarboxylic acids are the most suitable ones. *Figure 2* depicts an exemplary structure for the first category, namely a bis (2-ethylhexyl) adipate. Those esters have, compared to mineral oils, an improved

viscosity-temperature behavior and hence higher VI values. When the straight acid is replaced by a branched one, the VI value decreases, whilst the low-temperature properties are improved. VI values typically range from around 120 to 170 but can be enhanced with methacrylates as VI improves up to 180. Sterically hindered esters show the best thermal and hydrolytic stability. In general, the hydrolytic stability of aromatic diesters is higher than that of alkyl diester, due to a higher degree of steric hindrance [1], [7], [10].

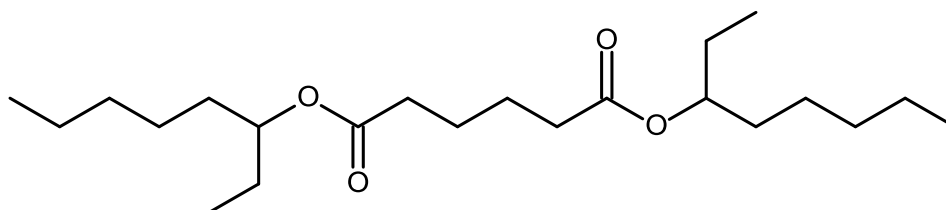


Figure 2: Structure of bis (2-ethylhexyl) adipate as exemplary synthetic ester base oil.

Diesters can be added to increase the additive solubility of PAOs. Moreover, they act as seal-swelling additives or lubricity additives. In engine oils, diesters positively affect the viscosity-temperature characteristics without negative impact on the low-temperature viscosity. Other applications include the usage in compressor or gear oils, as biodegradable hydraulic or metalworking fluids [1], [7], [10].

### 1.3 Lubricant additives

In order to add, avoid, modify or further improve properties of the base oil, various chemical components are known as lubricant additives are used [1]. The additives can be classified in three main groups:

- Lubricant protective additives to protect the base oil itself, e.g., antioxidants,
- performance additives to influence the physical properties responsible for performance characteristics, e.g., viscosity improvers, and
- surface-protective additives to preserve the condition of surfaces in contact with the lubricant, e.g., antiwear additives and corrosion inhibitors.

Table 2 gives an overview of the most important lubricant additives of all three categories in engine oils [15] and representative compounds serving as the mentioned types of additives. Some of them are multifunctional products such as zinc dialkyldithiophosphate (ZDDP), which serves as an antiwear additive but also as an antioxidant and sometimes as a base reserve. Some additives show synergistic effects, whereas some combinations of chemistries lead to

antagonistic effects [1].

In general, the total content of additives as well as the additive types are dependent on the field of application of a lubricant. While engine oils contain a broad variety of additives [5] and contents up to 25 % (v/v) [2], hydraulic oils have typically lower additive contents of up to 10 % (v/v) [3] and turbine oils as little as 0.5 to 5 % (v/v) [15]. In the following, the main representatives of lubricant additives and their modes of action are described.

*Table 2: Overview of the most important additives in engine oils. The task of the additive in the lubricant or on surfaces as well as the most common representative components are listed (modified according to [15]).*

|                                | Type of additive      | Task of additive   | Representative components   |
|--------------------------------|-----------------------|--|---|
| Lubricant protective additives | Antioxidant           | Retardation of oxidative degradation                                     | Hindered or sulphurized phenols, aromatic amines, ZDDP  |
|                                | Metal deactivator     | Reduction of catalytic effect of metal                                   | Organic complexes containing nitrogen/sulfur, amines, sulphides or phosphites                                 |
|                                | Foam inhibitor        | Prevention of persistent foam formation                                  | Silicone polymers and organic copolymers  |
| Performance additives          | Viscosity modifier    | Reduction of viscosity change with temperature                           | (Co)Polymers of methacrylates, butadiene olefines and alkylated styrenes                                      |
|                                | Pour-point depressant | Improved flow properties at low temperatures                             | Alkylated naphthalene, phenolic polymers, polymethacrylates   |
|                                | Seal swell agent      | Swelling of elastomeric seals  | Organic phosphates, aromates, halogenated hydrocarbons  |
| Surface protective additives   | Antiwear additive     | Reduction of friction and wear   | ZDDP, organic and acid phosphates, organic sulphur and chlorine compounds, sulfides and disulfides            |
|                                | Detergent             | Prevention of deposits on surfaces and neutralisation of corrosive acids | Metallo-organic compounds of Ba, Ca and Mg phenolates, phosphates and sulfonates                              |
|                                | Dispersant            | Dispersion of insoluble soot in the lubricant                            | Polymeric alkylthiophosphonates and alkylsuccinimides, organic complexes containing nitrogen compounds        |
|                                | Friction modifier     | Modification of friction coefficient                                     | Organic fatty acids and amines, lard oil, high molecular weight organic phosphorus and phosphoric acid esters |
|                                | Corrosion inhibitor   | Protection of corrosion and rusting of metal parts                       | ZDDP, metal phenolates, basic metal sulfonates, fatty acids and amines  |

### 1.3.1 Antioxidants

Provoked by exposure to oxygen together with light or elevated temperatures, a degradation process (see chapter 3) of the lubricant results in the formation of oxidation products of the base oil (see mechanism of degradation in section 3.2) and additives. Corrosion caused by the generated acids, surface deposits formed by sludge, which are polymeric oxidation products, and an increased viscosity are the main consequences of oxidation. Hence, the oxidative degradation significantly influences the lifetime and performance of a lubricant [1]. The use of antioxidative additives can decelerate this process remarkably. These additives terminate the free-radical reactions during oxidation processes and are consumed by sacrificing themselves, while inducing a delay of lubricant oxidation.

According to their mode of action, antioxidants may be divided into two classes [16], [17]:

#### 1. Primary antioxidants

These are radical scavengers that block the initial step of the oxidation reaction, the radical formation, by donation of a hydrogen atom. This hydrogen reacts with the alkyl radicals or the alkyl peroxy radicals, and a hydrocarbon or an alkyl hydroperoxide is formed. The antioxidant, which can act as a hydrogen radical donor or a peroxide scavenger, forms a stable radical. Sterically hindered phenols and aromatic amines are the two most important examples of primary antioxidants used in lubricants. When the transfer of a hydrogen atom from the oxygen or the nitrogen to the radical takes place, quinones or quinonimines are formed.

#### 2. Secondary antioxidants

The so-called peroxide decomposers undergo almost stoichiometrical reactions with oxygen or hydroperoxides, thus reducing the alkyl hydroperoxides to alcohols. The sulfur or phosphorus compounds typically used for this purpose are consumed by oxidation instead of the base oil molecules. ZDDP, phosphites and thioethers are representative chemical classes of secondary antioxidants.

One widely used class of antioxidants are the sterically hindered mono-, di- or even polynuclear derivatives of phenols, which carry tertiary alkyl groups on C2 and C6. *Figure 3* depicts two representatives of mono- and dinuclear phenol derivatives, namely 2,6-di-*tert*-butyl-4-methylphenol (also known as butylated hydroxytoluene, BHT) and 4,4'-methylene-bis(2,6-di-*tert*-butylphenol) used in the experiments for *Publication 2* and *Publication 3*.

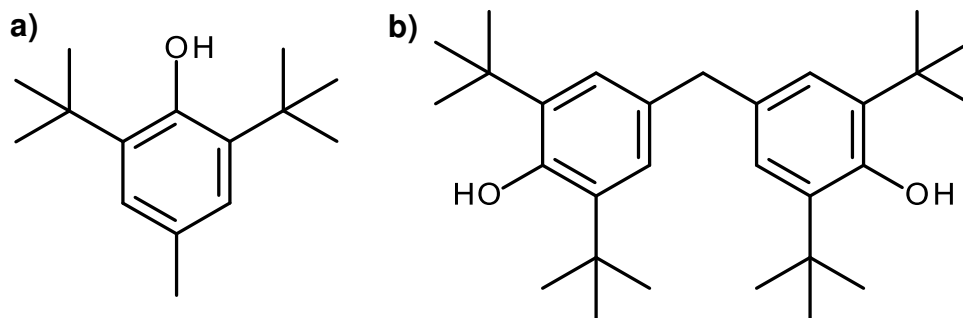


Figure 3: Chemical structures of two common antioxidants; a) 2,6-di-tert-butyl-4-methylphenol (BHT), b) 4,4'-methylene-bis(2,6-di-tert-butylphenol).

The substitution on C4 with higher-molecular-mass groups of di- and polynuclear phenols results in higher boiling points. Consequently, the lower volatility makes them suitable for high-temperature applications [1], [18].

### 1.3.2 Detergents

Detergents, together with antioxidants and dispersants, can be assigned to the additive group of stabilizers and deposit control agents [1]. The main tasks of detergents are on the one hand to control deposit formation on hot metal surfaces by formation of a protective layer on the surfaces and by covering sludge or varnish precursors to make them oil soluble. On the other hand, detergents serve to neutralize acids in the oil. With their alkaline or basic nature, detergents form the basis of the reserve alkalinity – also called base reserve – of engine oils to neutralize acidic components formed during the combustion process or by degradation [16]. The commonly used compounds in engine oils for this purpose are polar phenolates, phosphates, sulfonates and sometimes salicylates with magnesium, calcium or barium as bivalent metal counter ions [19]. Alkalinity is usually provided by CaCO<sub>3</sub>-based nanoparticles kept oil-soluble by a layer of detergents. Typically, detergent additives are applied in combination with dispersant additives.

### 1.3.3 Dispersants

Dispersants possess cleaning properties similar to detergents but are ashless and do not produce ash during combustion. Generally, they consist of three structural parts: a hydrocarbon polymer and a polar nitrogen or oxygen-containing group, linked by a connecting group such as a succinimide, a phenol or a phosphonate. The main function of detergents is to prevent agglomeration of particles deriving from contamination or degradation to prevent the formation of insoluble deposits in the oil. Due to their polar head and the oil-soluble oleophilic tail, detergents have the ability to form micelles by enveloping insoluble contaminants, e.g., soot

particles as depicted in *Figure 4* [15]. Hence, the combination to larger particles is interrupted [16], [20].

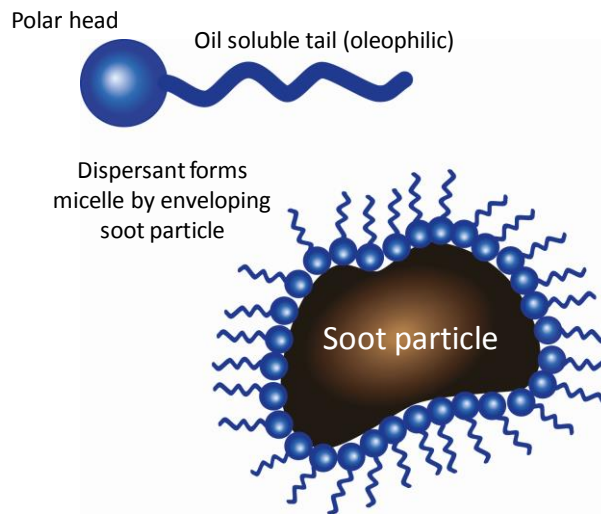


*Figure 4: Schematic depiction of a micelle with a polar head and an oleophilic tail and the mode of action as dispersants, modified according to [15]*

#### 1.3.4 Antiwear and extreme pressure additives

While operating in boundary and mixed lubrication regime, metal-to-metal contact of machine interfaces takes place. This results in scuffing, welding, seizure and surfaces damages. In order to protect machine parts and reduce wear, antiwear (AW) and extreme-pressure (EP) additives are important component in lubricants. When these additives react chemically with metal surfaces, a sacrificial film to minimize wear on the surface itself is formed and the additive depletes. A clear assignment of the compound to either AW or EP additives is difficult, as certain chemistries can act as both depending on the application and the existing conditions. However as general rule, AW additives form protective films to eliminate direct sliding contact of surfaces under moderate operating conditions such as in engines. EP additives operate under harsh conditions such as high strain and high temperatures, hence in surface contact with higher pressures. EP additives are typically composed of sulfur, phosphorus or boron compounds, while the most common AW additives are phosphates or sulfides [15], [16], [21].

ZDDP is the most frequently used AW additive and is applied in engine oils, hydraulic oils and transmission fluids. The distinct structure of ZDDP, in particular the structure of the alkyl chain, may vary according to application, requirements, and lubricant formulation [22]. *Figure 5* illustrates a representative structure of ZDDP. Besides the AW effect, ZDDP has antioxidative and corrosion-inhibiting properties [16]. However, the increasing commitment to eco-friendly,

zinc- and ash-free additives lead to enhanced attempts to replace ZDDP with ashless and metal-free compounds.

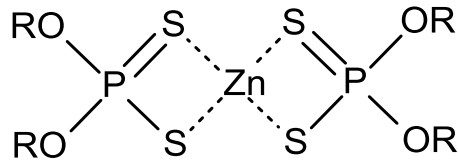


Figure 5: Representative structure of ZDDP

### 1.3.5 Viscosity modifiers

With the establishment of multi-grade oils, lower viscosity for engine starts at low temperature as well as adequate viscosity at higher temperatures to prevent engine wear became possible. This reduction of viscosity-temperature dependence is enabled by viscosity modifiers or viscosity index improvers [23]. Oil-soluble polymers of methacrylates [24], butadiene olefins or alkylated styrenes such as olefin-styrene copolymers are interacting with the lubricants according to the coil expansion model [25]. At low temperatures, the effect of thickening is minimized due to the coiled spherical shape of the polymer and less interactions with the lubricant. With increasing temperature, the solubility of the polymer in the base oil improves, the additive unravels and a thickening effect is caused by the voluminous conformation of the polymer [26]. However due to their large molecular weights, viscosity modifiers are prone to destruction by shearing forces, which can induce unfavorable changes in the viscosity-temperature behavior of oils in use [15].

### 1.3.6 Pour point depressants

Wax crystals formed at lower temperatures, particularly in paraffinic mineral oils, start to crystallize in large networks, and may cause the blocking of oil flow. The pour point indicates the lowest temperature, where the oil is still able to flow [1]. Pour point depressants are added to prevent large wax crystals formed by the aggregation of oil molecules and improve the low-temperature behavior [19], [2]. These additives consist of alkylated naphthalenes, phenolic polymers or polyalkylmethacrylates [16], [27]. When the wax crystallization is initiated, these molecules co-crystallize in the network. Hence, the crystal structure of the wax is modified and the steric hindrance inhibits the formation of three-dimensional, flow-inhibiting structures. The wax remains as a stable dispersion of tiny crystals in the lubricant.

### 1.3.7 Foam inhibitors

Gas entrainment and foam formation leads to decreased oil pressure and decreased cooling capability and hence may cause engine damage due to cavitation on the surface of the oil film among others. In order to avoid this effect, chemicals with low interfacial tension such as dimethylsiloxane polymers or alkylmethacrylate copolymers are applied. These materials are not supposed as oil-soluble but shall form fine dispersions in the lubricant. When the foam inhibitors come in contact with the interface to an air bubble, the surface tension is reduced and the bubbles tend to burst eagerly [21], [16]. Moreover, as the air-oil contact is reduced, they are considered to have a beneficial effect on the prevention of oxidation [28].

## 2 Liquid fuels

The application in automotive vehicles and industrial production made petroleum-based fuels one of the most important ones deriving from fossil energy sources within the last century [29]. The most important requirement to fuels used in internal combustion engines is of course combustibility. When the fuel is combusted, i.e., oxidized, heat energy is produced and converted to kinetic energy. Various gaseous and liquid, and less commonly, solid products are used as fuels. One usual classification is done in two main groups, namely in crude oil based and non-crude oil based fuels. The former comprises gasoline, diesel and kerosene, while the latter includes natural gas-based fuels, alcohol-based biofuels, biodiesel and biogas oil [30].

Further classification to categorize engine fuels more precisely can be done according to [30]:

- 1) Drivetrains
  - a. Fuels applied in gasoline engines, e.g., gasoline, ethanol, compressed natural gas
  - b. Fuels applied in diesel engines, e.g., diesel gas oils, dimethyl-ether, compressed natural gas
- 2) Origin
  - a. Products deriving from exhaustible energy carriers, i.e., fossil energy sources
  - b. Products deriving from renewable energy carriers, i.e., biofuels from biomass
- 3) Number of feedstock resources
  - a. One resource, e.g., fatty acid methyl esters (FAME) from only triglyceride and fatty acid containing feedstocks
  - b. Multiple resources, e.g., ethanol from sugar crops, from crops containing starch, lignocellulose, hydration of ethylene

While gasoline, diesel and kerosene are crude-oil derived and referred to as conventional fuels, all other fuels produced from other sources are so-called alternative fuels, either deriving from

fossil or biogenic energy sources [31], [32], [33].

All these materials, whether conventional or alternative, fossil or biogenic can be used in combustion engines alone or as blended components. In general, fuel selection is made based on the engine design, the choice of additives, the environmental and climate conditions, the availability of the energy source, safety technology and finally environmental protection issues and energy policy [30], [34], [35].

## 2.1 Gasoline

In general, the term gasoline describes a mixture of liquid, volatile hydrocarbons, which is suitable for application as fuel in spark-ignition internal combustion engines, also referred to as gasoline engines. A boiling point range of 30 up to 260 °C is covered. Nowadays, this fuel is typically unleaded, but contains small amounts of additives [30]. Specifications regarding the allowed components, the composition as well as the performance for so-called unleaded petrol automotive fuels are given in “EN 228 – Requirements and test methods” for the European market [36].

### 2.1.1 EN 228

In this European standard, the requirements and test methods for two different gasoline types supplied in the European market are given: it can be distinguished between gasoline with a maximum content of 10 % (m/m) ethanol and a maximum oxygen content of 3.7 % (m/m) and a second type with 5 % (m/m) maximum content of ethanol and 2.7 % (m/m) oxygen. The latter one is provided for older automotives, where the tolerance of the engines towards biocomponents is less. Despite these variations, both gasoline types have to fulfil certain requirements such as the maximum tolerable content of lead, sulfur or benzene, as well as the distribution of hydrocarbon groups. Due to these restrictions, limitations in the applicable additives occur. Additionally, requirements regarding density, appearance (e.g., turbidity) as well as research and motor octane value (RON, MON) are given (see 2.4.2). Thresholds are reported for further important performance characteristics such as oxidation stability, evaporation residues and corrosion impact the tolerable. The respective approved test methods are prescribed for all values to be determined. *Table 3* shows a brief overview of the main specifications regarding composition of both gasoline types [36].

Table 3: Maximum contents of specific components according to EN 228 for gasoline with 3.7 % (m/m) and 2.7 % (m/m) oxygen content.

| Content of       | Maximum level |
|------------------|---------------|
| Lead (mg/L)      | 5.0           |
| Sulfur (mg/kg)   | 10.0          |
| Manganese (mg/L) | 2.0           |
| Benzene % (v/v)  | 1.0           |
| Olefines % (v/v) | 18.0          |
| Aromates % (v/v) | 35.0          |

### 2.1.2 Biocomponents

Besides ethanol in a maximum content of 10 % (m/m) several other oxygen-containing biocomponents can be added in certain maximum contents. These compounds are given in Table 4 for gasoline with 3.7 % (m/m) and 2.7 % (m/m) oxygen content. The major amount of these biocomponents are short-chain alcohols or ethers, amongst them ethyl-*tert*-butylether (ETBE) [33], [37]. This component is not only used as a biocomponent, but also serves as a cetane improver (see 2.4.2) However, these limitations are not valid for synthetic hydrocarbons or hydrocarbons from renewable sources. Such biocomponents can be applied in unlimited contents as long as they fulfill the requirements set in EN 228 [36].

Table 4: Maximum content of oxygen-containing organic compounds (biocomponents) according to EN 228 for gasoline with 3.7 % (m/m) and 2.7 % (m/m) oxygen content.

| Content of oxygen-containing organic compounds % (v/v) | Gasoline with max. 3.7 % (v/v) oxygen | Gasoline with max. 2.7 % (v/v) oxygen                                   |
|--|---------------------------------------|---|
| Methanol   | 3.0                                   | 3.0   |
| Ethanol  | 10.0                                  | 5.0   |
| Isopropyl alcohol                                      | 12.0                                  | up to a total oxygen content of 2.7 % (v/v) additional to MeOH and EtOH |
| Isobutyl alcohol                                       | 15.0                                  |   |
| tert-Butyl alcohol                                     | 15.0                                  |   |
| Ether (5 or more C atoms)                              | 22.0                                  |   |
| Other oxygen containing compounds                      | 15.0                                  |   |

## 2.2 Diesel fuels

Diesel fuels are middle distillates from crude oil, consisting of numerous of hydrocarbon components with a boiling point range between 180 and 370 °C. These fuels are used in internal combustion engines where ignition is induced by pressure and not by an electric spark. The ignition point is around 350 °C (lower limit 220 °C) and comparatively low to gasoline with an ignition point around 500 °C. Besides conventional diesel from crude oil, biodiesel based on mono-alkyl esters of long-chain fatty acids, so-called fatty acid methyl esters (FAME), are used. This fuel derives mainly from vegetable oils or animal fats [30], [38]. While the term B0 indicates a pure mineral oil-based diesel fuel, the term B100 describes a fuel consisting of neat biodiesel. The most widely spread diesel fuel in the European Union is B7, which contains 7 % (v/v) of biodiesel. This specification as well as limitations regarding the allowed components, the composition as well as the minimum performance parameters for diesel fuels for the European market are given in “EN 590 – Requirements and test methods” [39].

### 2.2.1 EN 590

European standard EN 590 provides not only specifications regarding the maximum biodiesel content and the contents of sulfur, manganese, FAME and polycyclic aromatic hydrocarbons, but also requirements regarding residues related to combustion (see Table 5). Thresholds for physico-chemical properties such as density, water content or viscosity are reported as well as

parameters for performance such as the oxidation stability, copper corrosion tendency and the lubricity. The cetane number, which is the indicator for the ignitibility of diesel fuels and therefore is the inverse of the octane number for gasoline, must reach a minimum value of 51 (see 2.4.2).

*Table 5: Maximum contents of specific diesel fuel components and residues according to DIN EN 590.*

| Content of                               | Maximum level |
|--|---------------|
| FAME % (v/v)                             | 7.0           |
| Sulfur (mg/kg)                           | 10.0          |
| Manganese (mg/L)                         | 2.0           |
| Polycyclic aromatic hydrocarbons % (m/m) | 8.0           |
| Coke residue % (m/m)                     | 0.30          |
| Ash content % (m/m)                      | 0.01          |

Beyond these specifications, there are requirements for the cold filter plugging point (CFPP), which is defined as the lowest temperature at which a given volume of diesel fuel is still able to pass a standardized filtration device [38]. The 6 different classes (for moderate climate zones) range from thresholds of + 5 °C (Class A) to -20 °C (Class F). The specified class changes with the season and the expectable ambient temperatures [39].

### **2.2.2 Biodiesel components**

DIN EN 590 permits a maximum FAME content of 7.0 % (v/v) in diesel fuel, provided that the other requirements are fulfilled. This can be explained by the fact that there is no specification regarding the distinct FAME pattern or distribution, nor the respective source. Based on different feedstocks ranging from rapeseed, soybean or animal oil (first generation biodiesel) via non-edible oils (second generation) to algal oils (third generation), FAME components are produced by transesterification [34]. Thereby, caution has to be put on the selection of additives

blended for the improvement of the CFPP value, as not all are compatible with every FAME pattern, and incompatibilities may occur. Moreover, the use of FAME as components in a diesel fuel are known to reduce the storage stability [40]. Hence, the addition of antioxidants is recommended, whereas BHT or similar effective compounds are recommended [39].

In the same way as for gasolines, there are no limitations for non-petroleum deriving hydrocarbons such as hydrated vegetable oils (HVO) or hydrocarbons from gas-to-liquid or biomass-to-liquid processes. Unlimited contents can be applied as long as the resulting diesel fuel reaches the requirements stipulated in DIN EN 590 [39].

## 2.3 Kerosene

Kerosene is the umbrella term for jet aircraft fuels of different specifications. The most common aviation fuel for aircraft-powered gas-turbine engines is Jet A-1. This kerosene-type fuel consists of a hydrocarbon mixture with a carbon number range from 8 to 16 carbon atoms showing a remarkable maximum freezing point of  $-47\text{ }^{\circ}\text{C}$  [30], [41], [42]. Additionally, it is less volatile and flammable than gasoline (min. flash point for Jet A-1  $38\text{ }^{\circ}\text{C}$  [41]) and contributes to enhanced safety due to these characteristics. As it is used for global civil aviation, it must fulfil an international specification regarding composition, quality and performance to guarantee global availability [30]. These well-defined requirements are defined in ASTM D1655-19 “Standard Specification for Aviation Turbine Fuels” [41] and the British Ministry of Defence Standard DEF STAN 91-91/Issue 7 Amendment 3 [42], whereas both standards give the same limits.

### 2.3.1 Specifications for Jet-A-1 fuels according to ASTM D1655-19

The guideline of specifications and test methods for composition, volatility, fluidity, various other physico-chemical properties, combustion, corrosion, thermal stability, water separability, contaminants, and additives by ASTM D1655-19 ensures the controlled and constant quality of Jet A-1 fuels worldwide [41].

As Jet A-1 fuel is a complex mixture of hydrocarbons and the distinct composition varies depending on the crude oil source and manufacturing processes, the specification may be seen rather as a performance specification than a compositional one. However, Jet A-1 fuels shall predominantly consist of refined hydrocarbons derived from conventional sources, e.g., crude oil, natural gas liquid condensates and heavy oil, and the respective approved additives. *Table 6* summarizes the maximum contents for specific components and limitations regarding acidity and particulate contamination [41].

Specific specifications were elaborated due to the emerging requirement to control the use of

synthetic components from non-petroleum sources [43]. A permission of certain synthetic components requires the additional fulfillment of specific approvals given in Annex D of ASTM D1655-19 unless it is demonstrated that the alternative fuel type conforms to ASTM D7566-19. In this norm the “Standard Specification for Aviation Turbine Fuel Containing Synthesized Hydrocarbons” is described. All alternative fuel types fulfilling this norm are approved for use in aviation turbine fuels independently from Annex ASTM D1655-19 [44].

*Table 6: Maximum contents of specific components, particulate contamination and acidity resulting from the composition of Jet A-1 fuels according to ASTM D1655-19.*

| Content of                                       | Maximum level |
|--|---------------|
| FAME (mg/kg)                                     | 50            |
| Sulfur, total % (m/m)                            | 0.30          |
| Sulfur, mercaptan % (m/m)                        | 0.0030        |
| Total aromatics % (m/m)                          | 26.5          |
| Particulate contamination at manufacturer (mg/L) | 1.0           |
| Total acidity (mg KOH/g)                         | 0.015         |

In order to improve performance in general and to fulfil the requirements regarding conductivity, lubricity, and thermal stability blending with additives is permitted. However, for most of them not only a limited content but also a limited number of components is prescribed to guarantee a worldwide purchase of the respective additives. Annex A to ASTM D1655-19 lists the additives qualified for use, comprising the following additive classes [41]:

- Antioxidants (total concentration of min. 17.0 to max. 24.0 mg/L)
- Metal deactivator additives (initial doping max. 2.0 mg/L, redoping to a cumulative calculated or analytical value of max 5.7 mg/L)

- Static dissipator additives (initial doping max. 3.0 mg/L, redoping to a cumulative analytical value of max 5.0 mg/L)
- Lubricity improver additives (according to the respective compound and manufacturer min. 9.0 mg/L to max 23.0 mg/L)
- Fuel system icing inhibitor (added where mandated, min. 0.10 % (v/v) and max. 0.15 % (v/v) at the time of delivery to the purchaser)
- Leak detection additive (max. 1.0 mg/kg)

As for this work the permitted antioxidants are of particular interest, the allowed chemical structures are depicted in *Figure 6*. Besides the addition of either 2,6-di-*tert*-butylphenol, 2,6-di-*tert*-butyl-4-methylphenol (BHT) or 2,4-dimethyl-6-*tert*-butylphenol in a concentration of 17.0 to 24.0 mg/L, mixtures thereof may be applied. The content of the respective antioxidants in the permitted mixtures is specified for each compound, and the total content of all antioxidative additives must be in the range of 17.0 to 24.0 mg/L [41]. Due to the complex matrix of kerosene type fuels a reliable and precise determination of these additives in low levels is a challenge. For this purpose, sensitive analytical tools such as chromatographic methods and mass spectrometry may be used for identification and quantification [45], [46].

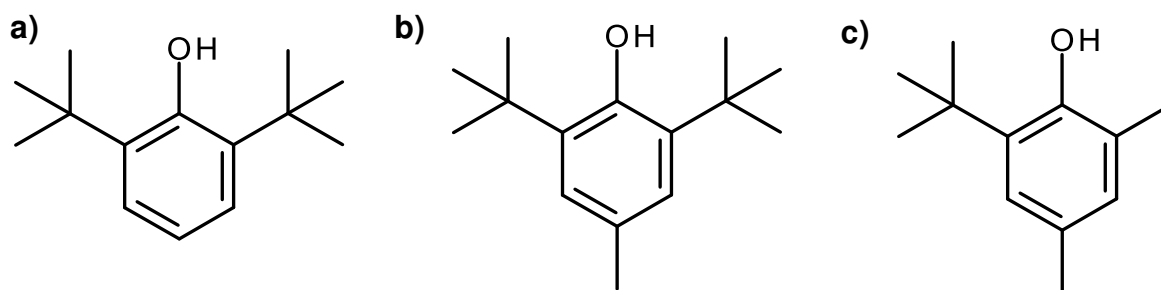


*Figure 6: Chemical structures of the antioxidants permitted for use in Jet A-1 fuels in concentrations of 17.0 to 24.0 mg/L. a) 2,6-di-*tert*-butylphenol, b) 2,6-di-*tert*-butyl-4-methylphenol, c) 2,4-dimethyl-6-*tert*-butylphenol.*

## 2.4 Fuel additives

In the same way as for lubricants (see section 1.3) additives are used to improve, reduce or avoid certain fuel characteristics. A combination of chemical additives is applied to achieve the requirements of the respective specifications for gasoline, diesel and kerosene-type fuels. Due to these and other restrictions such as European REACH regulations [47], there are also limitations in the applicable additive chemistries, e.g., for sulfur or emission levels.

In general, there are six main reasons to use additives in fuels [30]:

1. Improvement of handling properties and fuel stability
2. Improvement of combustion properties of the fuel
3. Reduction of emissions deriving from fuel combustion
4. Engine protection and cleanliness
5. Increase of fuel efficiency
6. Enhancement of the brand image of the fuel, e.g., by using dyes or deodorants

Based on the added concentrations one can distinguish between blending components (typically  $> 1 \%$ ), functional additives (typically  $< 1 \%$ ) and performance additives present in very low concentrations [30], [48]. As the permitted additives for Jet A-1 fuels are strictly limited as discussed in section 2.3.1, the following overview in *Table 7* lists the most important additives, their function and typical representative chemistries only for gasoline and diesel fuels. While some of the compounds are present in both fuel types, some of them are only used in diesel fuels [30]. The used compounds are depending not only on the type of fuel, but also the respective concentrations. As more and more alternative and biofuel components are used in gasoline and diesel fuels, the additive chemistries and contents have to be adapted according to the feedstocks and biocontents. Therefore, the given additive chemistries are subject to development, improvement and modification [49]. In the following, important additives for either used in gasoline, diesel or Jet A-1 fuels are discussed. Main emphasis is put on the antioxidative additives, in particular the ones permitted in Jet A-1 fuels.

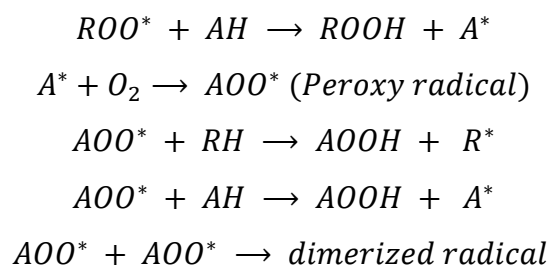
Table 7: Overview of the most important additives in gasoline and diesel fuels, their tasks in the fuel as well as the most common compounds [30].

|                     | Type of additive                    | Task of additive   | Representative components   |
|---------------------|-------------------------------------|--|---|
| Gasoline and diesel | <b>Antioxidants</b>                 | Increase of storage stability, inhibition of deposit formation       | BHT, sterically hindered phenols, alkyl/aryl-phenylene-diamines, ethylene-diamines                                  |
|                     | <b>Octane improvers (gasoline)</b>  | Increase of octane number  | Methyl-cyclopentadienyl-manganese-tricarbonyl (MMT), ferrocene, iron pentacarbonyl                                  |
|                     | <b>Cetane improvers (diesel)</b>    | Increase of cetane number  | Cetane: alkyl-nitrates/nitrites, peroxides, nitro/nitroso-compounds   |
|                     | <b>Metal deactivator additives</b>  | Deactivation of metal surfaces acting as oxidation catalysts         | <i>N,N</i> -disalicylidine 1,2-propane-diamine  |
|                     | <b>Friction modifiers</b>           | Reduced friction for lower fuel consumption                          | Fatty acid esters (e.g., glycerol monooleate) and fatty acid amides   |
|                     | <b>Corrosion inhibitors</b>         | Corrosion protection of the fuel system                              | Alkyl-succinates, amine salts, dimer acids, salts of carboxylic acids   |
|                     | <b>Anti-static additives</b>        | Increase of conductivity   | Chromium salts of alkylsalicylic acids, amine salts of carboxylic acids, calcium di(2-ethyl hexyl/sulpho succinate) |
|                     | <b>De-icing additives</b>           | Inhibition of ice formation on carburetor                            | Glycol-ethers   |
|                     | <b>Combustion improvers</b>         | Improve of combustion characteristics and reduction of emissions     | Organometallic compounds and complexes of iron (ferrocenes, naphthenates, succinates)                               |
|                     | <b>Detergents and dispersants</b>   | Deposit control  | Long-chain alkyl amines, amides, polybutene/polyether-amines, alkenyl-succinimides                                  |
| Diesel              | <b>Cold flow improver additives</b> | Improve of cold flow properties and inhibit wax settling             | Polymeric compounds containing nitrogen   |
|                     | <b>Antifoam additives</b>           | Inhibition of foam formation during filling                          | Silicones   |
|                     | <b>Demulsifier</b>                  | Inhibition of haze formation caused by water or insolubles           | Long-chain alkyl phenols and alcohols, long-chain carboxylic acids and amines                                       |
|                     | <b>Lubricity additives</b>          | Increase of ubricity for low sulfur fuels, decrease of boiling point | Carboxylic acids (C8 - C14) and their esters, amides and fsatty acids   |
|                     | <b>Biocides</b>                     | Supression of microorganism growth causing bad quality               | Succinimides and imidazolines   |

### 2.4.1 Antioxidants

Similar to base oils (see section 1.3.1.1), antioxidants are added to improve stability during storage and use by inhibition of fuel oxidation. In addition, the formation of sludge and deposits, affecting the fuel system and the vehicle performance, is prevented. The stability was improved by the reduction of sulfur in fuels. At the same time, however, the intrinsic antioxidative properties were also reduced. Moreover, there is a tendency towards cracked stocks driven by the increased demand for fuel products. These stocks show lower stability caused by the high amounts of olefins, aromatics, sulfur and nitrogen compounds that quickly degrade [30]. The oxidation tendency of diesel fuels containing biodiesel promoted by carbon-carbon double bonds is a well-known issue of these blends [40], [50], [51], [52]. For this reason, antioxidants are added to improve the resistance towards oxidation.

During the initial phase of auto-oxidation, the induction period, fuel radicals  $R^*$  are built from the dissociation of fuel molecules  $RH$  and  $RR$  (chain initiation). Next, oxygen from the atmosphere reacts with  $R^*$  to alkylperoxy radicals  $ROO^*$ . With further fuel molecules  $RH$  alkyl hydroperoxides  $ROOH$  and more radicals  $R^*$  are built, consequently (chain propagation). Similar to oxidation in lubricants, the process of oxidative degradation in fuels is a chain reaction (for detailed reaction steps see section 3.2). Typical end product thereof is an insoluble gum, which causes clogging in pipelines, tanks and fuel transportation systems [30]. In presence of an antioxidant  $AH$  donating the hydrogen atom to the alkylperoxy radical  $ROO^*$ , some complex reactions lead to the termination of the chain reaction and dimerization of the antioxidant radicals  $AOO^*$  takes place, shown in a simplified way [30], [53]:



In general, primary antioxidants are the antioxidative additives of choice in fuels (for a detailed description see 1.3.1.1). Similar to lubricant antioxidants, sterically hindered phenols and alkylated aromatic amines are commonly used. Sterically hindered phenols, amongst them the widely used BHT, are most effective in fuels with low olefin content [30], [54]. On the contrary, phenylenediamines like  $N,N'$ -di-*sec*-butyl-*p*-phenylenediamine and various aromatic amines are most effect in gasolines with higher amounts of cracked products [30].

## 2.4.2 Octane and cetane improvers

When the air-fuel mixture in gasoline engines shows uneven combustion, an undesired acoustic phenomenon called knocking occurs, especially pronounced in high-compression gasoline engines. It is caused by auto-ignition of the compressed air-fuel-mixture before the piston reaches the upper dead center in spark-ignition vehicles. This does not only produce unwanted noise, but also can damage engine parts, in particular the valves and the piston. Moreover, fuel efficiency is decreased due to heat loss [30], [55], [56].

The research octane number (RON) was introduced as a standard measure to indicate the performance of a gasoline fuel. In a test engine with variable compression ratios under controlled conditions, RON is determined against a mixture of isooctane (RON 100) and *n*-heptane (RON 0). The isooctane content in % (v/v) in this standard fuel with the same antiknock properties as the test fuel indicates the RON. The higher this number, the more tolerant is the fuel shows against compression before ignition, and hence it shows better antiknock properties [30], [55].

In order to improve these properties, octane number improvers are used as additives in gasoline fuels. The first widespread additives of this category were lead-tetramethyl and lead-tetraethyl. However, because of concerns about lead pollution and accumulative neurotoxicity, the use of these compounds has been banned in Western countries anymore and were replaced by several other chemistries:

- Methyl-cyclopentadienyl-manganese-tricarbonyl (MMT) [only limited use allowed as suspected to be a strong neurotoxin and respiratory toxin]
  - Ferrocene, consisting of two cyclopentadienyl rings bound on opposite sides of a central iron atom
  - Iron pentacarbonyl
  - Ashless antiknock additives, mainly consisting of carbon, hydrogen, oxygen and nitrogen, e.g., dialkyl ethers such as methyl-*tert*-butylether (MTBE) and ETBEAs
- counterpart to the octane number for gasoline fuels, the cetane number is the indicator for the ignitibility properties of diesel fuel components. As this characteristic is indispensable for the principle of function of a diesel engine, it is considered as an important quality indicator. A cetane number of 100 is represented by cetane (*n*-hexadecane), while alpha-methylnaphthalene has been assigned a cetane number of 0. Same as RON, the cetane number is determined using a test engine under defined conditions. In general, the cetane number is higher the more unbranched hydrocarbons

are present in the mixture, and the earlier autoignition in the engine occurs [30]. In summary, it can be concluded that octane and cetane number address inverse properties of gasoline and diesel fuel compositions, i.e., fuel compositions that promote spark ignition and those that favor autoignition.

Different chemistries are available on the market to improve the cetane number, amongst them the most important are:

- Organic peroxides, which are not containing nitrogen, show hardly any toxic effects and good anticorrosion properties, but are relatively expensive [57]
- Nitrites and nitrates, in particular alkyl nitrates such as amyl nitrate, hexyl nitrate and mixed octyl nitrates [30], [58], [59]

Due to the relatively low costs compared to organic peroxides, 2-ethylhexyl nitrate (2-EHN) as a representative of the second group is established as the commercially most used cetane improver [60], [61]. The structure is depicted in *Figure 7*. Ignitibility is improved by the breakdown of the alkyl nitrate and the provision of oxygen. However, this oxygen also promotes the oxidation during long-term storage of the fuel and may lead to sludge formation [30].

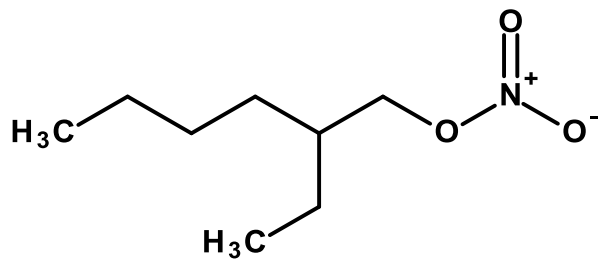


*Figure 7: Structure of 2-EHN, the most common cetane improver in diesel fuels.*

### 2.4.3 Lubricity additives

Lubricity additives protect the fuel pump against wear by film formation on metal surfaces. Accordingly, these additives are surface active and are enriched at the surfaces to form thin layers typically by physisorption or chemisorption. These molecular interactions between lubricity additive and metal surface alter adhesion, friction, and wear in a beneficial way. For this purpose, fatty acids with carbon numbers of 8 to 24 and their derivatives provided as esters and amides of fatty acids are added in small quantities to meet the lubricity requirements of modern engine fuels [30], [62].

#### 2.4.4 Antistatic additives

During fuel transfer and under turbulent fuel movement, e.g., during pumping or flow in the pipe, static electricity (separation of electrical charges) is generated. High pumping rates and equipment of a large surface area, such as water separators and fuel filters, promote this phenomenon. This may lead to high voltages, and spark discharges, which can cause the ignition of the fuel vapor.

To avoid this is of high importance for safety reasons but cannot be accomplished for fuels with low electrical conductivity. Fuels with a higher content of sulfur-containing molecules (> 500 mg/kg) inhibit sufficient intrinsic conductivity to disseminate the charge. As sulfur levels were subject to reduction during the last decades, these natural compounds were decreased. In the same way, electrically conductive ionic species are removed from highly refined petroleum products such as Jet A-1 fuels. Thus, conductivity must be enhanced by addition of anti-static additives. These salt-type additives in the fuel enable the transfer of the charge from the liquid to the container wall. Common antistatic additives are [30]:

- Chromium salts of alkylsalicylic acids such as chromium di(alkylsalicylate)
- Amine salts of carboxylic acid and polycarboxylic acids such as hydrocarbyl monoamine or N-hydrocarbyl substituted poly(alkyleneamine)
- Calcium salts of di(2-ethylhexyl)sulpho succinates such as manganese dodeceny succinate
- Quaternary ammonium compounds
- Organic polymers serving as stabilizing agent

### 3 Stability assessment

Degradation of lubricants and fuels – conventionally and simplified termed as ageing – is influenced by a large number of parameters, including their composition and operating conditions mainly characterized by materials, temperature, pressure, relative shear velocity of interfaces, presence of gases such as oxygen, humidity, and contaminations. To put it more simply, ageing is understood as any chemical and/or physical changes in lubricant and fuel parameterisation regardless of an improving or deteriorating effect on lubricating or other properties.

As the impact of degradation processes or ageing on the lubricant performance, either positive or negative, cannot be predicted, it is proposed to replace the term “ageing” by the neutral term “alteration”. The term alteration may be understood as any chemical and/or physical change of

the lubricant, either of improving or declining effect on the lubricating properties. Alteration includes ageing and degradation of the lubricant and deterioration of the additives [1], [16].

So-called artificial alteration is applied to elucidate and understand degradation mechanisms and kinetics of lubricants and fuels, simply denominated as ageing behavior. Such artificial alteration methods are laboratory-based simulations of lubricant and fuel degradation, which are performed according to standards or modified procedures to simulate specific operating conditions observed in the field.

The main processes dominating the alteration of lubricants are oxidative and thermal mechanism, followed by hydrolysis, shear stress and electric impact under certain operating conditions. Further the process of alteration can be driven by contamination, either pollution from machinery or biological or microbial contaminants. Table 8 gives an overview of the alteration mechanisms most relevant in fuel and lubricant degradation and the respective inducing factors.

*Table 8: The most relevant mechanisms of alteration of lubricants and fuels and the inducing factors thereof.*

| Mechanism of alteration | Inducing factor                        |
|-------------------------|--|
| Thermal                 | Temperature, heat                      |
| Oxidative               | Air oxygen                             |
| Hydrolytic              | Water                                  |
| Mechanical              | Shear stress                           |
| Contamination-based     | Pollution (from machinery environment) |
| Biological/microbial    | Presence/activity of micro-organisms   |
| Electrical              | Electric discharges, current flow      |

All these stress factors/mechanisms (can) occur simultaneously. The reactions with oxygen and water can be considered as the most relevant. Therefore, within this work mainly (thermo)-oxidative degradation is discussed. As during most alteration methods water is produced, the aspect of hydrolytic alteration is included, consequently.

## 3.1 Thermo-oxidative alteration methods

### 3.1.1 Standardized thermo-oxidative methods for lubricants

The major part of the established thermo-oxidative alteration methods for lubricants can be categorized in four classes:

1. Thermo-oxidative alteration at ambient pressure
2. Thermo-oxidative alteration under pressure
3. Thermo-oxidative alteration with catalysts
4. Thermo-oxidative alteration under pressure and with catalysts

In the following, one important standard of every class for the artificial alteration of lubricants is discussed exemplarily.

#### 3.1.1.1 Thermo-oxidative methods at ambient pressure – CEC L-48-A-00

CEC L-48-A-00 [63] describes the standardized determination of the oxidation tendency of automotive transmission lubricants including automatic transmission fluids (ATF) and gear oils. The standard consists of two parts and therefore two types of glassware are used. The first one is an Erlenmeyer flask with an air inlet and outlet, and an oil reservoir of 300 mL, which is exposed to a 10 L/h air flow. The second part is a flat-bottomed glass tube combined with a water-cooling device. In this tube, an air flow rate of 5 L/h is subjected to an oil sample of 100 mL via an air inlet. According to the conditions defined in the standard, the lubricant is heated to 160 °C in an oil bath and kept at this temperature for 192 h. An air flow is bubbling through the sample during the entire ageing time.

For the test evaluation, several parameters are evaluated. Besides the visual appearance, the kinematic viscosity at 40 °C and 100 °C is determined and compared to the fresh sample. The changes in acid number can be determined, optionally. Additionally, the oil aliquot from the Erlenmeyer flask is can be used to determine the content of heptane insolubles, which represents the amount of insoluble material and deposits. Moreover, a determination of the oxidation by Fourier Transform Infrared Spectroscopy (FT-IR) according to ASTM D7214-07a(2012) [64], which was developed for transmission oils and is used in the CEC L-48-A-00 test, can be done.

#### 3.1.1.2 Thermo-oxidative methods under pressure – pressure differential scanning calorimetry (PDSC)

In general, lubricant degradation can be monitored via the oxygen consumption correlating to the oxygen pressure during thermo-oxidative alteration processes under pressure. The standard ASTM D 6186 [65] determines the oxidation induction period by pressure differential scanning

calorimetry (PDSC). One benefit of this method is the minimal sample amount of 3 mg required that is placed in a so-called aluminum solid fat index sample pan and positioned in the test cell. In the test cell, a constant oxygen pressure of 3.5 MPa and a constant temperature between 130 and 210 °C are applied until an exothermic reaction is detected. The interval until this occurs is evaluated as extrapolated onset time and is reported as the induction period, which is an indicator of the oxidative stability. Besides the induction period, the entire thermal curve of the experiment is reported and therefore valuable for in-depth interpretation of the sample's oxidation behavior.

### 3.1.1.3 Thermo-oxidative methods with catalysts – turbine oil oxidation stability test (TOST)

In addition to elevated temperature and pressure, catalysts can be applied in the form of metals or metal soaps in an alteration method. The catalytic impact does not only accelerate the degradation process, but also mimics the impact of metal machine parts and their contact with the lubricant in field applications.

The turbine oil oxidation stability test (TOST) is one of the most frequently applied procedures in this category and exist in four parts described in DIN EN ISO 4263.

In part 1 [66], a method to determine the alteration behavior of mineral oils is described, in particular turbine oils of different categories with antioxidative additives and corrosion inhibitors. In detail, a mixture of 300 mL oil and 60 mL water are tempered by using an oil bath or metal block bath at 95 °C, while a constant oxygen flow of 3L/h through the sample is applied. A double coil of steel and copper, made from a wire of 1.6 mm diameter for steel and 1.63 mm diameter for copper, is immersed in the oil as a catalyst. Preparatory for the immersion, 3 m of each wire are cleaned with heptane, polished with silicone carbide abrasive cloth (100 grit) and dried with a cloth. A double coil with a total length of 225 mm is then produced with a hand winch. The oxidation cell made of borosilicate glass consists of a water-cooled mushroom-type condenser and an oxygen supply tube both made of borosilicate glass as well. The alteration process is monitored by the acid number determined of aliquots sampled in defined intervals of  $50 \pm 5$  h. In order to keep a constant liquid level, the amount of the obtained sample is restocked by the same amount of fresh fluid. An acid number of 2.0 mg KOH/g indicates the end of the alteration experiment but can be replaced by a predefined test duration. Finally, the oxidation lifetime  $L$  in hours is evaluated and reported.  $L$  is calculated by following equation:

$$L = A + (B - A) [(2.0 - C)/(D - C)]$$

Whereas  $A$  is the alteration time in hours of the last sample with an acid number below

2.0 mg KOH/g and  $B$  the time in hours of the first sample with an acid number larger than 2.0 mg KOH/g.  $C$  is the acid number after  $A$  hours, and  $D$  the acid number after  $B$  hours.

DIN EN ISO 4263 part 2 [67] describes the procedure for category HFC hydraulic fluids. On the basis of part 1, a slightly higher oil content of 360 mL in the water-oil-mixture is used. The pH value of the taken oil sample aliquots is determined instead of the acid number. The amount of insolubles is evaluated by filtration with a 0.4  $\mu\text{m}$  membrane filter and subsequent gravimetric analysis. Furthermore, a visual evaluation of the catalyst coil is reported. When a pH value below 4.0 and an insoluble content of more than 4.0 mass percent is measured, the end point of the test is reached, and both values together with the appearance of the catalyst coil are reported. However, the minimum test duration is given with 200 h. Similar to part 1, the test can also be finished after a defined duration.

Part 3 [68] outlines an anhydrous method for synthetic hydraulic fluids, in detail the categories HFDR, HFDU, HEES, and HEPG. The procedure is performed with an amount of 360 mL oil and sampling amounts from 2 to 5 mL at defined intervals to determine the change of acid number. The end point of the remaining oil is determined by an increase of the acid number of 2.0 mg KOH/g or after a predefined duration. As a result, the oxidation lifetime  $L$  analogue to part 1 is calculated. The content of insolubles, the appearance of the catalyst coil and the metal content of the oil sample can be reported optionally.

Part 4 [69] describes the alteration method for industrial gear oils of the categories CKC, CKD, CKS, and CKT. Part 4 is significantly different from part 1 to 3. The borosilicate glass oxidation cell is sealed with a slotted cork stopper and equipped with an air supply tube made from borosilicate glass. The alteration is carried out at an air flow of 10 L/h, under light exclusion and without any catalyst for 312 h. The temperature is selected according to the respective oil type in a range from 95 to 150 °C. Subsequent to the alteration procedure, the change in kinematic viscosity at 100°C is determined. The content of insolubles is reported as precipitation number as well as the appearance of deposits in the oxidation cell. Moreover, the content of sediments by filtration, the additive degradation by determination of the elemental content, and the oxidation by FT-IR can be analysed, optionally.

#### 3.1.1.4 Thermo-oxidative methods under pressure and with catalysts – rotating pressure vessel oxidation test (RPVOT)

Here, the accelerating impact of oxygen pressure and the catalytic influence of metals are combined. One important method of this category is the rotating pressure vessel oxidation test (RPVOT) described in standard ASTM D 2272 [70]. This method applies an oxygen pressure

vessel to evaluate the oxidation stability of new as well as in-service turbine oils in presence of water and a copper coil as catalyst. The method is meant as an assessment tool for the estimation of oxidation stability, for quality control between oil batches, and for the remaining useful life of in-service oils. However, it is not eligible to compare the service lives of different oil formulations.

Method A of ASTM D 2272 describes a procedure where 5 mL reagent water and a copper coil are added to 50 g of oil sample in a glass container that is placed in the pressure vessel. Another 5 mL water are added between the vessel and the outside of the glass. The vessel is closed tightly, pressurized via a valve with oxygen up to 620 kPa and heated to 150 °C in an oil bath. Throughout the entire test duration, an axial rotation at 100 rpm and an angle of 30° is applied and the oxygen pressure is monitored. When a defined pressure drop of typically 175 kPa is reached, the test is finished and the minutes until this pressure drop occurred are reported.

Method B is a variation of method A with a dry block bath instead of the oil bath and an alternative rotation mechanism based on a magnetic cup driven by a motor magnet.

*Figure 8* depicts the schematic set-up of the rotation device according to method A as well as the pressure vessel with the respective components except the copper coil. In *Figure 9* the metal block bath instrument according to method B is shown.

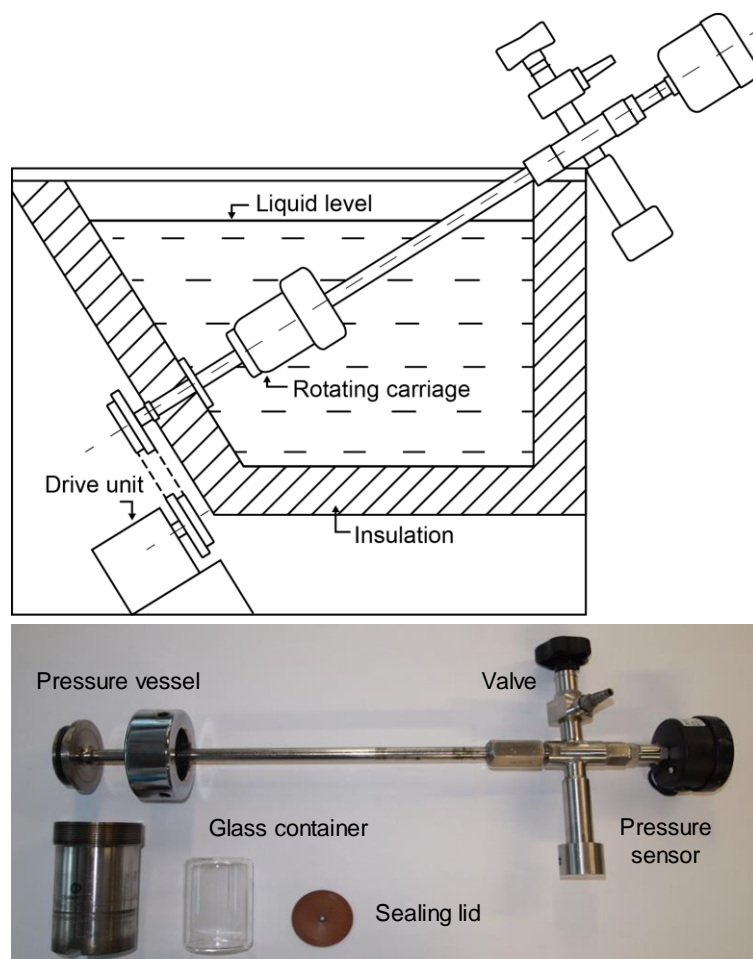


Figure 8: Schematic set-up of the RPVOT (rotating pressurized vessel oxidation test) device in the heating unit (top) and the components of the pressure vessel without the copper coil (bottom) according to method A [71].

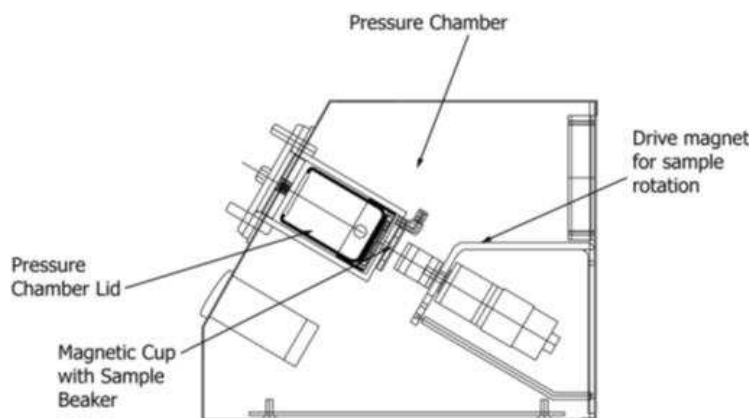


Figure 9: Schematic set-up of the metal block bath instruments according to method B [70].

The coil consists of a copper wire with a length of 3 m and a diameter of 1.63 mm. It is polished with silicone carbide abrasive clothes and cleaned with isopropyl alcohol. Subsequently, a coil with dimensions of 44 to 48 mm in diameter and 40 to 42 mm in height with a total weight of 55.6 g is formed.

### 3.1.2 Standardized thermo-oxidative methods for fuels

In the respective specifications for fuels standardized methods for the determination of oxidation stability are given. These stability assessment methods are mainly based on application of thermo-oxidative stress to fuel samples. Important oxidation stability tests for gasoline and diesel fuels with or without biocomponents are described in the following.

#### 3.1.2.1 EN ISO 7536

According to EN 228 (see chapter 2.1.1) the oxidation stability of gasolines is determined by the method EN ISO 7536 [72]. For this purpose, a pressure bomb is filled with 50 mL of the sample and closed tightly. At an initial temperature of 15 °C to 25 °C an oxygen pressure of 690 kPa is applied. The pressure bomb is heated in a water bath to a temperature of 98 °C to 102 °C, and the pressure is either monitored continuously or at pre-defined intervals, which is proposed every 15 minutes. The stability test is performed until the breakpoint is reached. This is defined as the point when a previous pressure decrease of exactly 14 kPa in 15 min is followed by a pressure drop of not less than 14 kPa in the next 15 min. The time from the start of the stability assessment until this point is gives the induction period and is used to calculate the induction period at 100 °C. This value is reported as the measure for oxidation stability of the samples. Besides motor gasolines, this standardized test can also be applied for aviation gasolines.

#### 3.1.2.2 EN ISO 12205

In EN 590 (see chapter 2.2.1) two methods to determine the oxidation stability of diesel fuels are described. EN ISO 12205 [73] is applied to estimate the storage stability of middle-distillate fuels with an initial boiling point above approximately 175 °C and a 90 % (V/V) recovery point below 370 °C without any FAME content.

Before the oxidation test filtration of 400 mL is done with a filter (47 mm diameter, nylon, 0.8 µm pore diameter) in a filter funnel and a suction flask to remove insoluble matter. In an oxidation cell consisting of a test tube, a cooler and a tube for oxygen supply 350 mL are heated up to 95 °C in a heating bath. Oxygen supply is set to 3.0 L/h and the stability test is conducted for 16 hours. Throughout the entire time the cell shall be protected from light. After cooling to room temperature, the amount of filterable insoluble matter of the entire sample is determined with the same filtration set-up used for sample preparation. The oxidation cell is rinsed with three parts (each 50 mL) of 2,2,4-trimethylpentan, all aliquots are filtered with separate filters and the weight of all the filters is determined after drying. For the determination of adhering insoluble matter the oxidation cell as is rinsed with a total amount of 75 mL trisolvent (one part

acetone, one part toluene, one part methanol each) and all aliquots are collected in a beaker. Subsequently, the trisolvent is evaporated at 135 °C and the residue gives the adhering insoluble matter. The amount of filterable insoluble matter, the amount of adhering insoluble matter and the total matter content is reported in g/m<sup>3</sup> as a result of the stability test.

### 3.1.2.3 EN 15751

The second method described in EN590 to determine the oxidation stability is EN 15751 [74], which is based on EN 14112 [75]. The latter one was elaborated to determine the oxidative stability of FAME samples. However, this method does not take mixtures of diesel blends containing FAME in account. As most of the commercially available diesel fuels in the European Union contain 7 % (V/V) FAME, EN 15751 gives an adapted version suitable for diesel blends containing at least 2 % (V/V) FAME.

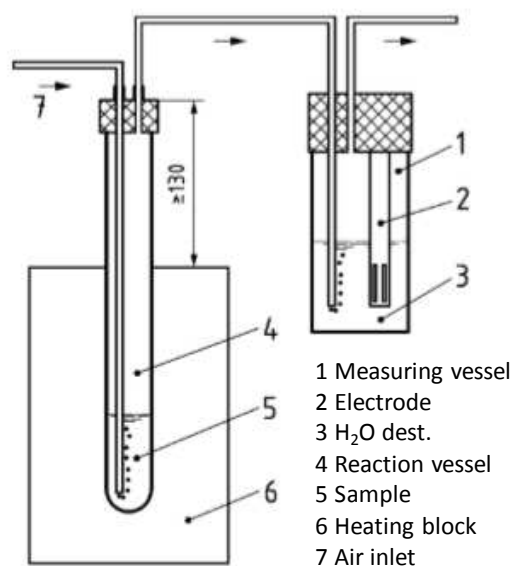


Figure 10: Schematic set-up of the main parts of the measuring cell used in EN 15751 [74].

For this purpose, the measuring cell schematically depicted in Figure 10 is filled with 7.5 g of sample. During the entire stability test the cell is heated to 110 °C and the sample is bubbled with a flow of purified air (10 L/h). The oxidation process releases volatile components, which are transferred into the measuring cell. This cell is filled with 60 mL distilled water (H<sub>2</sub>O dest.) and contains an electrode for the determination of conductivity. The change of this value is induced by volatile oxidation products such as carboxylic acid, which are absorbed by the water. It is recorded throughout the stability test to give the data for the test evaluation. As a results, the induction time, which is the period from the start of the measurement to the point of maximum increase of the oxidation products (equally with the change of conductivity) is reported in hours.

### 3.1.3 RPVOT and modifications

As presented in section 3.1.1 and 3.1.2, the range of procedures to determine the stability of lubricants and fuels is wide. However, each method comprises specific drawbacks, e.g.,

- application of open vessels and, hence, the loss of volatile alteration products,
- insufficient sampling (either due to rare sampling or too small sample aliquots) making it impossible to monitor a lifetime curve of the oil or fuel condition,
- small total sample amount resulting in limited possibilities for subsequent analysis, or
- inadequate analytical methods for a comprehensive lubricant and fuel condition monitoring at the molecular level.

Out of that reasons, the RPVOT device according to ASTM D2272 method B (see section 3.1.14) was selected as method of choice for the evaluation of lubricant and fuel stability in the presented study (see section 5). For that purpose, the standard device was thoroughly modified to meet requirements regarding safety, chemical purity and post analyses. The steel magnetic cup with the glass sample container was replaced by a tailor-made Teflon cup equipped with a gas conduit in the outer wall for appropriate gas flow from the gas inlet into the cup. Thus, the deposition of condensed volatile sample components between beaker and pressure chamber described in ASTM D2272 was avoided. Moreover, the standard sampling kit enabling regular withdrawal of sample aliquots was adapted to allow the reduction of total sample amount in the pressure vessel as well as to ensure mechanical and thermal stability of the syringe set-up. The described modifications are depicted in *Figure 11*.

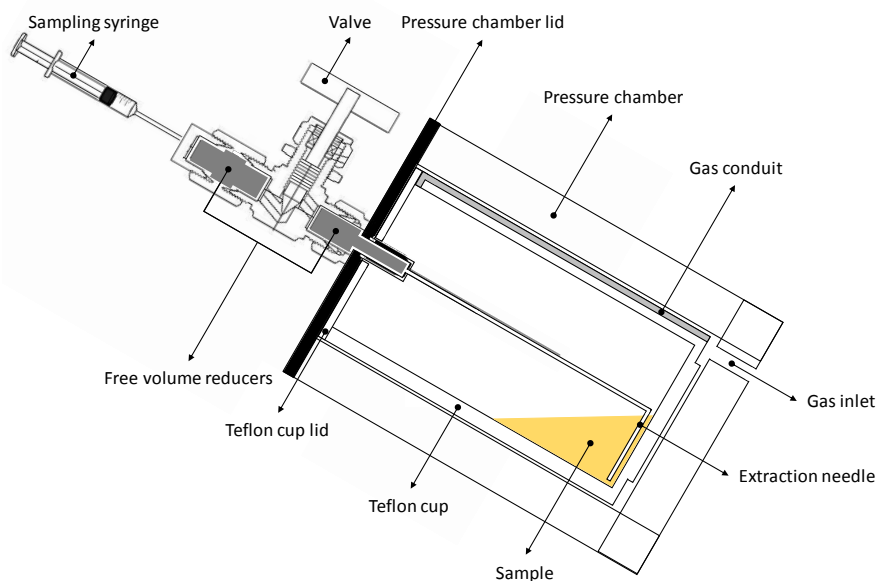


*Figure 11: Modifications of the used pressurized vessel to applied.*

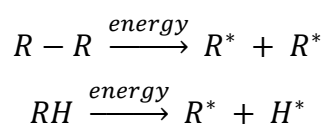
By means of this modified RPVOT, it was possible to comprehensively study and rate the stability of various lubricants and fuels, since the closed vessel apparatus allowed the investigation of solid (deposit formation), liquid (bulk), and gaseous (volatiles) sample fractions in one experiment at the same time.

## 3.2 Oxidative oil degradation mechanisms

Thermal degradation at elevated temperatures leads to cracking of hydrocarbon molecules. The impact of thermal degradation can be reduced by application of lubricating oils with high thermal stability. However, the main degradation processes in oils are oxidation reactions. The main pathway of oxidation is auto-oxidation, where the main steps are following a radical chain reaction first described by Farmer *et al.* [76] and Bolland [77] in the years 1942 and 1949, respectively. In the following, these steps of auto-oxidation are described in detail.

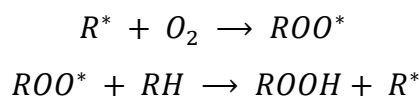
### 3.2.1 Chain initiation

Auto-oxidation is initiated by energy transfer, either from UV light, heat, or mechanical shear stress, to a hydrocarbon molecule. The process, which can be supported by catalysis of metal ions, results in a bond breakage of C-C bonds or hydrogen abstraction from C-H bonds as depicted. Both reactions result in the formation of alkyl radicals. The likeliness of a homolytic cleavage of the R-H bond is determined by the C-H bond strength and the radical stability. Thus, hydrogen atoms bound to tertiary carbon atoms and those in *alpha* position to a C-C double bond or aromatic ring are more prone to hydrogen abstraction.



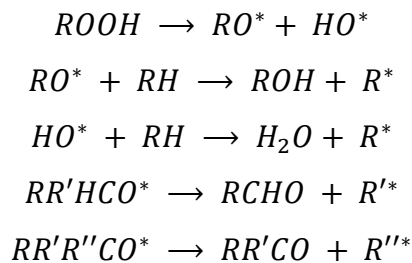
### 3.2.2 Chain propagation

At the beginning of the chain propagation, an alkyl peroxy radical  $ROO^*$  is formed by an rapid and irreversible reaction with oxygen. Thereby, the reaction rate is determined by the substituents of the radical. This explains the higher oxidation stability of linear and unbranched hydrocarbons compared to branched, aromatic and unsaturated hydrocarbons [78]. After this step, the hydrogen abstraction from a hydrocarbon molecule  $RH$  by an alkyl peroxy radical  $ROO^*$  takes place and results in an alkyl hydroperoxide  $ROOH$  and another alkyl radical  $R^*$ . Due to the higher reaction rate and the high concentration of oxygen, the concentration of alkyl peroxy radicals  $ROO^*$  is higher than that of the alkyl radicals  $R^*$ .



### 3.2.3 Chain branching

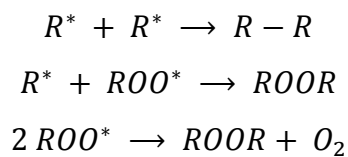
Chain branching starts with the cleavage of the alkyl hydroperoxide  $ROOH$  into an alkoxy  $RO^*$  and a hydroxy  $HO^*$  radical. This reaction only becomes significant at temperatures higher than  $150\text{ }^\circ\text{C}$  due to the high activation energy required. The reaction of the alkoxy  $RO^*$  and hydroxyl  $HO^*$  radicals with hydrocarbons generate, beside alcohols and water, more alkyl radicals  $R^*$  which in turn can react with oxygen according to the chain propagation. Alkoxy radicals formed from secondary and tertiary carbons readily provide aldehydes and ketones, respectively. Further typical oxidation products generated by these processes are carboxylic acids, ethers, esters, as well as  $H_2O$  and  $CO_2$ . Condensation of these molecules may lead to polymeric degradation products that eventually form sludge and varnish deposits in engines. In the following, some exemplarily reaction during chain branching are given:



### 3.2.4 Chain termination

The combination of radicals leads to chain termination. Either two alkyl radicals  $R^*$  combine to a hydrocarbon molecule, or one alkyl radical  $R^*$  and an alkyl peroxy radical  $ROO^*$  form a dialkyl peroxide  $ROOR$ . Furthermore, two alkyl peroxy radicals  $ROO^*$  can combine to form a peroxide  $ROOR$  under release of oxygen.

Nevertheless, dialkyl peroxides  $ROOR$  are prone to break down and regenerate alkyl peroxy radicals.



## 3.3 Conventional analytical methods for condition monitoring

According to the type and application of lubricants and fuels, different standardized analytical methods to characterize the most important properties are mandatory. Besides the characterization of fresh oils and fuels, these methods are suitable for condition monitoring of lubricants and fuels in use [79], [80]. Amongst them, one can find the determination of color, viscosity, total base number, neutralization number, acid number and water content. Furthermore, the elemental composition can be determined by optical emission spectroscopy

with inductively coupled plasma (ICP-OES) [81]. This results in qualitative and quantitative information regarding the additive components containing sulfur, phosphorus, zinc or calcium. Moreover, metal particles caused by corrosive or abrasive wear can be detected in in-service lubricants [40]. Beyond elemental information by ICP-OES, FT-IR spectroscopy also provides structural information of the base oil, additives, and contaminants and changes thereof during use. This is achieved by interpretation of the characteristic absorption bands given by the respective substances and functional groups [79], [80], [82].

In the following, the most important conventional analytical methods are discussed in detail. Moreover, their relevance as a tool for condition monitoring of lubricants and fuels and the meaning of changes in the respective values is described. These methods provided valuable preliminary data to gas chromatography coupled with mass spectrometry (MS) as stated in the attached publications (see *section 2 Publications*).

### 3.3.1 Dynamic and kinematic viscosity

One commonly applied method is the determination of the most important physic-chemical oil parameter, the viscosity. It describes the flowability of an oil sample under distinct temperature, shear, and pressure conditions. This property is responsible for the hydrodynamic film formation of lubricants. It can be differentiated between kinematic and dynamic viscosity. The latter is defined as one poise to be “*the force in dynes to move 1 cm<sup>2</sup> of surface in the fluid past a parallel 1 cm<sup>2</sup> at a distance of 1 cm within the fluid, and at a speed of 1 cm/second*” given in the more convenient unit centipoise (cP). In SI units, it can also be expressed in 1 milliPascal second (1 cP = 1 mPa × s). The kinematic viscosity is given by a fluid falling under its own weight, which results in a value reported as centistokes (cSt), or mm<sup>2</sup>/second according to SI units. Depending on the method for measurement, either by capillary viscosimeters [83] (for kinematic viscosity) or rotational viscosimeters (for dynamic viscosity) [84] the value can be obtained. Based on the dynamic viscosity, one can calculate the kinematic value via the oil density at the respective temperature of measurement, and vice versa [84].

Mechanical stress, chemical reactions and contaminations may alter the viscosity during application, either showing an increase or decrease of viscosity. The former is induced by oxidation products of the base oil, suspended and accumulated wear particles and insoluble materials. Dilution with lower viscous components such as fuel or the breakdown of viscosity modifier molecules by shear stress results in the opposite effect and, hence, a decreased viscosity. The change in viscosity can be considered as an evidence for the condition of used lubricants.

### 3.3.2 Neutralization number (NN) and acidification number (AN)

Both NN and AN describe the content of acidic components in a lubricant or fuel sample. One has to distinguish between three types of NN: 1) acidic, 2) alkaline and 3) water-soluble acid number [85].

1. The acidic acid number, also known as total acid number (TAN) [86], gives the base amount in mg potassium hydroxide (KOH) needed for the neutralization of all acidic components in 1 g of the respective sample.
2. The alkaline acid number, also known as strong base number, is the base amount in mg KOH representative for all alkaline components in 1 g of the respective sample.
3. The water-soluble acid number, also known as strong acid number, specifies the base amount in mg KOH needed for the neutralization of all water-soluble acidic components in 1 g of the respective sample.

In order to determine the acidic and alkaline NN, a mixture of toluene, isopropanol and water is used to dissolve the sample and titration is carried out with an alcoholic KOH or HCl solution. The end point is determined by a colour change of the indicator p-naphtholbenzein. For the determination of the water-soluble acid number, the sample is extracted with hot water, and a titration of the water phase with KOH and methyl orange as indicator is done.

The AN, also known as total acid number (TAN), is defined by the base amount in mg KOH per g sample necessary to potentiometrically titrate the acidic components in the respective sample [87]. Therefore, an aliquot of the sample is dissolved in a mixture of dimethylsulfoxide, isopropanol, and toluene. Titration is executed with a tetramethylammonium hydroxide solution and monitored potentiometrically by a glass electrode and a reference electrode. End point is the last inflexion point of the titration curve. Alternatively, the sample can be dissolved in a mixture of toluene, anhydrous isopropanol, and water and the titration can be done with alcoholic potassium hydroxide [86].

### 3.3.3 Total base number (TBN)

While in use, the oxidation of lubricants and fuels results in the formation of acidic compounds. These components are neutralized by the total base reserve (TBN) provided by basic additives (see section 1.3). With progressing lubricant degradation, the TBN decreases as a result of neutralization processes [88]. In contrast, NN and AN increase and the acidic components can cause serious damage (see section 1.3) Hence, there are defined thresholds for these values, and NN and AN are an important indicator in condition monitoring [89].

### 3.3.4 Water content

The content of water in petroleum products is determined by Karl-Fischer titration as described in DIN 51777 [90], [91], [92]. It can be distinguished between the volumetric and the coulometric method, for both a commercially available Karl-Fischer solution (KFS) in dried methanol as solvent is used. For the former, a sample aliquot is dissolved in this methanolic solution, and titration is done with an automated Karl-Fischer titrator until the end point is reached. As a titrant, a mixture of alcohol (commonly ethanol), a base (most commonly pyridine or imidazole) and sulfur dioxide with a known concentration of iodide is used. According to the used volume of titrant, the water content is calculated and reported in mg/kg.

For the latter, the water is evaporated from the sample via a nitrogen flow at 120°C to the titration cell. After solution in methanol at room temperature, the titration is performed coulometrically. The required iodine amount is produced electrically at the working electrode. Iodine reacts with the present water to iodide and the measuring electrode detects the amount of not-consumed (free) iodine when the end point is reached. The water content in mg/kg corresponds to the charge used for the reaction with water.

During oil degradation (see section 3.2), more precisely when chain branching occurs, water is formed amongst other oxidation products. In addition, the water content in lubricants and fuels can increase due to water uptake by contamination. Higher water amounts may provoke corrosion and can influence viscosity. Thus, monitoring of the water content provides valuable information regarding contamination and oil deterioration.

### 3.3.5 FT-IR spectroscopy

FT-IR spectroscopy is a fast and powerful tool to characterize lubricants and fuels. Besides information regarding composition and quality control [93], it is widely used for characterization of differences between fresh and used samples. It is a well-established method to determine contaminations such as water, glycol or soot, but can also be used to monitor additive depletion or oxidation [94], [95], [96], [97].

For this purpose, the interactions between radiation energy and the sample are typically detected in the range of 4000 to 650  $\text{cm}^{-1}$ . Since functional groups are known to absorb light at specific wavelengths, this information can be used for elucidation of the chemical composition despite a complex matrix [98], [99]. After measurement with a Michelson interferometer, the interferogram is transformed by FT to provide a spectrum of intensity versus wavelength, typically absorbance as a function of wavenumber. The Lambert-Beer law provides the ratio between the intensity of light before the interaction ( $I_0$  given in  $(\text{W}/\text{m}^2)$ ) and the intensity of

light after the interaction ( $I$  given in  $(\text{W}/\text{m}^2)$ ) depending on the concentration and the thickness of the sample. This results in following expressions

$$\text{for transmission: } T = \frac{I}{I_0} = 10^{-c*d*e}$$

$$\text{for absorption: } A = c * d * e$$

$$\text{and the relationship between absorption and transmission: } A = -\lg T$$

whereupon  $T$  stands for dimensionless transmission,  $c$  for concentration given in  $(\text{mol}/\text{L})$ ,  $d$  for thickness of sample layer in  $(\text{mm})$ ,  $e$  for absorption coefficient in  $(\text{m}^2/\text{mol})$ , and  $A$  for dimensionless absorption. Based on these equations, the absorption is proportional to the concentration of the respective component, which allows a quantitative analysis. General working principles are defined by DIN 51451 [100].

For condition monitoring by FT-IR three parts can be divided, first the monitoring of component degradation, second the monitoring of external contamination, and third the formation of alteration products. To obtain the desired information, spectra can be analysed directly (direct trending), or a difference spectrum between fresh and used sample can be calculated (spectral subtraction) [82]. By spectral subtraction, parameters such as oxidation, nitration, sulfation or additive depletion as well as contaminations including water, fuel and soot are calculated.

Due to oxidation processes during alteration, carbonyl-containing degradation products such as esters, aldehydes, ketones or carboxylic acids are built up (see section 3.2). This carbonyl formation is used as representative to estimate the oxidation. Therefore, the maximum peak height between  $1800$  and  $1650 \text{ cm}^{-1}$  with the baseline taken at  $1950 \text{ cm}^{-1}$  is used and spectral subtraction is applied. In order to avoid interference provoked by the ester group of lubricant components, this region can be shifted to the region between  $1710$  and  $1660 \text{ cm}^{-1}$  for ester-based synthetic oils [82].

According to their functional groups, additives show characteristic absorption in infrared spectra. For condition monitoring, these regions are observed to calculate the remaining additive concentration. For commonly used additives, procedures to determine the additive content are proposed, e.g., for ZDDP [82], [88], [101], which is monitored as a negative peak in the difference spectra. The residual additive content is calculated by the peak minimum in the range from  $1020$  to  $930 \text{ cm}^{-1}$ .

### 3.4 Gas chromatography mass spectrometry (GC-MS) for advanced condition monitoring

In 1906, Mikhail Tswett was the first to describe the principle of chromatography [102]. According to the definitions of the International Union of Pure and Applied Chemistry (IUPAC), chromatography is “a physical method of separation in which the components to be separated are distributed between two phases, one of which is stationary (stationary phase) while the other (the mobile phase) moves in a definite direction”. For gas chromatography (GC), this mobile phase is a gas [103]. Since 1952, when Martin and James [104] developed the first gas-liquid chromatography, this technique has rapidly gained in importance. Nowadays, it has become the method of choice for separation and analysis of volatile, thermally relative stable compounds of both, organic and inorganic nature, and molecular weights from 2 to over 1000 Dalton (Da) [105]. Due to the separating capabilities of GC, complex samples such as flavors, perfumes, environmental residues or petroleum products can be resolved into hundreds of components. Direct coupling with mass spectrometry (MS) enables the identification of the separated analytes. Hence, GC-MS offers the opportunity to separate, quantify and characterize complex mixtures, from hydrocarbon mixtures in oils, fatty acid methyl esters in biodiesel to distinct isotopes in samples of interest [106], [107]. In the following sections, the most relevant principles of GC including injection techniques, columns and detectors are discussed, as well as the coupling with different types of mass analyzers in single MS and MS/MS (tandem) mode.

#### 3.4.1 Capillary gas chromatography

Prior to injection to the GC system, the volatile and thermally stable sample is dissolved in a volatile organic solvent, e.g., dichloromethane or hexane, and the desired concentration is adjusted. In addition, sample treatment may include derivatization to

- improve volatility and thermal stability, e.g., for large or thermally labile molecules,
- avoid unwanted retention, e.g., for acidic hydrogen, or
- introduce isotopic tracers, e.g. deuterated groups [108], [109], [110].

Sample injection into the GC is mostly done via liquid injection (see section 3.4.1.1) or injection of a gaseous sample via headspace injection, but also solid samples can be introduced via pyrolysis techniques [106].

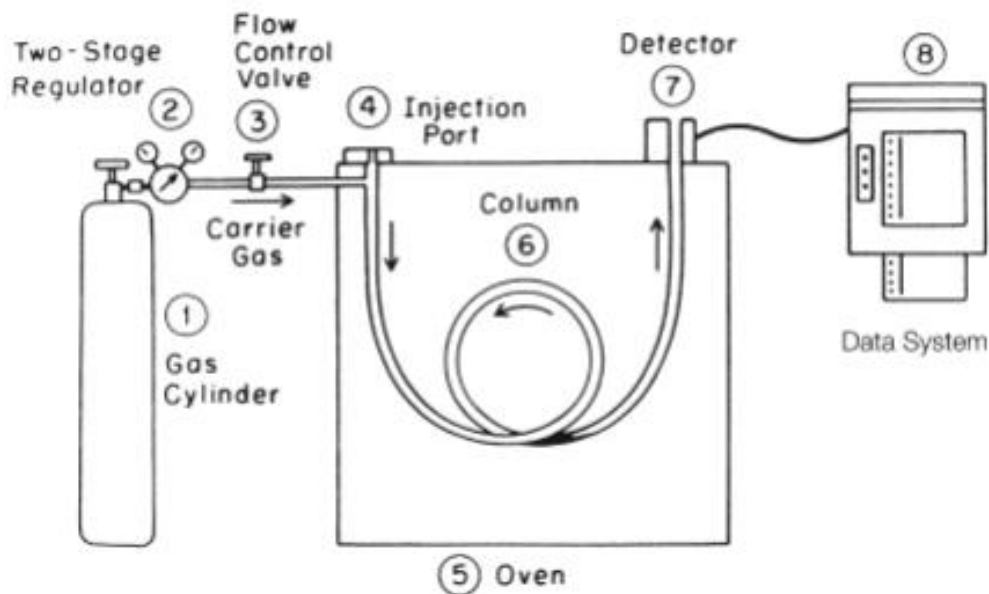


Figure 12: Schematic illustration of a GC system with the main components (figure by McNair and Miller [105]).

Figure 12 depicts a schematic GC system with its main components. Through a flow control valve (3), the carrier gas comes from the gas supply system (1) and (2) via the injection port (4) to the column (6). This highly pure and inert carrier gas, commonly He or H<sub>2</sub>, serves as mobile phase and enables the transfer of the analytes along the column (6) to the detector (7). The gas flow and, hence, the applied pressure is regulated via the flow control valve (3). In order to introduce the vaporized sample to the column, several direct injection techniques and the respective ports are available, which are discussed in section 3.4.1.1. The oven (5) is one of the centrepieces of the GC system to keep the column (6) at a certain temperature, either isothermal or with a gradient program. A broad variety of different columns, either packed or capillary columns, are commercially available and may be selected according to the analyte and the analytical task (see section 3.4.1.2). Subsequent to separation, the analyte elutes to the detector (7), which is coupled with a data processing system (8). Different commonly used detectors are discussed in section 3.4.1.3 [105].

Although several fairly complex interactions and processes occur during chromatography, and a complete prediction is not possible, assumptions based on general principles can be made a priori. The separation depends on migration rates of the analytes by interactions with the stationary phase. These rates are different for the various components according to the sum of the transport rates of the sample through the column – in dependence of the operating parameters – and the retention in the stationary phase. The sum of both generates the different

migration rates, which account for the separation of the analytes.

Retention is based on the distribution of the analyte between stationary and mobile phase, and is given as the distribution constant  $K$ . It is defined as

$$K = C_s/C_m$$

with  $C_s$  as the concentration of the analyte in the stationary phase, and  $C_m$  as the concentration in the mobile phase. The larger  $K$ , the longer the dwell time of the component and the slower the migration rate through the column. Separation is achieved when  $K$  of the sample components is different [105], [111], [112].

In general, there are three modes to run a GC separation [105], [106], [112]:

1) Gas-liquid chromatography (GLC)

A packed column with a liquid stationary phase coated onto inert support particles is used.

2) Gas-solid chromatography (GSC)

A packed column in which the solid surface of the particles, e.g., alumina or cross-linked polymer, forms the stationary phase is used.

3) Capillary column GC

Open tubular capillary columns are used. The liquid or solid stationary phase is coated onto the inner wall of the column tubing. Wall coated (WCOT), porous layer (PLOT) and surface coated open tubular columns (SCOT) can be differentiated.

In the following, the discussion will focus on the third mode, the capillary column GC as used for the described analytical research (see section 2).

### 3.4.1.1 Liquid injection techniques

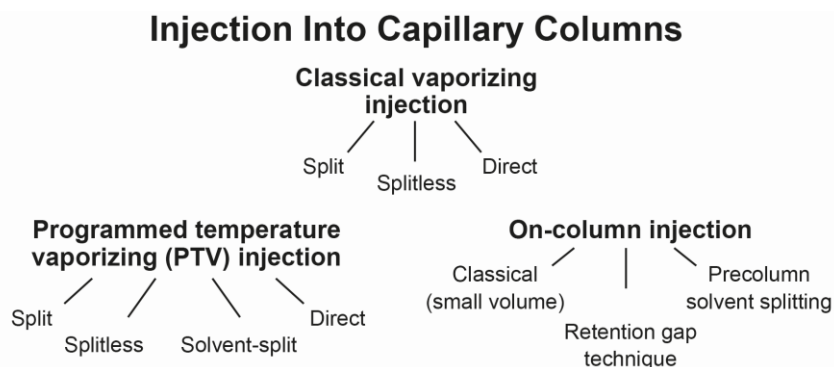


Figure 13: Different injection techniques to capillary GC columns according to Grob et al. [113].

For liquid samples, which are dissolved in a volatile organic solvent, several injection techniques can be applied according to the analytic task as well as the nature of the sample. *Figure 13* depicts the 3 main groups of liquid injection techniques. The sample can be introduced by on-column injection, by programmed temperature vaporizing (PTV) injection or by classical vaporizing injection. Each of these techniques can be accomplished in several modes, which are explained briefly in the following [105], [113].

- Classical vaporizing injection

Prior to transfer into the column, the sample is injected by a micro-syringe via a septum into a permanently hot vaporizing chamber (also called liner or inlet) and is evaporated.

From there, 3 injection modes are possible:

1. Split injection: Only a small part of the vapor reaches the column, the rest is vented. This is the method of choice for analysis of highly concentrated samples.
2. Splitless injection: Almost the entire sample vapor is introduced into the column. For this technique, a split injector is necessary. It is often applied for trace analysis of contaminated samples.
3. Direct injection: All the vapor is transferred into the column via an injector without split outlet. This method is used for trace analysis and is also suitable for packed columns.

- PTV injection

The sample is injected by a micro-syringe via a septum into a cool chamber, and subsequent heating vaporizes the samples. This is an advancement of the classic vaporizing injection. There are four different ways of PTV injection:

1. Split injection: Analogue to classical vaporizing injection as described above.
2. Splitless injection: Analogue to classical vaporizing injection as described above.
3. Direct injection: Analogue to classical vaporizing injection as described above.
4. Solvent splitting: The major part of the solvent vapor is vented, and the solute material enters the column in splitless mode. It is the method of choice for large volume injections in trace analysis.

- On-column injection

Injection of the liquid sample is done directly into the column inlet or to a temperature capillary precolumn. This technique cannot be applied with highly contaminated samples. On-column injection can be performed in three different modes:

1. Retention gap technique: An uncoated precolumn is used to avoid band broadening resulting from sample flooding in the inlet. This is an important technique for large volume injection and for on-line coupling of liquid chromatography with GC.
2. Classical small-volume injection: Similar to direct injection as for classical vaporizing injection.
3. Precolumn solvent splitting: Injection is done into a precolumn, which is connected to a vapor exit. Through this, most of the solvent vapor passes out. This method is applied for large volume injection.

Split and splitless injection are two of the most commonly introduction methods. The concentration of the analyte as well as the type of column determine, which of the two techniques is applied. Each method has its advantages and drawbacks.

Capillary GC columns only have a small capacity of sample that can be injected and tend to overload, which results in overlapping peaks and bad peak shape. Such small volumes (around 0.01  $\mu\text{L}$ , depending on the column size) can barely be dosed reproducibly [114]. Hence, a larger gas flow is applied, and only a small part of it is transferred into the column, while the major part is vented. During splitless injection, a total inlet flow with the carrier gas, mostly He, equal to the column flow is applied, and the split vent is closed. The carrier gas in the injector port is divided into three streams. One is used to purge the septum to avoid contamination, another part is directed out of the system via the split valve, and a small part of the gas flow carrying the samples is transferred into the column. Commonly applied split ratios range from 1:50 to 1:500 depending on the column diameter and stationary phase thickness [113], [115]. For optimum chromatographic results, a careful selection of the inlet liner, the injector temperature, the splitless hold time, the initial oven temperature and the solvent is necessary. Then split injection provides very satisfying chromatography results by rapid sample transfer and sharp peaks. However, most of the sample is lost by vent, and is sometimes not suitable for trace analysis [116].

For trace component applications, splitless injection may be the method of choice. It is applied for analytes at low concentrations or wide boiling range. During sample injection, the split vent is closed, and almost the entire volume of the vaporized sample is transferred into the column. Subsequently, the split vent is opened to eliminate residual solvent vapors. This prevents solvent peak tailing and masking of eluted analytes. Overloading of the capillary column may be prevented to some degree by dilution with appropriate solvents. Hereby, the difference

between the vapor pressure of the analytes and the solvent must be sufficiently large to prevent peak overlapping. Moreover, discrimination effects between analytes with highly different boiling points must be considered. Nevertheless, peaks deriving from splitless injection are typically less symmetrically shaped and show fronting [113], [114], [115].

### 3.4.1.2 Capillary columns

In the recent decades, a major part of the GC systems and applications have been running with capillary, also known as open-tubular, columns instead of the traditional packed columns. They offer a number of advantages over packed columns including tremendously improved separation with higher resolution, reduced time of analysis, smaller sample size requirements, and often, higher sensitivities [117]. According to the theory of Golay [118], [119], who was the first to present the concept of capillary columns, a very high efficiency is enabled for columns without packing, 10-100 m length, 0.1-0.7 mm internal diameter and an inner wall coated with a thin layer of stationary phase. Since 1979 [120], these capillary columns are often made of fused silica quartz with a polyimide coating on the outside to improve durability [117], [121], [122].

In general, a GC column can be characterized mainly by following parameters: the type of stationary phase used, the film thickness ( $\mu\text{m}$ ), the column inner diameter (mm) and the column length (m). Based on the inner diameter and length, a carrier gas flow from 1 up to 25 mL/min is applied.

The purpose of the stationary phase in the column is the separation of the sample in the individual components. According to the condition of their stationary phase, a common classification of capillary columns is done. *Figure 14* shows the set-up of PLOT, SCOT and WCOT columns.

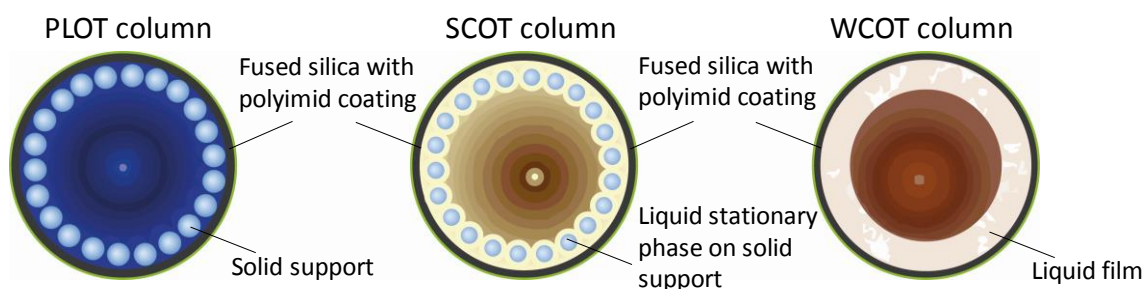


*Figure 14: Set-up of PLOT, SCOT and WCOT capillary columns [117], [123].*

PLOT columns consist of a wall made from fused silica and polyimide coating on the outer side. On the inner side, a solid stationary phase is applied. As the amount of stationary phase is relatively high, it is well suited for analytes, which are not separable with a liquid stationary phase, such as highly volatile compounds, gases like nitrogen, argon or oxygen, or short-chain hydrocarbons.

For SCOT columns, an adsorbed layer of very small solid support coated with a liquid phase is used. They can be used for highly volatile compounds which are retarded too strong on PLOT columns. Compared to the thin films of WCOT columns in its early days, SCOT columns usually have a higher sample capacity. As nowadays stable thick films are available for WCOT columns as well, SCOT columns are hardly used anymore.

WCOT have a thin liquid film on the inner side of the capillary as a stationary phase. They exhibit the largest separation efficiency and are used in trace analysis. Typically, only small sample amounts are used [105], [106], [117], [123].

The polarity of both the stationary phase and the analyte controls the retention of the analyte on the column. Accordingly, the material of the stationary phase and the composition of the analyte determine the elution order of the analytes. With regard to the latter, various characteristics such as the dipole moment and charge distribution are important characteristics. Based on the chemistry of the analyte, a selection of the suitable stationary phase is done. In general, similar polarities of the stationary phase and the sample are purposeful. If the appropriate stationary phase is selected, analytes will successively elute from the column due to their specific affinities towards the stationary phase, while the least interacting analyte will exit the column as the first one.

The stationary phase film has to be non-volatile, thermally stable and chemically inert. The most popular material is polydimethyl siloxane with 100% methyl groups for non-polar interactions. The methyl groups can be substituted by functional groups such as phenyl and cyanopropyl to adjust the polarity. Another option are polyethylene glycol based stationary phases [121], [122].

The diameter of capillary columns ranges from 50  $\mu\text{m}$  for supercritical fluid chromatography up to 750  $\mu\text{m}$  for preparative separation. Commonly used standard capillaries have a diameter between 250 and 320  $\mu\text{m}$ . The more different the concentrations of the individual analytes in a sample, the wider the inner diameter should be in order to benefit from the higher sample capacity [117], [122], [123].

Film thickness is another parameter that influences column selection. The thickness influences

the retention behaviour of the analytes as well as the column capacity. Common thicknesses range from 0.1  $\mu\text{m}$  for high-boiling analytes up to 5  $\mu\text{m}$  for gaseous samples. For samples with an elution temperature up to 300  $^{\circ}\text{C}$ , the standard film thickness of 0.25 to 0.5  $\mu\text{m}$  is used [117], [122], [123].

A longer column length means a longer separation time, which has to be considered in particular for isothermal analysis. This means a column temperature throughout the analysis is applied, which is recommended for sample with similar boiling points. Although double length means double analysis time, the separation improvement is only 40 %. Even longer columns are suitable for analysis with a temperature gradient. Gradient temperature program is recommended for analysis of samples with a wide boiling range, and the increase is either applied continuously or stepwise. While 30 m is the most popular column length, columns from 10 up to 200 m are also commercially available [105], [117], [122], [123].

Hence, successful separation of a component mixture must consider not only the stationary phase material, but column diameter and length, film thickness, injection conditions, carrier gas flow and temperature program based on the composition and concentration of the individual analytes [105].

#### 3.4.1.3 Detectors

When the carrier gas containing the analytes elutes from the column, the detector provides a response signal for the separated chemical compounds. The response signal is characteristic of a physical or chemical property of the chemical compounds being monitored by the detector. It can either be dependent on the concentration of the analyte in the carrier gas, or on the mass flow. Hence, detectors are classified in mass or concentration dependent types. The resulting chromatogram is a plot of the amplified detector signal over time to obtain information about the presence and amounts of analytes in the carrier gas [105], [106], [112], [124].

In general, there are several parameters of a detector to consider [105], [106], [112]:

- Linearity and linear range

In the linear range, the detector signal is proportional to the concentration or mass of an analyte. The detector responds with the same sensitivity in this range.

- Sensitivity

The sensitivity is defined as the change in detector signal with a change of mass or concentration of the analyte. Hence, it is the slope of the calibration plot.

- Limit of detection (LOD)

This value describes the minimum quantity or concentration of an analyte to generate a

signal, either peak height or area, which is above a certain signal to noise (S/N) ratio. Commonly, an S/N ratio of 3 is used as a threshold. This is a response with 99 % probability that the signal represents a sample peak.

- Response factor and response time

The response factor is given by the ratio of signal magnitude to sample size. The response factor is defined either via peak area or peak height. The response time describes the ability of a detector to respond to a change in the concentration of the analyte

- Noise characteristics

Noise is the signal produced by a detector in absence of any sample due to electric signal processing. Influencing parameters are for example the pump system or the temperature. The noise is also known as background and generates the baseline.

- Selectivity

This term refers to the types of analytes that can be detected. It can be distinguished between universal and selective detectors. While the former can be used for detection of a numerous types of analytes, the latter are used for either structure- or elemental-selective detection of certain components.

In the following, the most used detectors are discussed based on three important characteristics. When the concept of a detector shall be described, it must be distinguished between

- concentration or mass flow dependent detectors,
- selective or universal detectors and
- destructive and non-destructive detectors.

Various detection systems are available for GC. A selection has to be done according to the application based on the above described parameters and characteristics. The most popular ones are the thermal conductivity detector (TCD), the electron capture detector (ECD), the nitrogen-phosphorus detector (NPD) and the most commonly used one, the flame ionization detector (FID) [105], [106], [112], [124].

In the early days of GC, most of the instruments were equipped with a TCD. It is a universal, concentration dependent detector. The concept is based on the measurement of the thermal conductivity of the eluent and translation into an electric signal. For successful detection, a difference between the conductivity of the analyte and the carrier gas is crucial. As this system is non-destructive, it can be coupled with other detectors [125].

The ECD makes use of a concentration dependent principle and a high selectivity towards

compounds that capture electrons, which means electronegative substances, e.g., halogenated materials like pesticides. Consequently, it is widely used in pesticide residue analysis. Coupling with other detectors is possible, as it is a non-destructive system. A  $\beta$ -radiation source (commonly  $\text{Ni}^{63}$ ) ionizes argon in the carrier gas mixture (95 % Ar and 5 % methane), and a base current is induced between 2 electrodes. When electrophilic analytes are in the carrier gas, an electron uptake takes place and the ionization of the carrier gas decreases. This induces a reduction of the current between the electrodes, which is detected as signal. Hence, analytes are detected by causing a decrease in the level of ionization [126], [127].

The set-up of an NPD is highly similar to that of an FID. Hence, it is mass flow rate dependent and destructive. Addition of a bead of rubidium or caesium silicate, which is electrically heated in the flame, enables the selective detection of substances containing phosphorus, nitrogen and sometimes halogen. The alkali silicate bead emits excited atoms, and electrons are transferred to radicals built by the analyte. Consecutive reactions form free electrons, which are causing a detector signal at the collector. As the flame temperature is lower than in an FID, no carbon hydrogens are ionized [128], [129].

The FID is a mass flow rate dependent and destructive detector that offers the advantage of being highly sensitive. The dynamic range from LOD up to the saturation limit covers  $10^7$  units. It is selective for all compounds carrying an oxidizable carbon.

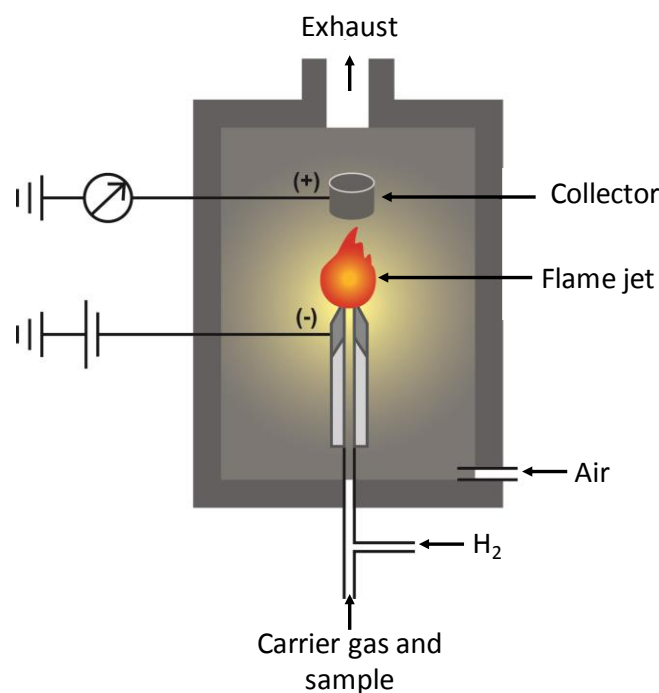


Figure 15: Schematic working principle of an FID modified according to [124].

*Figure 15* depicts the schematic detection concept of an FID. Pure H<sub>2</sub> and synthetic air are burnt at temperature around 250 °C, and during this process a chain reaction mechanism takes place. The collector is used as anode, while the flame jet is working as a cathode. During rinse of the FID with carrier gas, which is rather freely selectable, no current is detected. As soon as ionizable analytes are eluted, carbon-containing radicals are formed. Excitation of O<sub>2</sub> and reaction thereof with a radical lead to electron dissociation and consequently ionization. The free electrons are collected at the anode and can be detected as current. Hence, a detectable current is produced and reported as detector signal by ionization of the analyte in the flame.

One of the most important advantages of this detector is its robustness. It is generally self-cleaning due to the combustion process. Special care must be taken with silicon-containing compounds, as silicon oxide deposits are formed in the FID. Besides this and normal bleeding of capillary columns, regular maintenance with fluorine-containing solvents is required. In addition, sample preparation by previous separation is necessary, when sample components are forming solid combustion residues. A high stability offered by almost independence of temperature or flow fluctuation makes the FID the most widely used detector in GC systems. However, FIDs of different construction modes cannot be compared with each other, as the detector geometry is responsible for the sensitivity. The FID is most suitable for analytes with C-H or C-C bonds, but also works well for C-O, C-N and C-S bonds. However, there is a number of compounds which are hardly detectable, such as inert gases, H<sub>2</sub>O, CO<sub>2</sub>, CO, O<sub>2</sub>, N<sub>2</sub>, H<sub>2</sub>, H<sub>2</sub>S, NO<sub>2</sub>, CS<sub>2</sub>, and CCl<sub>4</sub> [124], [130], [131], [132].

Although a qualitative information can be obtained, e.g., by comparison of retention times or standard analytes, the described detectors are typically used to quantify known components in a sample mixture [112]. In order to identify unknown structures subsequent to a prior separation of complex mixtures, GC can be coupled with a mass selective detector. A GC-MS system combines the benefits of both systems enabling the separation, quantification and identification by structure analysis.

### 3.4.2 Mass spectrometry

*Figure 16* depicts the main components of a mass spectrometer. The effluent gases come from the GC and are directed through the transfer line and via the sample inlet into the ion source. This is enabled either by open split or the today most common direct GC-MS coupling. Beginning with the sample inlet, all parts until the detector are in a vacuum system. In the ion source, ionization of the eluted analytes takes place, and – depending on the ionization technique – molecular and fragment ions are produced. In the mass analyzer, these ions are

separated according to their mass-to-charge number ( $m/z$ ) ratio. The detector records the intensity of the ions, and a data processing system plots the relative intensity of the ions against their  $m/z$  value. Since most ions produced in GC-MS systems are singly charged, the  $m/z$  values correspond to their masses [133], [134], [135]. In the following, the various types of ionization, mass analyzers and tandem MS systems are discussed.

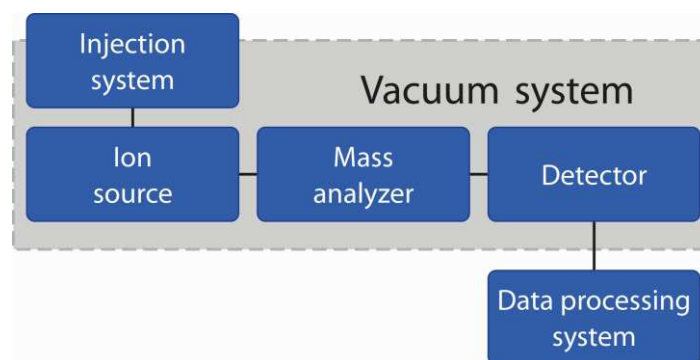


Figure 16: Main components of a mass spectrometer [135].

### 3.4.2.1 Gas phase ionization

Different fragmentation patterns occur during different ionization techniques depending on the internal energy transfer during ionization and the properties of the analyte. So-called “hard” techniques are highly energetic, which results in extensive fragmentation. Electron impact ionization (EI) is the most common hard ionization in GC-MS. In comparison, “soft” techniques such as chemical ionization (CI) produce less fragmentation and more molecular ions. Besides EI and CI, there is a third technique suitable for gas-phase ionization, the field ionization [136].

#### 3.4.2.1.1 Electron ionization

EI is the most commonly used technique for gas-phase molecules. Molecular ions are not always observable due to extensive fragmentation. *Figure 17* depicts the set-up of the EI ion source. Centerpiece is a heated filament emitting electrons, which are accelerated towards an anode. Depending on the potential difference applied between the cathode and the anode, the emitted electrons acquire a certain energy. When collision with the gaseous sample molecules takes place in the ionization chamber, ionization occurs due to the high-energy electron bombardment [136].

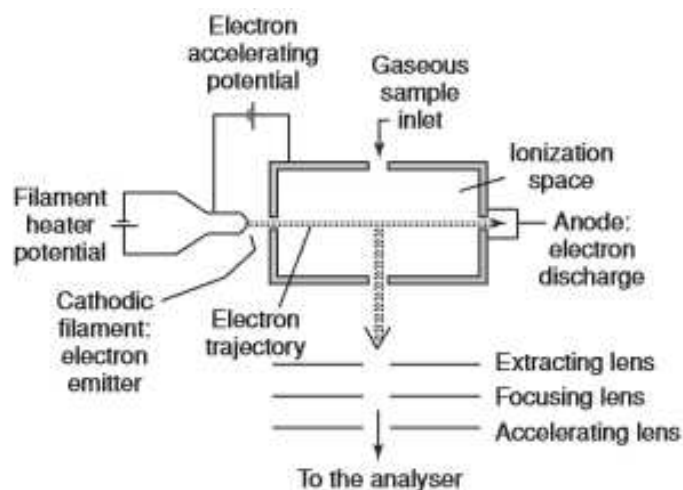


Figure 17: Set-up of an EI ion source [136].

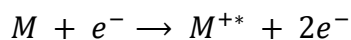
Every electron is associated to a certain wavelength  $\lambda$  which is given by

$$\lambda = \frac{h}{mv}$$

where  $m$  is the mass,  $v$  the velocity and  $h$  the Planck's constant. For the most commonly used electron energy of 70 eV, this wavelength is 1.4 angstrom ( $\text{\AA}$ ). When this  $\lambda$  is close to the bond length, it may lead to electronic excitation, and an electron can be expelled.

When 70 eV are selected, 10 to 20 eV of energy are transferred to the molecule. The lowest potential difference during which the sample ionization occurs is called first ionization potential. For most organic molecules this threshold energy leading to ionization is approximately 10 eV.

The transferred energy causes the loss of a valence electron ( $e^-$ ), which leads to the formation of a molecular ion, the radical cation  $M^{+*}$ .



Extensive fragmentation may occur due to excess energy above the first ionization potential. This fragmentation pattern provides structural information, as the extent of fragmentation depends on the molecule bond strengths and the stability of the fragment ions. This can be used to elucidate unknown analytes. EI at 70 eV generates very reproducible mass spectra and fragmentation patterns characteristic for distinct compounds. For this reason, this value is the most widely used one. Thus, entries in MS libraries are produced with 70 eV to easily identify analytes based on pattern recognition.

Besides the formation of a positive molecular ion and fragment ions, also negative ions can occasionally occur. [134], [136], [137], [138], [139], [140].

### 3.4.2.1.2 Chemical ionization

CI is known as a “soft” ionization technique, as the analyte molecules are not directly ionized, but by collision with primary ionized gas molecules. CI ion sources are highly similar to EI ion sources and are often constructed as EI/CI combination sources. The ion chamber must be gas-tight and exhibit comparatively high pressure (some  $10^2$  Pa), as the reagent gas is directly introduced to the ion chamber. CI requires a sufficiently large number of ion-molecule collisions during the dwell time in the ion source. This is achieved by significant increase of the partial pressure of the reagent gas. The reagent gas, applied in high excess, is ionized by an electron beam. Charge transfer to analyte molecules takes place without huge excess of energy. Therefore, the ionization process is rather soft, and little fragmentation occurs. Pseudo-molecular ions originate ( $[M+H]^+$ , protonated molecule or  $[M-H]^+$ ), and the determination of the molecular weight is possible [134].

In detail, the formation of ions in positive ion CI can be described by four general pathways:

- 1)  $M + X^{+*} \rightarrow M^{+*} + X$  charge exchange
- 2)  $M + [XH]^+ \rightarrow [M + H]^+ + X$  proton transfer
- 3)  $M + X^+ \rightarrow [M + X]^+$  electrophilic addition
- 4)  $M + X^+ \rightarrow [M - A]^+ + AX$  anion abstraction

The first reaction mainly occurs due to charge transfer reactions with the reagent gas. This reaction takes place when the ionization potential of the reagent gas is higher than the one of the analyte. The excess in energy, which is transferred to the analyte, is equal to the difference of both ionization potentials. Thus, when the reagent gas and the analyte exhibit equal values for this parameter, the main reaction is the formation of pseudo-molecular ions. However, as samples are often complex mixtures, other ion-molecule reactions including proton transfer, electrophilic addition and anion abstraction (as given in reaction equation 2 to 4) happen simultaneously. Besides formation of positive pseudo-molecular ions, the uptake of an electron may generate negative ions. This reaction occurs when substances exhibit a high electron affinity, such as chlorinated organic substances or polycyclic aromatic hydrocarbons (PAHs). This tendency is exploited in negative chemical ionization (NCI) [136], [141], [142].

The selection of the reagent gas is based on the analytic task and the analyte. There are several commercially available gases in highest purities available. Among the most common gases are methane, iso-butane and ammonia. According to the selected gas, the fragmentation yield can be controlled. Protonation of the analytes takes place, when their proton affinity is higher than that of the reagent gas. As already mentioned, the lower this difference between the two

components is, the lower the fragmentation and the higher the yield of pseudo-molecular ions. In general, a lower degree of fragmentation is observed with ammonia and iso-butane than with methane.

The second fact to be considered is the selective ionization of certain compounds by specific reagent gases. Again, this behavior is influenced by the proton affinity and the ionization potential of both. To give an example, ionization with ammonia as reagent gas only works for highly basic compounds. This may be utilized for the analysis of highly complex mixtures containing basic analytes such as alkylamines of interest [143].

#### 3.4.2.2 Mass spectrometric analyzers

In the mass analyzer, the gas-phase ions produced in the ion source are separated according to their  $m/z$  ratio prior to detection. As in some ionization processes also multiply charged ions may occur, the apparent  $m/z$  values are fractional parts of the actual masses. Several types of mass analyzers are available. Either static, dynamic electric or magnetic fields or combinations thereof are used, and all of them have their advantages and limitations.

Based on the various principles of ion separation, analyzers can be classified into [136]

- sector field analyzers based on deflection of the ion beam in an electric or magnetic field,
- mass filters (quadrupole, ion trap and ion cyclotron resonance mass analyzer) by filtering ions with different  $m/z$  values in alternating electric fields and
- time-of-flight analyzers in which the separation is performed according to different times of flight of the ions in a field-free space.

A further classification can be made according to various other properties such as scanning analyzer versus transmission of all ions, continuous versus pulsed analysis, ion beam versus ion trapping types, or low versus high kinetic energies [134].

Mass analyzers are characterized by several characteristic parameters on the basis of which a selection is made for the respective application [136], [144]:

1.  $m/z$  range

This range defines the lowest and highest  $m/z$  a mass analyzer is able to measure. The limits are determined by the applied separation principle.

2. Ion transmission

This term describes the number of ions which reach the detector referred to the number of ions produced in the ion source. The higher the transmission, the better is the sensitivity of a mass analyzer.

3. Resolution

The resolution denotes the ability of a mass analyzer to differentiate between two ions with different masses. In order to distinguish ions with minor mass differences, a sufficient resolution is necessary.

4. Accuracy

This term is a measure for proximity of the experimentally determined mass to the calculated exact mass.

5. Scan time

This value defines the velocity of the measurement. It is determined by the time of one scan, including measuring time and reset. The scan time is particularly important for time-dependent measurements such as in GC-MS systems.

In the following the most commonly used mass analyzer are described. The quadrupole mass analyzer applied for all measurements in section 2 part B is described in detail in the following subsection (see 3.4.2.2.1).

In a time-of-flight (TOF) analyzer, ions of different  $m/z$  are dispersed according to their velocities in a vacuum flight tube and, hence, the needed time during their flight along a field-free drift path of known length. Under the assumption that all ions start their flight at the same time, the lighter ones arrive earlier at the detector than the ones with a higher mass. To enable the same starting time, the combination with a pulsed ionization method – or less common by pulsing ion packages out of a continuous beam – is necessary. Additionally, this analyzer is appropriate for separation of high molecular weight analytes. This makes a TOF analyzer the ideal for coupling with matrix-assisted laser desorption/ionization (MALDI), a pulsed “soft” ionization technique without extensive fragmentation. One benefit of this type of analyzer is the high ion transmission efficiency which leads to a high sensitivity. The mass spectra recorded are a sum of several hundred individual mass spectra enabled by high analysis speed. Mass resolution in TOF analyzer is proportional to the flight time. Therefore, an increase by use of

longer flight tubes is possible. An additional improvement of resolution can be achieved by application of delayed ion extraction or a reflectron (RTOF). The former is an introduced time delay before the ion extraction from the source, which is used to reduce the kinetic energy dispersion of ions of the same  $m/z$  ratio. The latter are reflectron lenses that act as an ion mirror deflecting the ions and sending them back through the flight tube in the opposite direction. Thus, it improves resolution by flight path increase [134], [136].

In a sector field analyzer, accelerated ions are distracted by a magnetic or/and an electric field. Centerpiece of this analyzer is a curved metal tube with an angular between 60 and 180 degrees operated in high vacuum. When the ions exit the source, they are accelerated into the tube and a magnetic/electric field is applied vertically to their directional movement. The ions are directed on a circular orbit. The radius of this orbit depends on the  $m/z$  ratio of the ions. A dispersion of the ion beam based on  $m/z$  and kinetic energy is achieved.

For double-focusing sector instruments, a magnetic field and an electric field are arranged in a row. These instruments are large devices capable of very high resolution and accurate mass determination, and suitable for a wide variety of desorption/ionization methods [134], [136].

Ion trap (IT) mass analyzers filter ions according to their  $m/z$  ratio by a combination of oscillating and static electric field. Two different types can be classified, the 3D or Paul's ion trap and the 2D or linear ion trap (LIT). The latter one is today the most common and achieves a higher capacity of trapped ions, resulting in a higher trapping efficiency. LITs can guide, accumulate, store, and finally release ions. As the ions are focused along a central line instead of a point, less susceptibility to space charge effects is observed. Thus, an increase of sensitivity and dynamic range is enabled. The LIT is based on a four-rod quadrupole, often further divided in three segments. In the radial dimension, the ions are confined by the radio frequency (RF) quadrupolar field. In the axial dimension, confinement is realized by the electric field applied at the end of the trap. Ions trapped in the LIT collide with an inert gas and can be ejected in two ways. Either a radial ejection through two slots of opposite rods take place, or an axial ejection along the axis of the trap is done. One benefit of the LIT is the ability to perform soft fragmentation in the trap. Hence, it cannot only be used as a stand-alone mass analyzer, but as well for fragmentation in the time domain over several generations [134], [136], [145].

The Orbitrap mass analyzer is basically an ion trap without any RF or magnetic field for confinement. It consists of a barrel-shaped outer electrode and a coaxially placed central spindle-shaped electrode. The outer electrode is equipped with an off-axis entrance slit which serves for ion injection. Moving ions are trapped by application of an electrostatic field. An

electrostatic attraction occurring in the direction of the spindle-like central electrode is compensated by a centrifugal force, induced by the initially tangential velocity of ions. If a detection of positive ions is desired, a negative electrostatic voltage up to several kilovolts is applied on the central electrode. Meanwhile, the outer electrode is held at constant potential. An oscillation on the stable trajectories of the injected ions along the central axial electrode is induced. Their axial Eigen frequency during this harmonic oscillation is directly linked to their  $m/z$  ratio, which is computed via fast Fourier transformation into accurate  $m/z$  values. This frequency is determined by image current detection located at the outer electrode. When the ion cloud attracts (positive ions) or repels (negative ions) the electrons of the detection electrode, a minuscule image current result. This can be amplified and transformed in a voltage signal. Based on the highly coherent ion motion, a very sensitive detection as well as high mass resolution (max. over 1 000 000 full width at half maximum for newest devices) and mass accuracy ( $<1$  ppm with internal calibration) are achieved by Orbitrap. Both latter values are crucial for determination of the elemental composition. The Orbitrap is often coupled with an electrospray ionization source and can be run as a LIT-Orbitrap hybrid instrument to combine the LIT tandem capability with the high resolution and mass accuracy of the Orbitrap [134], [136], [146], [147].

#### 3.4.2.2.1 Quadrupole mass analyzer

In 1953, Paul and Steinwedel [148] described a new “mass spectrometer without magnetic field”. Today, this mass analyzer is known as quadrupole mass spectrometer, also simply called “quadrupole”, and its principle is related to the described LIT: the stability of the trajectories in ramped and oscillating electric fields is used to separate ions according to their  $m/z$  ratio.

This mass analyzer itself is built up of four electrode rods consisting of metal or metallized material in a square configuration (see *Figure 18 left*). A perfectly parallel alignment of the four rods is crucial for proper operation. In order to induce an electric field, the opposite pairs of rods are coupled together and RF and direct current (DC) potentials are applied between the pairs (see *Figure 18 right*). Ions that origin from the source are directed along the  $z$ -axis influenced by the electric field. This is made by a quadrupolar alternating field, superposed on a constant field which results from the potential applied on the rods. This total potential  $\Phi_0$  is given as:

$$\phi_0 = +(U - V_{RF}\cos\omega t) \text{ and } -\phi_0 = -(U - V_{RF}\cos\omega t)$$

Here,  $\omega$  denotes the angular frequency,  $U$  is the direct current voltage (range from 500 to 2000 V) and  $V_{RF}$  is the “zero-to-peak” amplitude of the RF voltage (range from -3000 to 3000 V).

During their travel, the ions are describing complex trajectories, either stable or unstable depending on  $m/z$  ratio. Only those that are following a stable oscillating pathway can pass the analyzer, while the latter are lost. The RF and DC voltages applied determine, which ions with their respective  $m/z$  values are transmitted. Ions above or below this value set are discarded. The path stability of an ion of a certain  $m/z$  value is based on the amplitude of the RF drive potential ( $V_{RF}$ ), the magnitude of its frequency  $\omega$  and the ratio of the amplitude of the DC ( $U$ ) to RF potential. A wide range of  $m/z$  values is able to transmit for  $U = 0$  [V]. With increasing value of the ratio  $U/V_{RF}$ , the resolution increases and, hence, the stability criterion allows only one single  $m/z$  value for a stable trajectory. Thus, all ions within the stability range are resonant and reach the collector and detector. In order to obtain a mass spectrum over the selected  $m/z$  range, the RF and DC voltages are scanned during the measurement. [134], [136], [149].

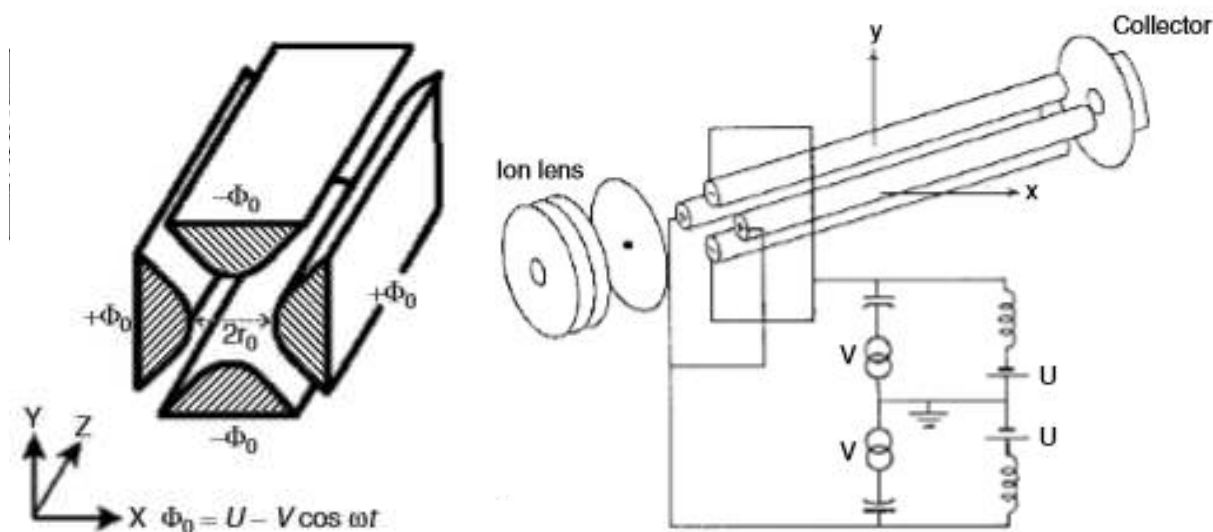


Figure 18: Left: Schematic of a quadrupole mass analyzer with four electrode rods in front view. The opposite two of them are paired and each pair is subjected to alternating potentials. The interelectrode spacing is given with  $2r_0$ . The  $x$ ,  $y$  and  $z$ -axis as well as the potential are denoted [136]. Right: Schematic of a quadrupole mass analyzer including the elements ion lens and collector in side view [149].

As already mentioned, a stable trajectory is required for a successful transmission of the ions through the mass analyzer. As depicted in Figure 18 left, the interelectrode spacing is  $2r_0$ . As long as the  $x$  and  $y$  coordinates of the trajectory of an ion are below  $r_0$ , which is half of the

interelectrode spacing, no collision with the quadrupole rods will occur. There are two parameters, namely  $a$  and  $q$ , which define the stability areas over a range of varying DC value  $U$  and RF value  $V_{RF}$ :

$$U = a \frac{m \omega^2 r_0^2}{z 8e}$$

$$V_{RF} = q \frac{m \omega^2 r_0^2}{z 4e}$$

where  $r_0$  is the radius of an imaginary cylinder within the center of the rods. The electron charge is defined by the term  $e$ , and  $m/z$  gives the mass-to-charge ratio. As a given quadrupole instrument operates at a constant  $\omega$ , the last term of both equations stays constant providing the stability parameters  $a_u$  and  $q_u$ .

When  $m/z$  is changed, a proportional multiplication with the stability parameters  $a_u$  and  $q_u$  occurs. For a graphical representation, the Mathieu stability diagram can be used to depict the stability of ions with different  $m/z$  values [150]. This diagram (see *Figure 19*) provides the stability areas  $A$  as a function of  $U$  and  $V_{RF}$  for single charged ions with different masses, where  $m_1 < m_2 < m_3$ . When  $U$  is changed linearly as a function of  $V_{RF}$ , a straight operating line is obtained. The triangular area  $A$  is the area between the operating line and the long side of the triangle. All ions within this area have a stable ion trajectory. Ions of different  $m/z$  are successively scanned along this line by increasing the magnitude of the RF and DC voltages, while keeping the  $U/V_{RF}$  ratio constant. The higher the slope, the higher is the achievable mass resolution, as long as it goes through the stability areas [134], [136], [149].

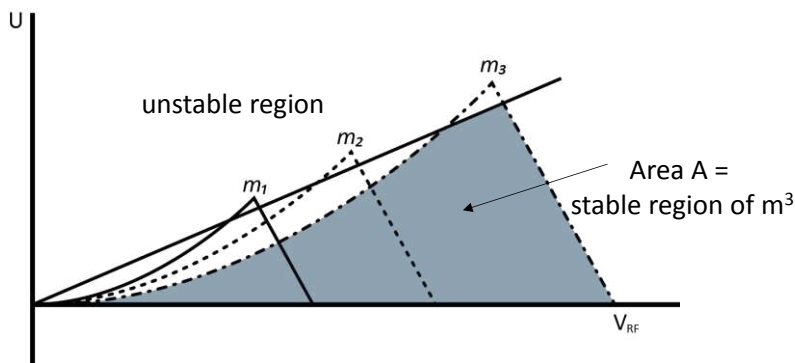


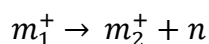
*Figure 19: Stability areas  $A$  as a function of  $U$  and  $V_{RF}$  for ions with different masses ( $m_1 < m_2 < m_3$ ) but same charge. Ions within this area  $A$  and the operating line have stable ion trajectories. Modified according to [136].*

An elemental analysis with a quadrupole is not possible, as they typically work at unit resolution over the whole mass range. Unit resolution means the ability to separate two peaks which are one mass unit ( $m/z$ ) apart. Therefore, these devices are classified as low-resolution instruments with a mass accuracy of several hundred ppm. As ion masses determined by a quadrupole do not depend on the kinetic energy of the ions at the time of leaving the source, they are real mass-to-charge ratio analyzer. For these two requirements must be fulfilled: first, the time of the ions to cross the analyzer has to be short compared to the time necessary for switching from a mass to another. Second, the ions have to remain at least for a few oscillations. This requires that the ions leaving the source are accelerated to kinetic energies from one up to a few hundred eV to enable quadrupole scans to be obtained over the desired  $m/z$  range.

Quadrupoles are well suitable for coupling with capillary GC as high scan speeds of 1000 Da/s or even higher are possible. Typically, around 10 full scan mass spectra can be obtained within one GC peak. The additional robustness and the relatively low costs make this mass analyzer a popular instrument [134], [136], [149].

### 3.4.2.3 Tandem mass spectrometric systems

Tandem mass spectrometry (MS/MS) is a term for methods that comprise at least two stages of mass analysis. In a first step (MS1), ions from the source are separated by  $m/z$  ratio. Subsequently, ions with a particular  $m/z$  value, so-called precursor ions ( $m_1^+$ ), are selected. By different modes of fragmentation, fragment ions (product ions,  $m_2^+$ ) and neutral fragments ( $n$ ) are produced based on the precursor ions



The definition of a precursor ion, equivalent with a parent ion, according to IUPAC is, “*an electrically charged molecular moiety which may dissociate to form fragments, one or more of which may be electrically charged, and one or more neutral species. A parent ion may be a molecular ion or an electrically charged fragment of a molecular ion*” [103].

Product ions, equivalent with daughter ions, are defined as “*an electrically charged product of reaction of a particular parent ion. In general, such ions have a direct relationship to a particular precursor ion and indeed may relate to a unique state of the precursor ion. The reaction need not necessarily involve fragmentation. It could, for example, involve a change in the number of charges carried. Thus, all fragment ions are daughter ions, but not all daughter ions are necessarily fragment ions*” [103].

The resulting charged fragments are then separated and detected in a second MS step (MS2). For some devices, even more than 2 MS steps (MS $_n$ ,  $n$  refers to the number of generations of

ions being analyzed) are possible [134], [136].

In general, two instrumental concepts for MS/MS may be distinguished:

- Tandem-in-space MS
- Tandem-in-time MS

For the former concept, two sequential mass-analyzing steps in two mass analyzers are performed. In the first instrument section, the ions are selected according to their  $m/z$  value, an intermediate region performs fragmentation and the product ions are analyzed after transmission to a second instrument section. Hence, the product ion spectra are recorded in a separately located device. Popular devices are TOF/RTOF, QqRTOF and triplequadrupole (QqQ) instruments. Quadrupoles acting as a collision cell are describes with the term  $q$  instead of  $Q$ .

The latter concept is done with a single mass analyzer, e.g., a LIT or a Fourier-transform ion cyclotron resonance (FT-ICR) mass spectrometer. All steps from ion selection, fragmentation, to product ion analysis are executed in the same place, but sequentially in time [134], [136].

#### 3.4.2.3.1 Tandem-in-space scan modes

The selection of scan modes in tandem-in-space MS is strongly related to the used mass analyzer. In order to obtain the optimum results, the discussion of ion fragmentation cannot be separated from the instrumental set-up and the modes of operation [134], [136]. As QqQ are widely used devices in MS/MS applications, and all measurements in this PhD thesis were carried out with this type of instrumentation (see section 2), the different scan modes will be explained based on a QqQ.

In the early QqQ instruments, three quadrupoles were connected in series.  $Q_1$  served as  $MS_1$ ,  $q_2$  was an intermediate RF-only instrument, operating as a “field-free region” for ion guiding of metastable dissociations or collision cell for collision induced dissociation (CID).  $Q_3$  was equal to  $Q_1$  and served as a mass analyzer of the fragment ions exiting from  $q_2$  [151], [152]. In recent instrumentation, the collision cell is no RF-only device anymore, but a hexapole(h) or octapole (o), which improves the ion-guiding capabilities. Hence, nowadays most QqQ are in fact QhQ or QoQ instruments. The schematic depiction of a QqQ is depicted in *Figure 20*. Ion transition trough the QqQ is enabled by Einzel lenses in the separating gaps of the quadrupole [134], [136], [153].

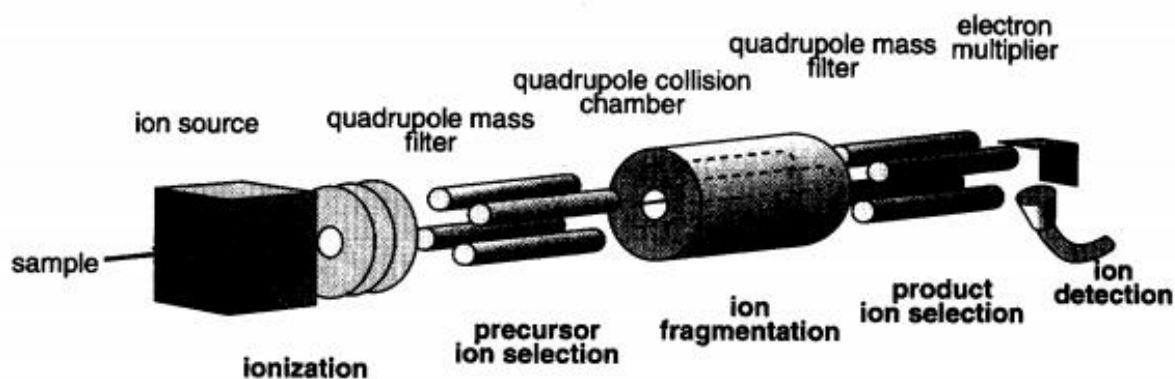


Figure 20: Schema of the components of a QqQ [153].

In order to perform a MS/MS analysis, the mass-selected ions coming from the Q1 are accelerated into the q2 used as ion guide or collision cell. Collision is enabled by a potential offset in a common range of 5 to 50 V. In q2, a collision gas, either N<sub>2</sub> or Ar, is applied at a pressure of 0.1 to 0.3 Pa. Accordingly, CID takes place at low energy. The mentioned parameters may be optimized for the respective analytes and applications to improve CID efficiency and resolution. As Q1 and Q3 operate independently from each other, the resulting fragment ions are scanned in Q3 according to the desired scan mode [134], [136].

In general, three main scan modes can be distinguished, which can be applied for all

$$m_1^+ \rightarrow m_2^+ + n:$$

- Product ion scan
- Precursor ion scan
- Neutral loss scan

For the product ion scan mode, Q1 operates at a constant  $m/z$  for selection of an ion  $m_1^+$  with defined  $m/z$  ratio. In q2, fragmentation by metastable dissociations or CID is performed, while the reaction products are scanned in Q3 with a range up to the  $m/z$  value of  $m_1^+$ .

In the precursor ion scan mode,  $m_2^+$  is defined and Q1 operates in scanning mode in a  $m/z$  range from  $m_2^+$  and higher to cover potential precursors. After fragmentation in q2, fragments are analyzed in Q3 at the selected  $m/z$  value of  $m_2^+$ .

For a neutral loss scan,  $n$  is defined. Either Q1 or both Q1 and Q3 are working in scanning mode. Q1 covers a desired  $m/z$  range, and fragmentation happens in q2. In Q3, a scan range shifted by a defined  $\Delta m$  is applied. To give an example, if the loss of a water molecule shall be detected, a neutral loss of 18 mass units will occur. Hence, Q3 is set to a scan range lowered by  $\Delta m$  from  $m/z$  of Q1.

The operation modes of Q1, q2 and Q3 for the different scan modes are given in *Figure 21* [134], [136], [153].

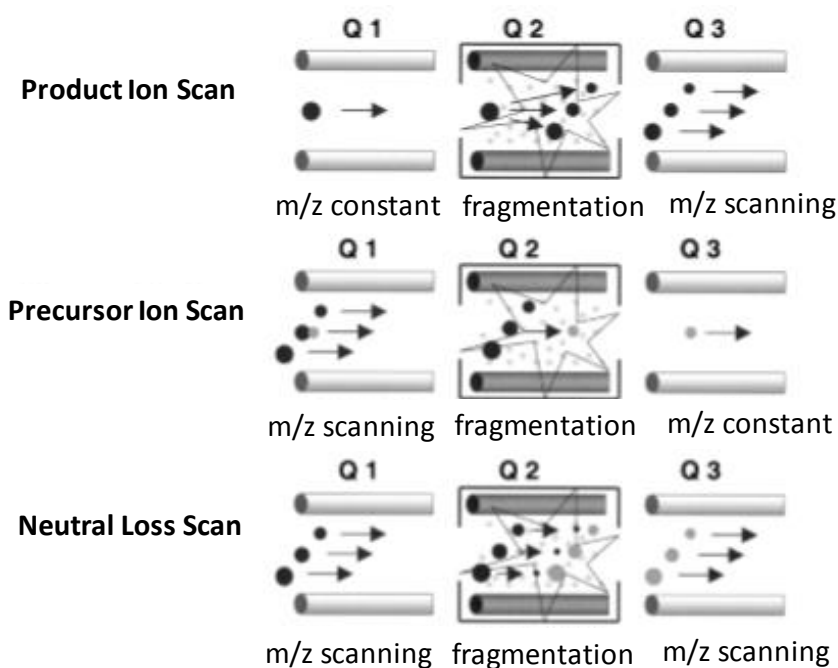


*Figure 21: Scan modes of qQq mass spectrometers, modified according to [134].*

In addition to these 3 scan modes, a method called selected reaction monitoring (SRM) can be used in MS/MS. For this purpose, an ion of a particular  $m/z$  value is selected in Q1, and after fragmentation in q2 one specific product ion of this precursor ion is selected in Q3. Thus, it reveals the fragmentation reaction by acquiring a spectrum selectively. For a successful SRM, the ionic fragmentation pathways have to be figured out. If more than one ionic fragmentation is performed, a so-called multiple reaction monitoring (MRM) is done [134].

#### 3.4.2.3.2 Modes of ion fragmentation

For MS/MS the fragmentation in the collision cell q2 is a crucial step. For this purpose, it is required that ions either possess or acquire sufficient internal energy. This step can be obtained in different ways. In QqQ-MS/MS, there are three commonly used methods:

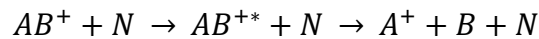
- Metastable Ion Dissociation (MID)
- Collision-Induced Dissociation (CID)
- Surface-Induced Dissociation (SID)

In the first case, ions react sufficiently fast for a dissociation during the transition through the analyzer. As this process takes  $10^{-6}$  to  $10^{-5}$  seconds, rate constants of unimolecular dissociation

in the order of  $10^{-6}$  to  $10^{-5}$  are required. The metastable ions possess internal energies close to the threshold of ion dissociation. Typically, such ions can be provided by EI and CI. The metastable ion dissociations occurring in the field-free region are detected when occurring between MS1 and MS2. However, ions with lower lifetime of metastable decomposition, which dissociate before MS1 are lost [134], [154].

CID is the most prominent collision technique and provides fragmentation of gaseous ions with neutral gas atoms or molecules which would otherwise be stable. Particularly, it is used for structure elucidation of ions with low internal energy or those obtained by soft ionization methods. The technique is performed in a collision cell where a collision gas (He, N<sub>2</sub> or Ar) is applied at a pressure that is clearly above the surrounding high vacuum to enable collision with gas molecules. For this purpose, a needle valve is used to introduce the gas into a tight part with a narrow entrance and exit slit to introduce and channel the ion beam. Effusing gas is removed by a vacuum pump, and a region with a pressure of  $10^{-4}$  Pa and a diffusion-controlled gas flow is created [134].

When the ion beam enters the collision cell and the ions interact with gas molecules, a two-step process takes place. These steps are given as:



The time range of the collision of ion  $AB^+$  carrying several keV kinetic energy with a neutral  $N$  is about  $10^{-15}$ s. As a first step, the reaction yields the activated species  $AB^{+*}$ . Subsequently, the occurring internal energy is randomized, and  $AB^{+*}$  dissociates. This reaction follows any pathway available at this level of internal energy  $E_{AB^{+*}}$ . This energy is given by the internal energy prior to collision  $E_{AB^+}$  and the energy  $Q$  transferred during collision:

$$E_{AB^{+*}} = E_{AB^+} + Q$$

In general, the internal energy before the collision is of minor relevance for the fragmentation behavior of the activated ion. The center-of-mass collision energy  $E_{CM}$  defines the upper limit of  $Q$  and is given as:

$$E_{CM} = E_{LAB} \frac{m_N}{m_N + m_{AB}}$$

In this equation,  $m_N$  is the mass of the neutral,  $m_{AB}$  the mass of the ion of interest and  $E_{LAB}$  the ion kinetic energy in the laboratory frame of reference. This term represents the kinetic energy that is acquired by the ion while passing through an acceleration stage defining its kinetic energy. To give an example,  $E_{LAB}$  of a singly charged ion after passing through a potential of 10 V is 10 eV [134], [155].

Besides single collisions, multiple collision events also may occur during CID: as the mass-

selected ions in the ion beam undergo collisions, this main beam is attenuated increasingly. With this attenuation, the probability for multiple collisions gets higher, and the fragments resulting from high activation energy processes increase. Assuming a high-energy collision experiment and a main beam with a transmission of 90 %, 95 % of the ions experience single collisions, and 5 % remain for double collisions. When the transmission decreases to 50 %, only 68 % of the ions remain for single collision, 23 % for double collision, and the remaining ions for three or four collisions [135], [156].

For SID, a collision with solid surfaces is performed instead of gaseous atoms as in CID. For this technique, collision of ions of some ten eV kinetic energy with a solid surface at an angle of 45° is induced. A linear Q mass analyzer is applied at right angle to the ion beam to analyze the arising fragments. The degree of fragmentation is adjusted by the SID conditions and energy of the incident ions. As there is no background from collision gas, a higher resolution compared to CID may be obtained. However, extensive instrumental modifications are necessary to perform SID, which is the main drawback of this technique.

Depending on the instrumentation, there are several other techniques for fragmentation available. Photodissociation is often applied in FT-ICR MS/MS. Electron capture and transfer methods are popular fragmentation methods in LIT and QIT instruments.

## **PART B: Aims, resulting publications and conclusion**

### **1 Aims of the thesis**

Lubricants and fuels are exposed to numerous stress factors that cause their degradation. The exposure to elevated temperatures, oxidation reactions in presence of air, and contaminations from environment or machine parts are just a few of them. Consequently, the composition, condition as well as the performance of lubricants and fuels undergo alterations during storage and in use. While some of these changes are visible by the naked eye such as color changes or deposits, others are only noticed after performance losses or even machine failure, e.g., due to corrosion caused by acids formed in the lubricant. In order to reveal the reasons, a careful assessment of the degradation processes and analysis of the underlying mechanisms are necessary. For this purpose, artificial alteration is the method of choice to simulate the ongoing reactions under well-defined, reproducible and variable conditions. Subsequently, a detailed analysis beyond conventional analysis using separation techniques coupled with MS enables the identification of degradation products in a complex sample composition.

This work aimed at a comprehensive study on the elucidation of the main pathways and involved molecules of oxidative degradation and the formation of oxidative degradation products over time. With increasing importance of eco-friendly and bio-based components, the number of oxygen-containing lubricant and fuel molecules such as esters is rising. However, an unambiguous identification of the oxidation reactions for these molecules is challenging as oxygen atoms derive from both the initial molecule and oxidation. In order to clearly identify the origin of oxygen atoms and, hence, clearly describe oxidation reaction pathways, a combined approach using artificial alteration, stable isotopic tracers and GC-EI-MS was applied.

## 2 Publications

### 2.1 Publication 1 - Oxidation products of ester-based oils with and without antioxidants identified by stable isotope labelling and mass spectrometry

Applied Sciences, vol. 7, no. 396, 2017

The publication is reprinted on the following page

Article

# Oxidation Products of Ester-Based Oils with and without Antioxidants Identified by Stable Isotope Labelling and Mass Spectrometry

Marcella Frauscher <sup>1,2</sup>, Charlotte Besser <sup>1</sup>, Günter Allmaier <sup>2</sup> and Nicole Dörr <sup>1,\*</sup>

<sup>1</sup> AC2T Research GmbH, Viktor-Kaplan-Straße 2C, 2700 Wiener Neustadt, Austria; marcella.frauscher@ac2t.at (M.F.); charlotte.besser@ac2t.at (C.B.)

<sup>2</sup> Institute of Chemical Technologies and Analytics, Vienna University of Technology, Getreidemarkt 9, 1060 Vienna, Austria; guenter.allmaier@tuwien.ac.at

\* Correspondence: nicole.doerr@ac2t.at; Tel.: +43-2622-8160-0150

Academic Editor: Jun Kubota

Received: 2 March 2017; Accepted: 10 April 2017; Published: 16 April 2017

**Abstract:** As lubricants with a high thermo-oxidative stability such as synthetic esters are gaining more importance in the lubricant market, a detailed knowledge regarding their oxidative degradation behaviour is of high importance. In order to reveal their degradation products and processes, a novel approach combining artificial alteration, isotope labelling based on oxidation with <sup>16</sup>O<sub>2</sub> and <sup>18</sup>O<sub>2</sub>, and mass spectrometry (MS), was applied to a bis(2-ethylhexyl) adipate base oil. The degradation products such as 2-ethylhexanol and its monoesters with short-chain fatty acids pinpointed the C–O ester bond as the site prone to oxidative attack, allowing the collection of information about the oxidation mechanisms. Furthermore, the influence of the antioxidant (AO) 4,4'-methylene-bis(2,6-di-*tert*-butylphenol) as an additive on the oxidation behaviour and resulting products was studied: blends containing AO showed a remarkably higher resistance against oxidation. However, similar degradation products were obtained after AO depletion and without AO. AO cleavage occurred at the carbon atom that bridges the phenols to give 2,6-di-*tert*-butyl-*p*-benzoquinone and 3,5-di-*tert*-butyl-4-hydroxybenzoic acid. By applying the isotope labelling approach, sites of preferential oxidative cleavage and hence differentiation of the origin of oxygen atoms—either from the atmosphere or from base oil components—can be unambiguously related in oxygen-containing base oils, as well as in blends with additives.

**Keywords:** oxidation; synthetic lubricant; ester base oil; antioxidant; thermo-oxidative stability; isotope labelling; mass spectrometry; degradation processes; lubricant chemistry; additive

## 1. Introduction

As a consequence of the trend towards machinery with an increasing performance, while scaling down in size, the appropriate selection of the lubricant quality, composition, and, hence, its performance profile, to fulfil the requirements of lubrication is becoming a more critical issue in the major fields of application. The base oil composition with regard to the application plays a crucial role in these considerations. Accordingly, group I base oils—among the five groups of base oils as defined by the American Petroleum Institute (API)—are in decline. In turn, mineral oil based group II and III base oils, which are more intensively refined petroleum crude oils, as well as fully synthetic polyalphaolefines (PAO) representing group IV, can be found in an increasing number of commercial lubricant formulations. Group V summarizes all of the other types of base oils such as silicones, phosphate esters, polyalkylene glycol (PAG) ethers, biolubes, and various synthetic esters [1,2]. With a global market size of USD 3.46 billion and a production amount of 652.2 thousand tons in 2015, the synthetic lubricants market represents a considerable economic factor [3].

In our paper, the focus is placed on ester-based oils according to their technical-economical potential and impact. Besides the growing market for environmentally friendly products, e.g., for hydraulic oils, an increasing demand from the heavy machinery industry is noticeable. Amongst the most important application fields, compressor oils have to be mentioned with a market share of 40.7% of 2013's global synthetic ester-based oil volume, followed by hydraulic fluids, engine oils, metalworking fluids, and other application fields including high temperature chain, aviation, and food lubricants.

The highly diverse fields of application of ester-based lubricants can be explained by their unique set of properties: they offer advantageous properties for high temperature and high stability applications, as well as a high flash point, low volatility, and good thermo-oxidative stability. Besides, they display an advantageous solubility for additives and an adequate inherent lubricity. Their low toxicity and good biodegradability are additional advantages [2,4]. Ester-based base oils can be distinguished in three main groups: (1) natural esters, including vegetable crops and animal fats; (2) synthetic oleochemical esters made by the reaction of alcohols and natural fatty acids; and (3) petrochemical esters derived from synthetic alcohols and acids [4]. Besides the above-mentioned general benefits of esters compared to high-quality hydrocarbons, they can exhibit a high thermal decomposition temperature of 275 °C according to ASTM D2879, a superior trade-off between a viscosity index (VI) of 124 and pour point of  $-68$  °C, as exemplarily given for the bis(2-ethylhexyl) adipate ester [2].

Despite the widespread applications of esters at high temperatures and under harsh conditions, the knowledge about their thermo-oxidative stability behaviour still remains a critical issue. Nowadays, an increasingly important application field where the thermo-oxidative stability of esters is in focus is that of renewable biolubricants being employed as esters based on synthetic and vegetable oils, opening a wide field for eco-friendly and biodegradable lubricants [5]. Thereby, a knowledge of structure-stability relationships lays the foundations for the adjustment of thermo-oxidative stability based on the application-related modification of molecule geometry and targeted synthesis [6–9].

The thermo-oxidative stability of esters is highly linked to the hydrogen configuration of the  $\beta$ -carbon, especially of the alcohol part, the second carbon atom next to the functional group of the C–O bond in the alcohol (see Figure 1). Hydrogen atoms which bond to these  $\beta$ -carbons are prone to thermal decomposition, as a six-membered cyclic intermediate can be built and decomposes to acid and alkene. The replacement of these hydrogen atoms, e.g., to give a quaternary  $\beta$ -carbon, disables this mechanism and degradation products have to be generated via the thermodynamically less favorable free-radical pathway. Thus, the stability is increased with a higher degree of substitution on this carbon atom [2,10]. This strategy is exploited in polyol esters by replacing all of the hydrogen bonds to the  $\beta$ -carbon by alkyl groups in the alcohol moiety. Thus, the thermal decomposition of polyol esters occurs via a free-radical pathway and proceeds remarkably slower, resulting in a significantly higher stability [10–12].

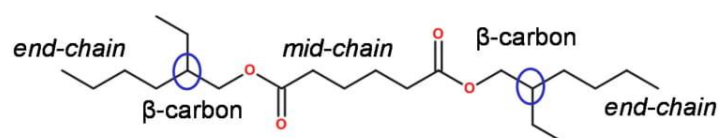


**Figure 1.** Diester bis(2-ethylhexyl) adipate with highlighted (blue circle)  $\beta$ -carbon atoms in the alcohol moiety (end chain).

The oxidative stability is increased with a decreasing mid-chain acid length, whereas the length of the end-chain alcohols shows less influence on the oxidative stability. However, branching of the alcoholic residue has a beneficial effect in terms of an improved oxidative stability, but is reduced by branched acid chains. While for the alcohol chain a complete H substitution at the  $\beta$ -carbons is particularly favourable, acid chain stability follows the order  $-\text{CH}_3 > -\text{CH}_2- > -\text{CH}-$  [2,13].

Beyond these considerations on the optimum base oil chemistries, an improvement of the thermo-oxidative performance with aminic and/or phenolic antioxidative additives is the most

common way to achieve higher resistance against oxidation and a longer functional durability of lubricants [14,15]. Lubricant degradation follows the free-radical chain reaction, based on four steps: (1) initiation; (2) propagation; (3) branching; and (4) termination. Within this study, the focus was laid on sterically hindered phenols suitable for high temperature applications to decelerate oxidation.

In order to evaluate the resistance of a base oil against thermo-oxidative stress and, thus, the impact of an antioxidant, several methods are available—either standardised or customised—such as the thermo-oxidative stability test (TOST) (DIN 51587) [16], corrosion and oxidation stability test (DIN 51808) [17], or the rotating pressurised vessel oxidation test [18] (RPVOT, see Section 2.3). Subsequent to the accelerated alteration of lubricant samples in laboratory devices, appropriate analytical methods have to be applied to determine the degree of degradation by oxidation. On the one hand, parameters regarding the degree of degradation can be obtained via conventional analytical methods based, for example, on infrared (IR) spectroscopy and the neutralisation number (NN) (see Section 2.4.1). However, these analytical methods do not provide detailed information related to the structures of degradation products or the mechanistic aspects of the process. For this reason, more advanced instrumental analytical methods have to be applied that are able to provide structure identification capabilities. Capillary gas chromatography coupled with electron impact ionization mass spectrometry (GC–EI–MS) is considered suitable for this task (see Section 2.4.2). With this hyphenated technique, the identification and characterization of the degradation products formed can be achieved after the high resolution chromatographic separation of the oil sample [19–21].

Nevertheless, a clear assignment of the origin of the degradation products, as well as the mechanistic aspects from oxygen-containing base oils and additives by oxidation, cannot be solely provided by chromatographic and mass spectrometric methods. In previous research work, a novel approach combining artificial alteration, isotope labelling, and mass spectrometry was developed to elucidate and track oxidation reactions in oxygen-containing fuel components [22]. In detail, the approach enables the unambiguous attribution of oxygen atoms in the degradation products either to the original ester, i.e., the starting material, or to the reaction process with oxygen (from the gas phase), and particularly hints to the mechanism of the formation of the degradation products. In the current publication, the methodology developed in [22] has been applied to a diester and a lubricant model mixture composed of the diester and a sterically hindered phenolic antioxidant. To the best of our knowledge, this is the first publication that reports on the artificial alterations of base oil containing a phenolic antioxidant using  $^{18}\text{O}_2$  labelling in combination with capillary GC–EI–MS.

## 2. Materials and Methods

### 2.1. Materials

As ester-based base oil component, bis(2-ethylhexyl) adipate (CAS 103-23-1, Sigma-Aldrich, St. Louis, MO, USA, structure is depicted in Figure 1) with a purity of 99% was applied. For the blends of antioxidant in base oil, 4,4'-methylene-bis(2,6-di-*tert*-butylphenol) (CAS 118-82-1, Sigma-Aldrich, St. Louis, MO, USA, structure is depicted in Figure 1) with a purity of 98% was applied at a concentration of 1 (*w/w*) %. Both chemicals were obtained from Sigma Aldrich (St. Louis, MO, USA).  $^{16}\text{O}_2$  and  $^{18}\text{O}_2$  gases were used in purities of 99.998% and more than 99%, respectively.  $^{16}\text{O}_2$  was obtained from AirLiquide (Paris, France) in conventional 50 L steel cylinders at 200 bar, and  $^{18}\text{O}_2$  in 1.0 L steel cylinders at 2 bar from Sigma Aldrich (St. Louis, MO, USA).

### 2.2. Approach of Isotope Labelling

In a previous study, an approach of artificial alteration in  $^{18}\text{O}_2$  atmosphere for producing isotope-labelled degradation products was developed and applied to the oxygen-containing model mixtures of fuel components [22]. Due to a noticeable lower abundance of oxygen isotope  $^{18}\text{O}$  (0.22%) than  $^{16}\text{O}$  (99.78%), a differentiation can be achieved between the oxygen atoms of the artificial  $^{18}\text{O}_2$  atmosphere and those comprised in the respective sample by means of mass spectrometry (MS). Thus,

different isotopes were used to track the oxidation mechanism via the assignment of the site of the oxidative attack. Figure 2 shows the scheme of the isotope labelling approach. For the present work, the above-mentioned ester-based base oil component and a blend with 1 (*w/w*) % antioxidant were subjected to accelerated degradation, due to the modified artificial alteration method described in Section 2.3 under two different oxygen atmospheres—plain  $^{18}\text{O}_2$  and standard  $^{16}\text{O}_2$ . Accordingly, the oxidation achieved with these gases yields the formation of degradation products either with or without  $^{18}\text{O}$  isotope labelling.

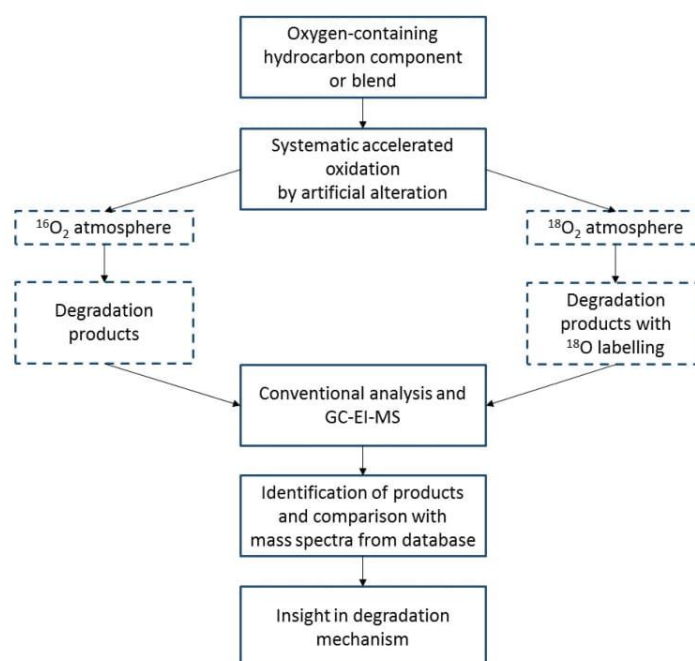


Figure 2. Scheme of the isotope-labelling approach.

Conventional analytical methods (see Section 2.4.1) revealed the general characteristics of the artificially altered samples compared to those which were fresh. A subsequent analysis with capillary GC–MS using the gas-phase ionization technique EI revealed, after comparison, the unambiguous origin of the oxygen atoms in the identified degradation products, as well as details related to the degradation mechanism [22].

### 2.3. Artificial Alteration

Most artificial alteration procedures of lubricants are performed within an open system. As a consequence, volatile compounds—both unreacted and reacted, i.e., newly formed—are removed by the gas flow and the elevated temperatures applied. Accordingly, they cannot react further, nor be investigated by subsequent fluid analysis.

In order to overcome this shortcoming, an artificial alteration procedure was utilised, based on standard ASTM D 2272 (Rotary Pressure Vessel Oxidation Test, RPVOT) [18]. In Figure 3, the respective alteration device is displayed.

For artificial alteration, 15 g of base oil—with and without antioxidant—is poured into a glass container and placed in the pressure vessel, which is closed tightly. The vessel is then filled with oxygen (either  $^{16}\text{O}_2$  or  $^{18}\text{O}_2$ ) until a pressure level of 1 or 2 bar, respectively, is reached at ambient temperature and heated to 150 °C in an oil bath. Over the entire duration of artificial alteration, the vessel is rotated by means of a rotary device in an inclined position to ensure a continuous circulation of the sample, as well as to improve the interaction with the oxygen gas-phase. The gas pressure is

monitored via a pressure sensor and recorded by a data processing computer. In contrast to ASTM D 2272, no copper wire catalyst or water addition was applied.

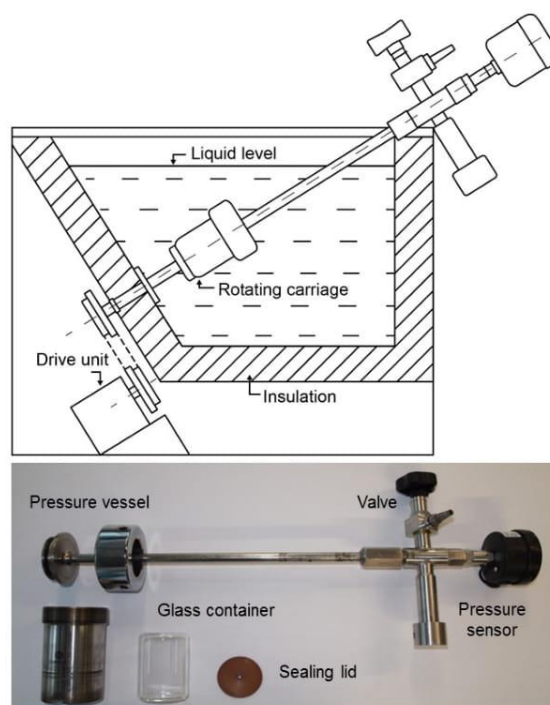


**Figure 3.** Schematic set-up of the RPVOT (rotating pressurised vessel oxidation test) device in the heating unit (above), RPVOT pressure vessel (below).

Tracking the oxygen pressure curve enables the monitoring of the alteration progress: stable pressure correlates to a stable sample condition, whereas a pressure drop (steep descent in the pressure curve) indicates increased oxygen consumption and, hence, the occurrence of oxidation reactions. By interrupting the experiment at selected points in time, an investigation of the samples with a defined condition is enabled, e.g., directly before the onset of oxidation or after the break down of pressure (see Figure 4).

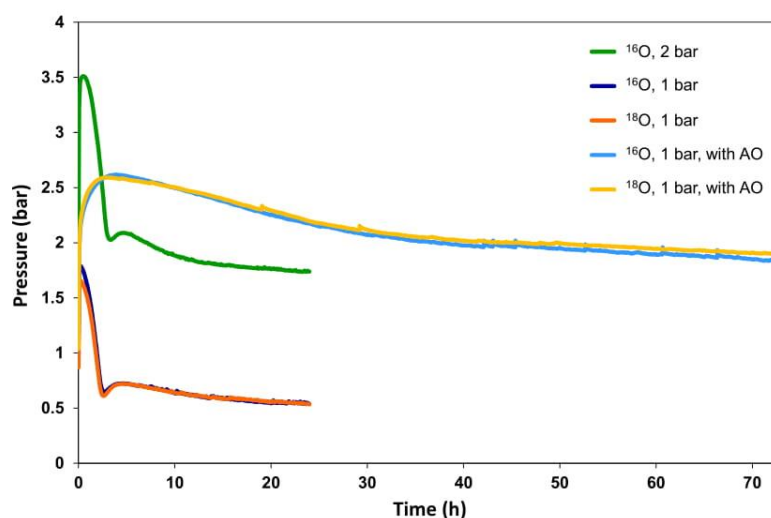


**Figure 4.** Progress of oxygen pressure during artificial alterations.

## 2.4. Analytical Approach

### 2.4.1. Conventional Analytical Methods

In [23], the neutralisation number (NN) and the water content of the conventional parameters were found to be the most important parameters involved in the degradation process during artificial alteration in the RPVOT device. According to these findings, the following conventional analytical parameters were chosen to characterise the fresh, as well as the altered, oil samples:

#### Neutralisation Number (NN)

The NN was measured in accordance with standard DIN 51558 [24], by means of colour indicator titration. It is defined as the amount of potassium hydroxide required for the neutralisation of all of the acidic compounds in 1 g of sample aliquot.

#### Water Content

The content of water in the oil samples was determined by Karl-Fischer titration, according to standard DIN 51777-2 [25]. The indirect method was applied by evaporating the water in the sample in an oven, inducing it in a measuring cell, and determining the concentration by coulometry.

### 2.4.2. Advanced Analytical Methods

In order to identify the degradation products, samples obtained from artificial alteration and in fresh condition were analysed with a capillary GC–EI–MS consisting of a TriPlus autosampler and a Trace capillary Ultra GC coupled to a TSQ Quantum XLS mass spectrometer, all of which were sourced from Thermo Scientific (Austin, TX, USA). Base components were applied as reference substances at various product concentrations: ester-based base oil component bis(2-ethylhexyl) adipate was injected with 0.02 (*w/w*) %, 4,4'-methylene-bis(2,6-di-*tert*-butylphenol) with 0.008 (*w/w*) %, and the blend of base oil component containing AO with 0.01 (*w/w*) %, which were all diluted in dichloromethane (DCM). The dilutions of all samples after artificial alteration were prepared with a concentration of 4 (*w/w*) % in DCM. The degradation products containing active hydrogen atoms such as acids were treated by silylation. The silylation reagent *N,O*-bis(trimethylsilyl) trifluoroacetamide (BSTFA) was applied to enhance the volatility for GC–MS and to avoid the undesired adsorption of the polar degradation products on the column material. BSTFA was added in a 2:1 mass excess of (*w/w*) % to the sample and aliquots were kept at 70 °C for 1 h to complete the reaction.

Samples were subjected to GC–EI–MS by injection via a programmable temperature vaporization injector (PTV) with a volume of 1 µL and a constant injector temperature of 300 °C. Split was selected with a ratio of 1:25, and the carrier gas was helium and kept at a constant flow of 2 mL/min. To separate the sample prior to mass spectrometric analysis, a TG–17MS capillary column obtained from Thermo Fischer Scientific (Waltham, MA, USA) was used, consisting of a 50%-diphenyl/50%-dimethylpolysiloxane stationary phase with a length of 30 m, a 0.25 mm inner diameter, and a film thickness of 0.25 µm. An oven temperature program starting at 50 °C for 2 min with a ramp of 7 °C/min up to 300 °C was applied, and the end temperature was kept constant for 15 min. The separated compounds were transferred to the mass spectrometer via a transfer line thermostated at 280 °C and were subsequently ionized in an EI source at 70 eV. The source temperature was set to 200 °C, and the analyser scan range was between *m/z* 40 and 650 for the full scan mode. Data acquisition and data processing were done with Xcalibur v2.0 software. For subsequent identification based on a full scan mass spectra comparison, the NIST library 2.0 (2011) with an update from the 2014 and reference substances was applied.

For the main degradation products, the calculated monoisotopic *m/z* value was given, based on the sum formula and the respective amount of <sup>16</sup>O or <sup>18</sup>O atoms based on the mass spectrometric data, as well as the detected monoisotopic mass pattern, i.e., the molecular ion peak. For analytes without a clearly visible, i.e., abundant molecular ion peak with a relative intensity (RI) of more than 1%, the highest unambiguously detected *m/z* value was reported.

### 3. Results and Discussion

#### 3.1. General Degradation Behaviour Determined by Conventional Analytical Methods

In Figure 4, the oxygen pressure in the reaction vessel throughout the artificial alterations is displayed. The pressure curves of base oil without AO show an abrupt rise in the first few minutes, due to the adjustment to the elevated temperature. Almost immediately, a steep pressure drop is observed, induced by oxidation processes. After 2 to 3 h of alteration, the lower plateau of pressure is reached, characterised by a slow pressure decrease.

In the case of the oxidation of ester-based base oils with AO, the pressure rise in the first hours of alteration is far higher, approximately twice that of blends without AO, and lasts longer, i.e., up to 5 h of alteration. After reaching the pressure maximum, a slow decrease begins, resulting in a drawn-out lower plateau with hardly any change in pressure.

Generally, prolonged alteration durations until the beginning of the pressure decrease and the achievement of the stable lower pressure plateau designate the effectiveness of the applied AO. Thus, on the one hand, the start of the oxidative processes is retarded, and on the other hand, the base oil degradation itself is decelerated. Without the application of AO, oxidation begins immediately, whereas blends with AO only start to significantly deteriorate after approximately 5 h. The overall duration until reaching a stable degradation condition strongly depends on the utilisation of AO: around 72 h in the case of blends with AO, compared to around 24 h for ester oils without an AO dosage.

Moreover, it has to be stated that the initial oxygen pressure in the vessel seems to possess little influence on the alteration behaviour, as a comparison of the alteration with 1 and 2 bar of the originally applied oxygen shows (Figure 4, dark blue curve versus dark green curve). Both alterations exhibit an identical pressure behaviour. In a first approach, the same degradation mechanisms, and hence the same reactions, can be assumed under both conditions.

A comparison of the oxygen pressure curves of alterations with  $^{16}\text{O}_2$  and  $^{18}\text{O}_2$  suggests that the isotope-labelled atmosphere does not have an impact on either the degradation behaviour or on the degradation mechanisms, strongly indicated by the almost congruent curve shapes in both cases.

The visual appearances of the fresh, as well as the artificially altered, ester-based oil samples are shown in Figure 5. It was found that all altered samples exhibit a bright yellow colour compared to colourless fresh blends. The only exception is the sample altered with 2 bar oxygen pressure with a dark brown colouring and significant turbidity. The latter can be attributed to an elevated water content, which was measured to be approximately five times higher than in all other investigated oil samples (see Figure 6).

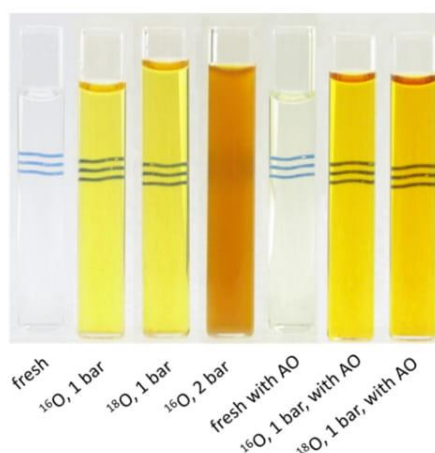


**Figure 5.** Visual appearances of ester-based oil samples with and without antioxidant (AO) before and after artificial alteration under the different oxygen atmospheres.

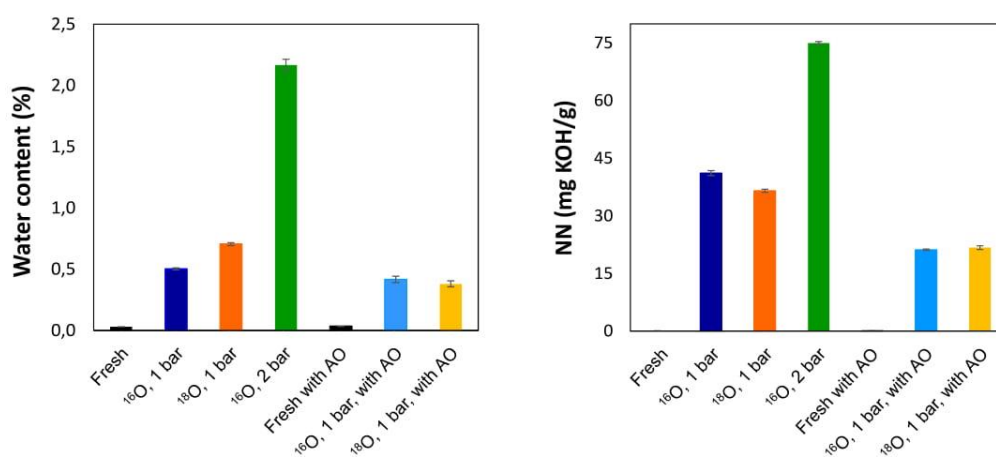


**Figure 6.** Water content (left) and neutralisation number NN (right) of oil samples before and after artificial alteration (under different oxygen atmospheres). The values for the fresh samples are <0.1 (*w/w*) % and <0.1 mg KOH/g.

Conventional condition monitoring was performed in terms of the NN and water content. Figure 6 compares the analytical data of the fresh oils with the respective results of the samples after artificial alteration. Fresh oil samples exhibited very low levels of water, as well as NN. On the contrary, a tremendous rise in both the water content and NN was detected in all samples after artificial alteration. Higher values for both parameters were found for oils without AO than for blends with AO, e.g., the NN for samples without AO was determined to be twice as high as the NN in samples with AO. The only outstanding exception is the oil sample after artificial alteration at a 2 bar oxygen pressure, which showed the highest values for both the NN and water content. In general, a good correlation was found between the detected water content and the NN in the oil samples after artificial alteration. This indicates an oxidative deterioration process producing acids, together with formation of water.

As a conclusion from the conventional oil analyses, it has to be stated that these methods provide valuable information on an oil sample which can be used to decide whether the oil has to be changed or can still be utilised in its respective application. Using these methods, equipment operators can rely on relatively rapid and cheap analyses as the basis for accurately timed counter-measures, e.g., in the case of an elevated acid concentration and/or a high water content, which may provoke corrosion. The most relevant shortcoming of conventional analysis is the lack of information on processes on the molecular level and of prognostic indications for counter-measures. Knowing these facts is essential to formulate adequate high performance oils operating at even harsher conditions or when applying them to completely new settings. Thus, conventional analytical tools have been extended by advanced analytical methods within this study to gain an insight into the degradation mechanisms and formation of degradation products, as well as the mode of action of the antioxidant.

### 3.2. Degradation Behaviour Identified by Advanced Analytical Methods

Figure 7 shows the total ion current (TIC) chromatograms of ester-based base oil samples without additives, altered at 150 °C and a pressure of 1 bar under <sup>16</sup>O<sub>2</sub> (A) and <sup>18</sup>O<sub>2</sub> (B) atmosphere, respectively. In accordance with the observations from the RPVOT pressure curves and conventional analyses, the same degradation products in a highly similar distribution were obtained for both alterations. Thus, no impact of the oxygen isotope on the type of degradation products formed was found, and a good reproducibility for the applied alteration method was demonstrated. The verification of these facts is essential for the successful application of the isotope labelling approach and the evaluation of the findings obtained.

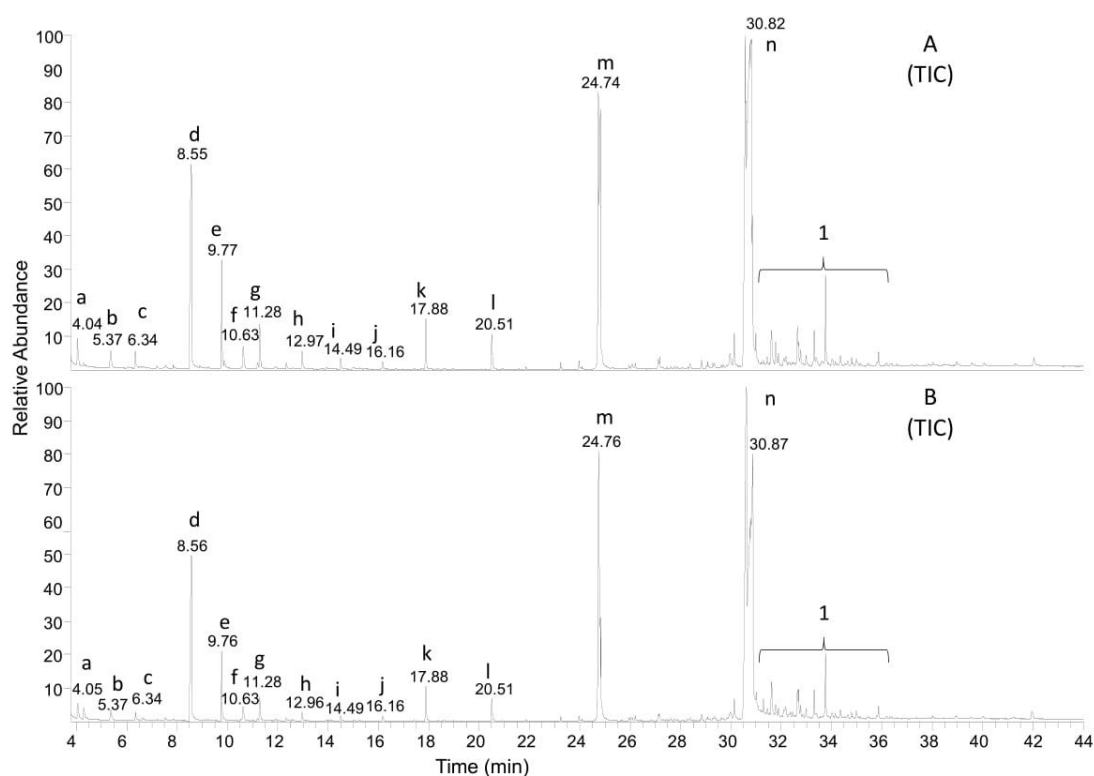


**Figure 7.** Total ion current (TIC) chromatograms of alteration products obtained under 1 bar  $^{16}\text{O}_2$  (A) and  $^{18}\text{O}_2$  (B) atmosphere without AO. Main products (a–m) and target molecule (n, starting material) are marked and given in Tables 1 and 2. Peaks under bracket with label 1 indicate oxidized molecules of ester-based base oil bis(2-ethylhexyl) adipate.

The target molecule (n), i.e., the starting molecule, and the main degradation products marked in Figure 7 are listed in Table 1 for  $^{16}\text{O}_2$  atmosphere and Table 2 for  $^{18}\text{O}_2$  atmosphere, respectively. Moreover, the retention time in minutes, calculated monoisotopic  $m/z$  value of the molecular ion, detected monoisotopic mass of the molecular ion with a relative intensity in % (RI %), and the highest detected  $m/z$  value are given. Besides linear carboxylic acids with short chain lengths such as propionic acid (a) and butanoic acid (b), detected as the trimethylsilyl (TMS) ester due to a prior sample silylation with BSTFA, hexanedioic acid TMS ester (k) referring to adipic acid in the base oil was found. 2-ethylhexyl moiety in the ester base oil was transformed into 2-ethylhexyl alcohol, detected as oxysilane (d), and 2-ethylhexanoic acid, detected as TMS ester (f). Esters of 2-ethylhexanol from formic acid up to pentanoic acid (e, g–j) were formed in distinct amounts, together with other esters (l, m) based on the alcohol moiety of the initial ester. Moreover, oxidation products with a ketone (c) structure were obtained after alteration, as well as a broad variety of oxidized molecules (peaks under bracket carrying the label 1) derived from the initial bis(2-ethylhexyl) adipate (n).

The benefit of using the isotope labelling approach to determine the degradation products related to the degradation mechanisms of the base oil is shown based on different molecules, either containing two (Figure 8), one (Figure 9 and Figure S1), or no (Figure S2)  $^{18}\text{O}$  atoms. In Figure 8, the positive ion EI mass spectra of the degradation product 2-ethylhexanoic TMS ester (f) obtained under  $^{16}\text{O}_2$  alteration atmosphere (A) and  $^{18}\text{O}_2$  alteration atmosphere (B) are shown. When comparing mass spectrum A (top) and B (bottom), some particular, close-by ions clearly differ in their  $m/z$  value, e.g., 128.9 (A) and 132.7 (B), 159.9 (A) and 163.9 (B), and 201.0 (A) and 204.9 (B). This shift of + 4 Dalton (Da) is obtained as the molecule contains two  $^{18}\text{O}$  atoms when altered under  $^{18}\text{O}_2$  atmosphere instead of  $^{16}\text{O}_2$ .

**Table 1.** Main degradation products of artificial alteration under  $^{16}\text{O}_2$  atmosphere without AO (antioxidant). Molecular ions of analytes e–m were not detected due to very low RI. Analyte n is the original of ester-based base oil. Structures of main degradation products are displayed in Figure S4.

| $^{16}\text{O}_2$ | Analyte                           | Retention Time (min) | Calculated Monoisotopic $m/z$ Value of Molecular Ion | Detected Monoisotopic Molecular Ion (RI %) | Highest Detected $m/z$ Value in the Mass Spectrum |
|-------------------|-----------------------------------|----------------------|--|--|---|
| a                 | Propionic acid TMS ester          | 4.04                 | 146.1  | 145.9 (0.6)                                | 130.9   |
| b                 | Butanoic acid TMS ester           | 5.37                 | 160.1  | 159.9 (1.0)                                | 144.9   |
| c                 | 3-heptanone                       | 6.34                 | 114.2  | 114.0 (13.5)                               | 114.0   |
| d                 | (2-ethylhexyl)oxy TMS silane      | 8.55                 | 202.4  | 202.1 (0.8)                                | 187.0   |
| e                 | 2-ethylhexyl formic acid ester    | 9.77                 | 158.2  | -( <0.5)                                   | 112.0   |
| f                 | 2-ethylhexanoic acid TMS ester    | 10.63                | 216.2  | -( <0.5)                                   | 201.0   |
| g                 | 2-ethylhexyl acetic acid ester    | 11.28                | 172.3  | -( <0.5)                                   | 124.8   |
| h                 | 2-ethylhexyl propionic acid ester | 12.97                | 186.3  | -( <0.5)                                   | 156.9   |
| i                 | 2-ethylhexyl butanoic acid ester  | 14.49                | 200.3  | -( <0.5)                                   | 156.9   |
| j                 | 2-ethylhexyl pentanoic acid ester | 16.16                | 214.3  | -( <0.5)                                   | 146.9   |
| k                 | Adipic acid TMS ester             | 17.88                | 290.5  | -( <0.5)                                   | 275.0   |
| l                 | 2-ethylhexyl 6-oxohexanoate       | 20.51                | 242.4  | -( <0.5)                                   | 139.8   |
| m                 | 2-ethylhexyl 2-oxobutyl adipate   | 24.74                | 328.4  | -( <0.5)                                   | 271.0   |
| n                 | <i>Bis(2-ethylhexyl) adipate</i>  | 30.82                | 370.6  | 371.1 (1.7)                                | 371.1   |

**Table 2.** Main degradation products of artificial alteration under  $^{18}\text{O}_2$  atmosphere without AO. Molecular ions of analytes e–m were not detected due to very low RI. Analyte n is the original of ester-based base oil. Structures of main degradation products are displayed in Figure S4.

| $^{18}\text{O}_2$ | Analyte                           | No. of $^{18}\text{O}_2$ Atoms | Retention Time (min) | Calculated Monoisotopic $m/z$ Value of Molecular Ion | Detected Monoisotopic Molecular Ion (RI %) | Highest Detected $m/z$ Value in the Mass Spectrum |
|-------------------|-----------------------------------|--------------------------------|----------------------|--|--|---|
| a                 | Propionic acid TMS ester          | 2                              | 4.04                 | 150.1  | 149.8 (<0.5)                               | 134.7   |
| b                 | Butanoic acid TMS ester           | 2                              | 5.37                 | 164.1  | 163.8 (1.0)                                | 148.8   |
| c                 | 3-heptanone                       | 2                              | 6.34                 | 116.2  | 115.8 (12.9)                               | 115.8   |
| d                 | (2-ethylhexyl)oxy TMS silane      | 2                              | 8.55                 | 202.4  | 201.9 (0.7)                                | 186.9   |
| e                 | 2-ethylhexyl formic acid ester    | -                              | 9.77                 | 158.2  | -( <0.5)                                   | 111.9   |
| f                 | 2-ethylhexanoic acid TMS ester    | 2                              | 10.63                | 220.2  | -( <0.5)                                   | 204.9   |
| g                 | 2-ethylhexyl acetic acid ester    | 1                              | 11.28                | 174.3  | -( <0.5)                                   | 126.8   |
| h                 | 2-ethylhexyl propionic acid ester | 1                              | 12.97                | 188.3  | -( <0.5)                                   | 158.8   |
| i                 | 2-ethylhexyl butanoic acid ester  | 1                              | 14.49                | 202.3  | -( <0.5)                                   | 158.8   |
| j                 | 2-ethylhexyl pentanoic acid ester | -                              | 16.16                | 214.3  | -( <0.5)                                   | 148.8   |
| k                 | Adipic acid TMS ester             | 2                              | 17.88                | 294.5  | -( <0.5)                                   | 278.9   |
| l                 | 2-ethylhexyl 6-oxohexanoate       | 1                              | 20.51                | 244.4  | -( <0.5)                                   | 141.8   |
| m                 | 2-ethylhexyl 2-oxobutyl adipate   | 1                              | 24.74                | 330.4  | -( <0.5)                                   | 271.0   |
| n                 | <i>Bis(2-ethylhexyl) adipate</i>  | -                              | 30.82                | 370.6  | 371.0 (1.8)                                | 371.0   |

Considering the structure of the initial molecule in addition to this information, the most likely pathway of degradation of the ester and formation of the degradation product can be revealed: the 2-ethylhexyl moiety cleaves between the alcohol's C1 and O atom, which is followed by the oxidative attack of O<sub>2</sub> from the atmosphere. Thus, 2-ethylhexanoic acid is obtained, detected as a TMS ester via sample preparation with the BSTFA silylation reagent. Nevertheless, as the initial ester molecule is symmetric, this reaction can take place on both alcohol moieties of the adipate. In Figure 8, the simplified reaction steps are exemplarily shown on one side of the initial molecule.

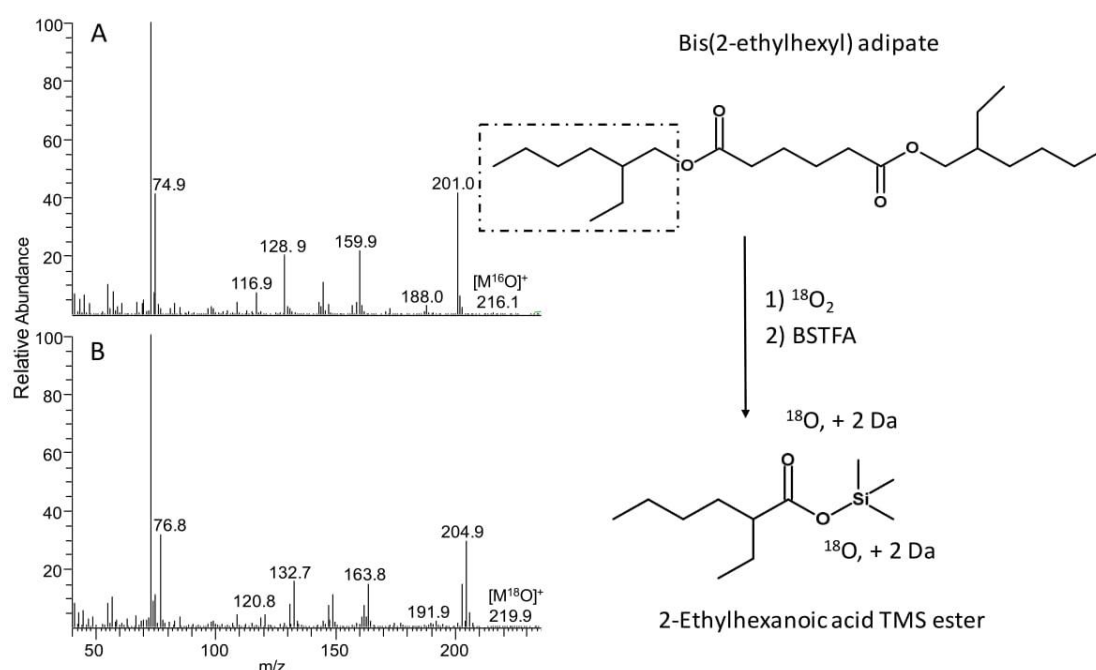


**Figure 8.** Positive ion mass spectra of 2-ethylhexanoic acid TMS ester (f) obtained after alteration under <sup>16</sup>O<sub>2</sub> (A) and <sup>18</sup>O<sub>2</sub> (B) atmosphere, respectively. Peaks of fragments where a change of the *m/z* value due to isotope labelling occurred are labelled with the respective values. A simplified oxidation reaction is suggested for the respective molecule.

3-heptanone (c) is a degradation product containing only one isotope-labelled oxygen atom, as shown in Figure S1. When comparing the mass spectra obtained under <sup>16</sup>O<sub>2</sub> and <sup>18</sup>O<sub>2</sub> atmosphere, the presence of one <sup>18</sup>O atom is confirmed: besides fragments containing oxygen, i.e., *m/z* 57.0 and 58.9, 72.0 and 73.9, 84.9, and 86.6, the molecular ion peak with a shift from *m/z* 114.0 to 115.8 is also effortlessly visible. It can be assumed, that thermal decomposition takes place via the six-membered cyclic intermediate involving the hydrogen on the β-carbon, as reported in the literature (see Introduction). This results in an alkene counting eight C atoms and an (di)acid. With these fragments, further reactions can take place. Due to oxidation, evoked by the oxygen from the atmosphere, 3-heptanone is built, carrying one <sup>18</sup>O atom. However, when looking closely at the mass spectra of this molecule, one may also see low abundant fragments without isotope labelling such as 114.0, 84.9, and 72.0 (Figure S1B). This observation may lead to a second possible formation mechanism of 3-heptanone, without involving <sup>18</sup>O<sub>2</sub>. Hence, the application of the isotope labelling approach is not only feasible for explaining issues of interest, but also raises new ones.

Figure S2 in the supplement shows an example of a degradation product without any isotope-labelled oxygen, 2-ethylhexyl alcohol detected as (2-ethylhexyl)oxy TMS silane (d). Due to the fact that in none of the mass spectrometric fragments found in the mass spectrum of the compound formed under <sup>18</sup>O atmosphere a shift of *m/z* values (+2 or 4 Da) is obtained, there is no hint of a participation of oxygen from the atmosphere in the formation of this product. Thus, by using the

isotope labelling approach, one can conclude that the molecule was formed by an unspecified cleavage of the C–O ester bond. Besides radical cleavage, the more likely mechanism can be hydrolysis of the ester bond. This mechanism requires conditions provided by proceeding alteration, in particular, an acid catalyst (see increased NN value for altered samples in Section 3.1) and a sufficient amount of water (see water formation for altered samples in Section 3.1). Accordingly, in the following passages, the term “cleavage of the C–O ester bond” refers to an unspecified mechanism of cleavage.

Besides the degradation products containing either  $^{18}\text{O}$  or  $^{16}\text{O}$  at the sites of the oxidative attack, molecules with a mix of isotopes are also possible. Figure 9 provides a 2-ethylhexyl acetic acid ester (g) as an example of this. Based on the shift in the molecular ion peak, as well as the highest detected shift of +2 Da, the presence of one  $^{18}\text{O}$  atom can be confirmed. A comparison with the NIST library identifies the molecule as 2-ethylhexyl acetic acid ester, containing two oxygen atoms. The correlation of the fragment ions with the structure only gives a shift for these fragments, where either both oxygen atoms are involved or exclusively the C=O group, i.e., the fragment ions at  $m/z$  43.1 and 45.0. This observation leads to the finding that the C=O group contains the  $^{18}\text{O}$  atom. Most probably, cleavage of the C–O ester bond and the combination with a  $\text{CH}_3\text{CO}$  moiety results in the identified ester. The  $\text{CH}_3\text{CO}$  moiety is most possibly derived by the cleavage of the ethyl side chain of 2-ethylhexanol and subsequent oxidation.

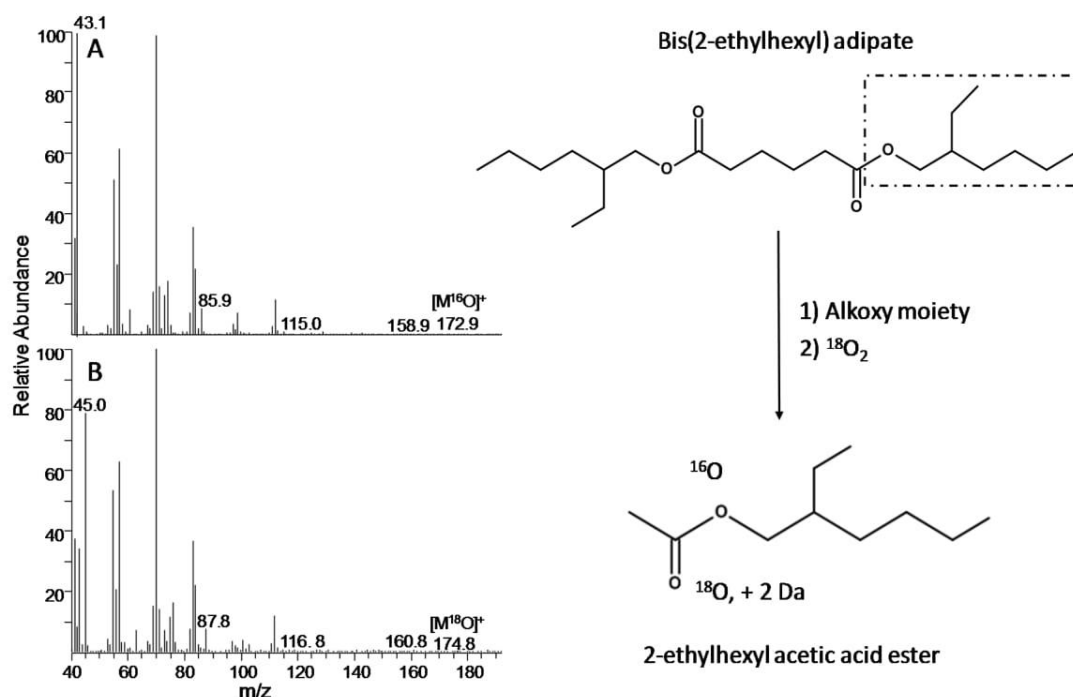


**Figure 9.** Positive ion mass spectra of 2-ethylhexyl acetic acid ester (g) obtained after alteration under  $^{16}\text{O}_2$  (A) and  $^{18}\text{O}_2$  (B) atmosphere, respectively. Peaks of fragments where a change of the  $m/z$  value due to isotope labelling occurred are labelled with the respective values. A simplified oxidation reaction is suggested for the respective molecule.

Summarizing the above described results of the neat base oil, relevant fragments of the oxidation mechanism could be identified: preferential sites of cleavage are between the C–O ester bond, resulting in products such as 2-ethylhexyl alcohol (d) and 2-ethylhexyl fatty acid esters with various acid chain lengths (e, g–j), and a bond cleavage between the O atom and C1 of the alcohol, providing 2-ethylhexanoic acid (f). Such a structure can be further oxidized to 3-heptanone (c) and, after a second cleavage step, to propionic and butanoic acid (a, b). For one of the main degradation products, adipic acid (k), the two  $^{18}\text{O}$  atoms are present in each of the ester bonds (C– $^{18}\text{O}$ ), whereas  $^{16}\text{O}$  was

found in the carbonyl groups ( $C=^{16}O$ ) of the acid chain of the initial ester. Hence, a combination of oxidative cleavage of the C–O ester bond and subsequent acid formation occurs on both sides. Moreover, the highly abundant 2-ethylhexyl 2-oxobutyl adipate (m) results from bond dissociation and oxidation between C2 and C3 of the alcohol chain, whereas the rest of the initial molecule stays intact. The formation of short-chain fatty acids as found in esters (e, g–j) is assigned to the cleavage and oxidation of 2-ethylhexyl alcohol. In contrast to the expected oxidation mechanism, formic acid (in e) and pentanoic acid (in j) do not carry  $^{18}O$ . Furthermore, the oxidation mechanism of 2-ethylhexyl 6-oxohexanoate (l) could not be revealed.

An alteration of the neat base oil was not only performed at 1 bar, but also at a pressure of 2 bar, to estimate the influence of pressure on the formation of degradation products. Figure S3 illustrates chromatograms of alteration under 1 bar  $^{16}O_2$  atmosphere (A) and 2 bar  $^{16}O_2$  atmosphere (B). For both alteration samples, the main products were marked and given in Table 1. Based on the degradation products obtained, it can be concluded that there is hardly any influence of the enhanced pressure on the structure of the degradation products formed, at least in the time frame and temperature regime applied. However, particular peaks show a noticeably lower abundance, e.g., (2-ethylhexyl)oxy TMS silane (d) at retention time  $t_R = 8.55$  min, and 2-ethylhexyl 2-oxobutyl adipate (m) at  $t_R = 24.74$  min, while some of them increased with increasing pressure, e.g., adipic acid bis(TMS) ester (k) at  $t_R = 17.90$  min. Therefore, an effect of pressure on the degradation mechanism and, consequently, on the quantities of the products formed can be assumed, whereas the quality of the degradation products is not influenced.

In addition to the neat base oil, blends with 1 (w/w) % AO were subjected to artificial alteration. GC–MS analysis obtained from these samples altered under  $^{16}O_2$  atmosphere and  $^{18}O_2$  atmosphere, respectively, showed identical products and distribution. The most abundant degradation products in the artificially altered samples have already been given in Table 1. Additionally, the degradation products of AO under both atmospheres are listed in Table 3.

Compared to alteration without AO (see Figure 10A), not all of the products were formed in similarly significant amounts and are therefore not marked as main degradation products. Exemplarily, short-chain fatty acids such as propionic acid (a) and butanoic acid (b), were detected as TMS esters in only minor amounts. Accordingly, 2-ethylhexyl fatty acid esters (e, g–j) with various acid chain lengths are generated in noticeably lower quantities. The lower amount of acidic degradation products of blends with AO is in good accordance with the results from NN analyses, which show values which are only half of the ones without AO. However, (2-ethylhexyl)oxy TMS silane (d) and adipic acid TMS ester (k) were formed in similar quantities. Regardless of the amounts of degradation products formed, qualitative analysis revealed almost completely the same list of degradation products for both the neat base oil and the blend containing AO.

In addition to the ester degradation products discussed above, the degradation products of the AO were also detected: 2,6-di-*tert*-butyl-*p*-benzoquinone (o) and 3,5-di-*tert*-butyl-4-hydroxybenzoic acid TMS ester (p) were found in TIC and are shown in Figure 10B. Figure 11 shows the positive ion mass spectra of  $^{16}O_2$  and  $^{18}O_2$  atmosphere alteration of the AO degradation product 3,5-di-*tert*-butyl-4-hydroxybenzoic acid TMS ester. Due to a shift of +4 Da for the molecular ion from  $m/z$  322.0 to 326.0, as well as for  $m/z$  307.0 to 311.0, the oxygen atoms in the carboxyl acid group can be identified as  $^{18}O$  isotopes. Hence, one can conclude that the oxidation of the AO leads to a bond cleavage between the C bridge-atom and one of the phenols, and the C bridge-atom is oxidized to a carboxyl acid by oxygen from the atmosphere, detected as a TMS ester after silylation. Furthermore, the oxidation of the residual phenolic residue results in the second degradation product, detected as 2,6-di-*tert*-butyl-*p*-benzoquinone.

**Table 3.** Main AO degradation products of artificial alteration under  $^{16}\text{O}_2$  and  $^{18}\text{O}_2$  atmosphere.

| $^{16}\text{O}_2$ | Analyte  | Retention Time (min) | Calculated Monoisotopic $m/z$ Value of Molecular Ion | Detected Monoisotopic Molecular Ion (RI %) | Highest Detected $m/z$ Value in the Mass Spectrum |
|-------------------|--|----------------------|--|--|---|
| o                 | 2,6-di- <i>tert</i> -butyl- <i>p</i> -benzoquinone         | 18.11                | 220.3  | 220.0 (40.2)                               | 220.0   |
| p                 | 3,5-di- <i>tert</i> -butyl-4-hydroxybenzoic acid TMS ester | 25.50                | 322.20   | 322.0 (14.5)                               | 322.0   |
| $^{18}\text{O}_2$ | Analyte  | Retention Time (min) | Calculated Monoisotopic $m/z$ Value of Molecular Ion | Detected Monoisotopic Molecular Ion (RI %) | Highest Detected $m/z$ Value in the Mass Spectrum |
| o                 | 2,6-di- <i>tert</i> -butyl- <i>p</i> -benzoquinone         | 18.11                | 220.3  | 220.0 (38.3)                               | 220.0   |
| p                 | 3,5-di- <i>tert</i> -butyl-4-hydroxybenzoic acid TMS ester | 25.52                | 326.2  | 326.0 (12.8)                               | 326.0   |

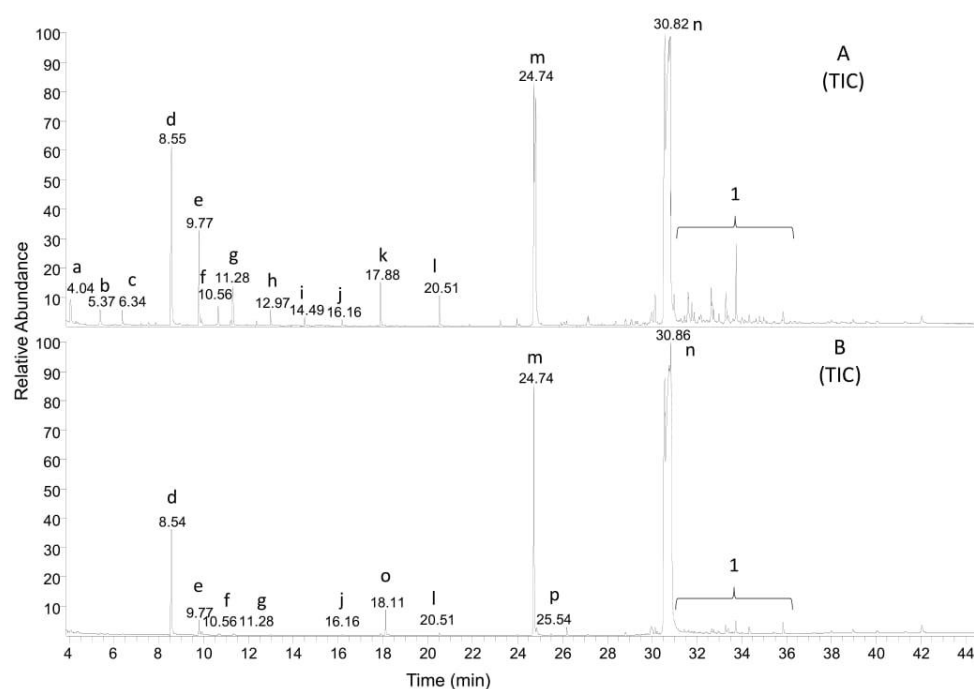


**Figure 10.** TIC chromatograms of alteration products obtained under 1 bar  $^{16}\text{O}_2$  atmosphere without (A) and with 1 (*w/w*) % AO (B). Main products (a–m), AO degradation products (o, p), and target molecule (n, starting material) are marked and given in Tables 1–3. Peaks under bracket with label 1 indicates oxidized molecules of ester-based base oil bis(2-ethylhexyl) adipate.

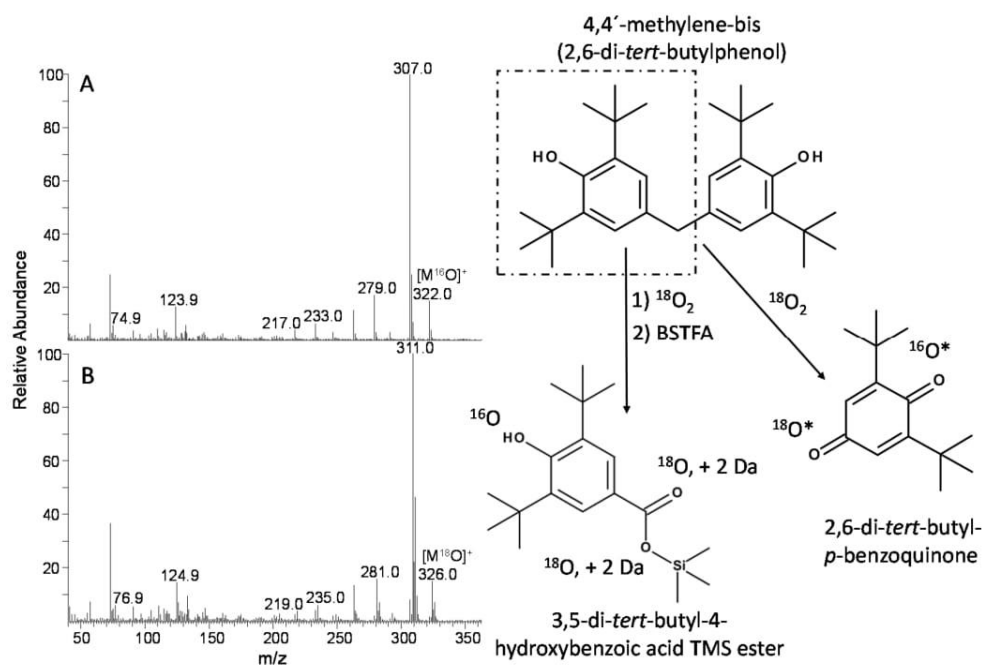


**Figure 11.** Positive ion mass spectra of 3,5-di-*tert*-butyl-4-hydroxybenzoic acid TMS ester (p) obtained after alteration under  $^{16}\text{O}_2$  (A) and  $^{18}\text{O}_2$  (B) atmosphere, respectively. Peaks of fragments where a change of the *m/z* value due to isotope labelling occurred are labelled with the respective values. A simplified oxidation reaction is suggested for the respective molecule. \* signifies assignment of  $^{16}\text{O}$  or  $^{18}\text{O}$  atoms according to the most likely degradation pathway.

#### 4. Conclusions

The unique usefulness of the isotope labelling approach based on mass spectrometry for the investigation of the thermo-oxidative stability of oxygen-containing lubricant components could be clearly demonstrated in this study. With a satisfactory reproducibility (in terms of the retention times and mass spectrometric peak pattern), neat diester bis(2-ethylhexyl) adipate, and a blend containing 1 (*w/w*) % antioxidant, 4,4'-methylene-bis(2,6-di-*tert*-butylphenol) was artificially altered in a closed vessel under  $^{16}\text{O}_2$  and  $^{18}\text{O}_2$  atmosphere, and subsequent high-performance capillary GC–EI–MS analysis was applied to identify the main degradation products containing varying numbers of  $^{18}\text{O}$ . Isotope labelling in combination with MS allowed a clear assignment of the location of the isotope-labelled oxygen in the degradation product, even in the case of a mix of  $^{16}\text{O}$  and  $^{18}\text{O}$ .

The findings revealed the preferential bond cleavage sites in the diester molecule between the C–O ester bond and subsequent oxidative attack, resulting in 2-ethylhexyl fatty acid esters and 2-ethylhexyl alcohol. Furthermore, 2-ethylhexanoic acid is generated by the bond scission between the O atom and C1 of the alcohol, and is followed oxidation during alteration under the applied conditions. Moreover, the main degradation products were built after oxidative cleavage on one side or on both sides of the initial ester groups, to give 2-ethylhexyl 2-oxobutyl adipate and 2-ethylhexyl 6-oxohexanoate, respectively. 2-ethylhexyl 2-oxobutyl adipate was produced in distinct abundance, based on the oxidation between C2 and C3 of the alcohol chain. An increased pressure during the alteration seems to have no considerable impact on the quality of the formed degradation products, but the quantities vary, depending on the pressure level.

Base oil blends containing AO showed a far higher stability, resulting in an enhanced alteration duration until the end point. Although mainly the same degradation products were built, almost all of them showed a significantly lower abundance, in particular, short-chain fatty acids and esters thereof, as well as oxidized ester base oil molecules. The two main degradation products of the AO were obtained: 2,6-di-*tert*-butyl-*p*-benzoquinone and 3,5-di-*tert*-butyl-4-hydroxybenzoic acid.

In sum, the advanced analytical approach combining artificial alteration, isotope labelling, and mass spectrometry, proved to be an appropriate and powerful tool to unambiguously determine the degradation products of oxygen-containing lubricant components. Hence, the foundations have been laid for the elucidation of the underlying oxidation mechanisms.

Prospectively, the sampling of alteration aliquots at points of interest, e.g., before the pressure curve starts to drop, are planned. This opens up the way to develop a reliable prognostic tool (on the status of lubricant in certain devices for acting at an early stage) based on the early detection of certain quantities of degradation products long before NN or IR spectroscopy would indicate anything. GC–MS analysis shall reveal the time- and alteration state-dependent formation of major degradation products. For blends containing AO, the determination of the residual AO content at different alteration states is of high interest. For this purpose, various GC-MS techniques such as selected ion monitoring (SIM), multiple ion detection (MID), or low energy (collision induced dissociation) CID MS/MS will be applied. Moreover, this work showed that the conventional and advanced analytical data are in good accordance, e.g., lower NN values for samples containing less acidic compounds obtained with MS analysis. Based on the knowledge gained with such an advanced analysis, a correlation of the degradation products formed with conventional oil data such as NN and that obtainable by IR spectroscopy shall be achieved.

**Supplementary Materials:** The following are available online at [www.mdpi.com/2076-3417/7/4/396/s1](http://www.mdpi.com/2076-3417/7/4/396/s1). Figure S1: Positive ion mass spectra of 3-heptanone (c) obtained after alteration under  $^{16}\text{O}_2$  (A) and  $^{18}\text{O}_2$  (B) atmosphere, respectively. Peaks of fragments where a change of the *m/z* value due to isotope labelling occurred are labelled with the respective values. A simplified oxidation reaction is suggested for the respective molecule. Figure S2: Positive ion mass spectra of (2-ethylhexyl)oxy TMS silane (d) obtained after alteration under  $^{16}\text{O}_2$  (A) and  $^{18}\text{O}_2$  (B) atmosphere, respectively. Random peaks of fragments where a change of the *m/z* value could have occurred due to isotope labelling are labelled with the respective values. A simplified oxidation reaction is suggested for the respective molecule. Figure S3: TIC chromatograms of alteration products obtained under 1 bar  $^{16}\text{O}_2$  (A) and 2 bar  $^{16}\text{O}_2$  (B) atmosphere without AO. Main products (a–m) and target molecule (n, starting

material) are marked and given in Tables 1 and 3. Peaks under bracket with label 1 indicate oxidized molecules of ester-based base oil bis(2-ethylhexyl) adipate. Figure S4: Structures of the main degradation products according to Tables 1 and 2.

**Acknowledgments:** The work presented was funded by the Austrian COMET program (project XTribology, no. 849109) and carried out at the “Excellence Centre of Tribology” (AC2T research GmbH).

**Author Contributions:** Marcella Frauscher established the experimental matrix and performed advanced analyses of the samples obtained by artificial alteration. Furthermore, she was responsible for the evaluation and interpretation of the derived data and main parts of the manuscript. Charlotte Besser carried out the conventional analysis, including the data evaluation, and wrote the results in this aspect and the experimental background. Nicole Dörr conducted the presented study and gave professional input. Günter Allmaier gave scientific support concerning mass spectrometry and revised the manuscript.

**Conflicts of Interest:** The authors declare no conflict of interest.

## References

1. American Petroleum Institute (API), API 1509 2016, Appendix E. Available online: [www.api.org](http://www.api.org) (accessed on 5 December 2016).
2. Rudnick, L.E. *Synthetics, Mineral Oils, and Bio-Based Lubricants*, 2nd ed.; CRC Press: Boca Raton, FL, USA, 2014; pp. 47–74.
3. Global Market Insights Inc. Synthetic Lubricants Market Size to Exceed USD 5 Billion by 2023. Available online: [www.gminsights.com](http://www.gminsights.com) (accessed on 5 December 2016).
4. Eastwood, J. Esters—The most versatile of base stock technologies. *Lube Mag.* **2015**, *129*, 32–37.
5. Nagendramma, P.; Kaul, S. Development of ecofriendly/biodegradable lubricants: An overview. *Renew. Sustain. Energy Rev.* **2012**, *16*, 764–774. [[CrossRef](#)]
6. Erhan, S.Z.; Sharma, B.K.; Perez, J.M. Oxidation and low temperature stability of vegetable oil-based lubricants. *Ind. Crop. Prod.* **2006**, *24*, 292–299. [[CrossRef](#)]
7. Salimon, J.; Salih, N.; Yousif, E. Improvement of pour point and oxidative stability of synthetic ester basestocks for biolubricant applications. *Arab. J. Chem.* **2012**, *5*, 193–200. [[CrossRef](#)]
8. Wu, Y.; Li, W.; Zhang, M.; Wang, X. Improvement of oxidative stability of trimethylolpropane trioleate lubricant. *Thermochim. Acta* **2013**, *569*, 112–118. [[CrossRef](#)]
9. Cavalcante, I.M.; de Rocha, N.R.C.; Maier, M.E.; Lima, A.P.D.; Neto, D.M.A.; Brito, D.H.A.; Petzhold, C.L.; Schanz, M.T.G.F.; Ricardo, N.M.P.S. Synthesis and characterization of new esters of oleic acid and glycerol analogues as potential lubricants. *Ind. Crop. Prod.* **2014**, *62*, 453–459. [[CrossRef](#)]
10. Housel, T. Synthetic esters: Engineered to perform. Available online: <http://machinerylubrication.com/Read/29703/synthetic-esters-perform> (accessed on 14 April 2017).
11. Gryglewicz, S.; Piechicki, W.; Gryglewicz, G. Preparation of polyol esters based on vegetable and animal fats. *Bioresour. Technol.* **2003**, *87*, 35–39. [[CrossRef](#)]
12. Bünnemann, T.F.; Vank Aken, R.P. Synthetische Ester—Wie kann man die Lebensdauer von biologisch schnell abbauenden Hydraulikflüssigkeiten verlängern. In *Tribology 2000—Plus, Proceedings of the 12th International Colloquium, Ostfildern, Germany, 11–13 January 2000*; Emerald Group Publishing Limited: Bingley, UK, 2000; pp. 109–110.
13. Moser, B.R.; Sharma, B.K.; Doll, K.M.; Erhan, S.Z. Diesters from Oleic Acid: Synthesis, Low Temperature Properties, and Oxidation Stability. *J. Am. Oil Chem. Soc.* **2007**, *84*, 675–680. [[CrossRef](#)]
14. Alias, N.H.; Yunus, R.; Idris, A.; Omar, R. Effects of additives on oxidation characteristics of palm oilbased trimethylolpropane ester in hydraulics applications. *Eur. J. Lipid Sci. Technol.* **2009**, *111*, 368–375. [[CrossRef](#)]
15. Chao, M.; Li, W.; Wang, X. Influence of antioxidant on the thermal-oxidative degradation behavior and oxidation stability of synthetic ester. *Thermochim. Acta* **2014**, *561*, 16–21. [[CrossRef](#)]
16. Deutsches Institut für Normung. *4263 Petroleum and Related Products—Determination of the Ageing Behaviour of Inhibited Oils and Fluids Using the TOST Test*; Deutsches Institut für Normung: Berlin, Germany, 2016.
17. Deutsches Institut für Normung. *51808 Testing of Lubricants—Determination of Oxidation Stability of Greases—Oxygen Method, Deutsches Institut für Normung (Draft)*; Deutsches Institut für Normung: Berlin, Germany, 2015.
18. ASTM International. *D 2272 Standard Test Method for Oxidation Stability of Steam Turbine Oils by Rotating Pressure Vessel*; ASTM International: West Conshohocken, PA, USA, 1998.

19. Santos, J.C.O.; Santos, I.M.G.; Souza, A.G. Thermal degradation process of synthetic lubricating oils: Part I—Spectroscopic study. *Petrol. Sci. Technol.* **2015**, *33*, 1238–1245. [CrossRef]
20. Keller, M.A.; Saba, C.S. Gas chromatographic monitoring of hydroxyl components in oxidized turbine engine lubricants. *Tribol. Trans.* **2003**, *46*, 576–579. [CrossRef]
21. Tripathi, A.K.; Vinu, R. Characterization of thermal stability of synthetic and semi-synthetic engine oils. *Lubricants* **2015**, *3*, 54–79. [CrossRef]
22. Frauscher, M.; Besser, C.; Dörr, N.; Allmaier, G. Unambiguous identification of degradation products related to elucidation of the degradation mechanism of oxygen containing fuel components by shared use of isotope labelling and mass spectrometry. *Anal. Chem.* **2017**. submitted.
23. Besser, C.; Pisarova, L.; Frauscher, M.; Hunger, H.; Dörr, N.; Litzow, U.; Orfanotis, A. Oxidation products of biodiesel in diesel fuel generated by artificial alteration and identified by mass spectrometry. *Fuel* **2017**, submitted.
24. Deutsches Institut für Normung. *DIN 51558 Testing of Mineral Oils, Determination of Neutralization Number by Color-Indicator Titration*; Deutsches Institut für Normung: Berlin, Germany, 1979.
25. Deutsches Institut für Normung. *DIN 51777-2 Testing of Mineral Oil Hydrocarbons and Solvents, Determination of Water Content According to Karl Fischer; Indirect Method*; Deutsches Institut für Normung: Berlin, Germany, 1974.



© 2017 by the authors. Licensee MDPI, Basel, Switzerland. This article is an open access article distributed under the terms and conditions of the Creative Commons Attribution (CC BY) license (<http://creativecommons.org/licenses/by/4.0/>).

## **2.2 Publication 2 - Elucidation of oxidation and degradation products of oxygen containing fuel components by combined use of a stable isotopic tracer and mass spectrometry**

Analytica Chimica Acta, vol. 993, pp 47-54, 2017

The publication is reprinted on the following pages



# Elucidation of oxidation and degradation products of oxygen containing fuel components by combined use of a stable isotopic tracer and mass spectrometry



Marcella Frauscher<sup>a, b</sup>, Charlotte Besser<sup>a</sup>, Günter Allmaier<sup>b</sup>, Nicole Dörr<sup>a, \*</sup>

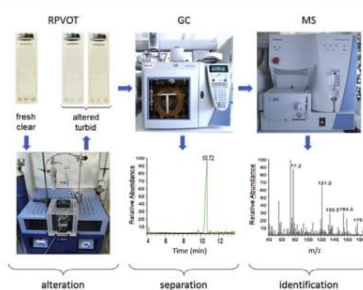
<sup>a</sup> AC2T Research GmbH, Viktor-Kaplan-Straße 2C, 2700 Wiener Neustadt, Austria

<sup>b</sup> Institute of Chemical Technologies and Analytics, TU Wien (Vienna University of Technology), Getreidemarkt 9/164, Vienna, Austria

## HIGHLIGHTS

- An approach combining artificial alteration, isotopic tracer and MS is presented.
- It is appropriate to monitor the build-up of oxidation products.
- Thermo-oxidative stability of oxygen-containing components is determined.
- Their role in oxidative degradation mechanisms on the molecular level is enabled.

## GRAPHICAL ABSTRACT



## ARTICLE INFO

### Article history:

Received 22 June 2017  
 Received in revised form  
 30 August 2017  
 Accepted 7 September 2017  
 Available online 19 September 2017

### Keywords:

Thermo-oxidative stability  
 Stable isotopic tracer  
 Mass spectrometry  
 Oxidation  
 Degradation products

## ABSTRACT

In order to reveal the degradation products of oxygen-containing fuel components, in particular fatty acid methyl esters, a novel approach was developed to characterize the oxidation behaviour. Combination of artificial alteration under pressurized oxygen atmosphere, a stable isotopic tracer, and gas chromatography electron impact mass spectrometry (GC-EI-MS) was used to obtain detailed information on the formation of oxidation products of (9Z), (12Z)-octadecadienoic acid methyl ester (C18:2 ME). Thereby, biodiesel simulating model compound C18:2 ME was oxidized in a rotating pressurized vessel standardized for lubricant oxidation tests (RPVOT), i.e., artificially altered, under  $^{16}\text{O}_2$  as well as  $^{18}\text{O}_2$  atmosphere. Identification of the formed degradation products, mainly carboxylic acids of various chain lengths, alcohols, ketones, and esters, was performed by means of GC-EI-MS. Comparison of mass spectra of compounds under both atmospheres revealed not only the degree of oxidation and the origin of oxygen atoms, but also the sites of oxidative attack and bond cleavage. Hence, the developed and outlined strategy based on a gas-phase stable isotopic tracer and mass spectrometry provides insight into the degradation of oxygen-containing fuels and fuel components by means of the accurate differentiation of oxygen origin in a degradation product.

© 2017 Elsevier B.V. All rights reserved.

\* Corresponding author.

E-mail addresses: [marcella.frauscher@ac2t.at](mailto:marcella.frauscher@ac2t.at) (M. Frauscher), [charlotte.besser@ac2t.at](mailto:charlotte.besser@ac2t.at) (C. Besser), [guenter.allmaier@tuwien.ac.at](mailto:guenter.allmaier@tuwien.ac.at) (G. Allmaier), [nicole.doerr@ac2t.at](mailto:nicole.doerr@ac2t.at) (N. Dörr).

<https://doi.org/10.1016/j.aca.2017.09.009>

0003-2670/© 2017 Elsevier B.V. All rights reserved.

## 1. Introduction

Influenced by the decline of natural resources and global warming, mainly caused by release of greenhouse gases by burning of fossil fuels, restrictions in gas emission regarding transportation

and notable governmental support for alternative fuels have increased over the last decade. According to the United Nations Framework Convention on Climate Change at the 21st Conference of the Parties (COP 21), mobility should be possible without fossil fuels by 2050 at the latest. Norway even intends to prohibit gasoline and diesel vehicles from 2025 on [1]. Influenced by these developments, diesel blending with distinct amounts of biodiesel has gained more and more importance over the last decades [2–5]. Europe is among the world leaders in biofuel production, regarding biodiesel even the world's largest producer. For the year 2014 a production amount of 13,341 million (mio.) liters (L) biodiesel and renewable diesel was achieved. An estimated amount for 2017 of 14,155 mio. L should be produced within Europe. Feedstock used for the production in 2014 is given with 11.21 kilo tons (kt), whereof 6,1 kt were from rapeseed oil, which corresponds to 55 percent (%) [6].

Biodiesel produced from rapeseed oil shows a distinct fatty acid methyl ester (FAME) pattern affected by the feedstock. The FAME composition of rapeseed oil methyl ester (RME) is mainly based on C18:1 (60.7 (w/w) %), C18:2 (19.6 (w/w) %), C18:3 (9.8 (w/w) %), C16:1 (4.4 (w/w) %) and C18:0 (1.8 (w/w) %) fatty acids [7].

In the past, the free radical oxidation of unsaturated lipids was investigated mainly due to medical interests [8–10]. Especially linoleate and its autoxidation mechanisms were of special research interest [11,12]. In previous work including RME-based FAME, focus was put on one of the most important issues of biodiesel, the storage stability [13]. Due to a high content of unsaturated fatty acids, FAME fractions are highly prone to oxidation, which is affected by storage conditions such as temperature, air exposure, or impact of sun light. Formed deposits are one consequence of oxidation reactions, which may cause damage to the engine or the fuel supply [14,15]. In order to determine the storage stability of biodiesel fuel blends, studies typically applying the Rancimat method according to DIN EN 15751 [16] are executed. Moreover, oxidative stability can be influenced and improved by addition of antioxidants, mainly hindered phenols or amines as well as combinations [17].

However, in order to improve oxidative stability of biodiesel formulations by well-directed measures, extensive analyses are necessary to understand the oxidation reactions taking place and to identify or characterize the degradation products built up during the oxidation process. For edible oils, the main pathway of oxidation is autoxidation, where hydroperoxides are formed as a first step. The steps of the following radical chain reaction were already described by Farmer et al. and Bolland in the years 1942 and 1949, respectively [18,19]. However, in the field of fuels, hydrocarbon-based lubricants, and their additives, there is still a lack of information about reactions taking place during the degradation process. Conventional analytical methods can provide information like acid number, viscosimetric data, peroxide number, degree of oxidation, or water content. In order to identify and/or characterize degradation products, mass spectrometry (MS) is the technique of choice. To mention some of the possible techniques, gas chromatography coupled with electron impact (EI) MS with analyzers such as quadrupole (Q), ion trap (IT), or quadrupole reflectron time-of-flight (QRTOF) is one of the first to be considered. However, high performance liquid chromatography (HPLC), on-line coupled or direct infusion with electrospray ionization (ESI) with a variety of analyzers, also seems to be suitable, as demonstrated in Refs. [7,20–22]. To give an example with direct infusion ESI-QRTOF-MS, Catharino et al. achieved fingerprint typification of biodiesel samples [22]. Moreover, information of the used alcohol, the state of degradation and the residual glycerol and glycerides was obtained.

As mentioned above, previous research work was focused on

storage stability evaluation of diesel and various diesel-FAME blends by their analytical characterization in different degradation states. Therefore, standard artificial alteration methods currently in use had to be modified to fulfil the required tasks. The term artificial alteration is used to describe the accelerated, lab-based procedure to change the properties of the respective model fuels or generally applied fuels. Here, the defined and reproducible conditions play a crucial role. The online monitoring throughout the alteration as well as the complete collection of degradation products was of high interest, directing investigations towards the technique GC-MS. Subsequently, the sample aliquots (from different time points) were analyzed using GC-EI-MS to identify and characterize degradation products in the various blends [13].

Although the characterization of degradation products and the correlation with conventional fuel analysis showed insightful results, several questions were left unanswered by this conventional approach. Beside the origin of the degradation products, possible ways of degradation of the initial molecule was of high importance, but it is still unclear and should be explained on the molecular level. In order to reveal more and in particular detailed information concerning the path of degradation, i.e., obtaining mechanistic information, of FAME, the development of a new approach for the elucidation of oxidation reactions became necessary. In case of oxygen-containing lubricants and components, e.g. ethers and esters, a differentiation of oxygen origin in a degradation product, either from lubricant or via oxidation, is still difficult to determine. Hence, tracking of the reactions taking place while degradation is complicated. Therefore, we propose the novel approach using a  $^{18}\text{O}$  stable isotopic tracer of the formed degradation products during artificial alteration with subsequent analysis by GC-EI-MS presented in this paper.

With 99.78% natural abundance,  $^{16}\text{O}$  is the most common oxygen isotope followed by stable  $^{18}\text{O}$  with 0.22% [23,24]. These different abundances can be used, e.g., to study atmospheric gas, marine carbonate deposits, or for stable isotopic tracer methods. This has been applied to improve methods for protein quantification and gain insight in their functions and dynamics [25]. Another highly interesting approach for use of isotopic tracer is the use of stable isotopic tracers to track chemical changes or reactions on the molecular level. Exemplarily, usage of ammonium-based ionic liquids (IL) was simulated by means of artificial accelerated alteration. Subsequent evaluation of degradation products by mass spectrometry showed that certain cation moieties are prone to degradation. However, a comprehensive proposal of degradation mechanisms were not obtained so far [26].

To gain the maximum degree of information during artificial alteration of molecules of interest, a novel approach was designed. Not the target molecule itself was labelled with an isotopic moiety, but the atmosphere involved in the oxidative degradation of these substances consists solely of  $^{18}\text{O}$  isotopes to track the oxidation products derived from the gas-phase. The unique element of this approach is the application of a gas-phase stable isotopic tracer for the formation of degradation products to monitor this process instead of the more common labelling of the target molecule. Hence, a completely new approach in lubricant analysis was elaborated. In order to determine fuel component degradation on a molecular level, a combination of artificial alteration under oxygen pressure, a stable isotopic tracer, and GC-EI-MS was used to obtain detailed information on the oxidation products of oxygen-containing fuel components. This approach was applied to the fuel additive/replacement (9Z), (12Z)-octadecadienoic acid methyl ester (C18:2 ME) to develop the proof of concept. The elucidation of degradation process in case of oxygen-containing fuels and fuel components by means of the definite differentiation of oxygen origin in a degradation product proved to be feasible.

## 2. Materials and methods

### 2.1. Strategy

Fig. 1 gives an overview of the main elements of the approach developed and applied for the first time. As first step, this strategy was applied to a binary model mixture of fuel components. For developing the proof of concept discussed in this publication, a blending of C18:2 ME in n-dodecane (C12) was generated. Artificial alteration of these mixtures was then performed in a rotating closed pressurized vessel (RPVOT), one aliquot under  $^{16}\text{O}_2$  atmosphere, the other one under  $^{18}\text{O}_2$  atmosphere. From this setup, we obtained conventional degradation products on one hand, and products with a stable isotopic tracer on the other under otherwise identical conditions. Both aliquots were subjected to GC-EI-MS measurement to identify and characterize the degradation products based mainly on the retention time, molecular ions, and mass spectrometric fragmentation pattern (and database comparison). Comparison of alterations under both atmospheres then revealed the degree of oxidation and, moreover, exact determination of the origin of the oxygen atom was possible. This allowed the proposal of possible ways of formation for some of the main degradation products.

### 2.2. Model fuels

In order to reduce the complexity of the analytes and, hence, subsequent degradation products, model fuels simulating a simplified biodiesel blend were prepared at first hand. Therefore, n-dodecane (C12) was selected as reference representing a non-additive-containing, simplified diesel fuel. (9Z), (12Z)-Octadecadienoic acid methyl ester (C18:2 ME), one of the FAME in RME used for biodiesel, was added in 2 (w/w) % to the C12 to represent the biodiesel, both obtained from Sigma Aldrich (St. Louis, MO, USA) in GC grade quality ( $\geq 99\%$ ). Based on the findings regarding autoxidation of unsaturated FAME [8–12], C18:2 ME may be regarded as

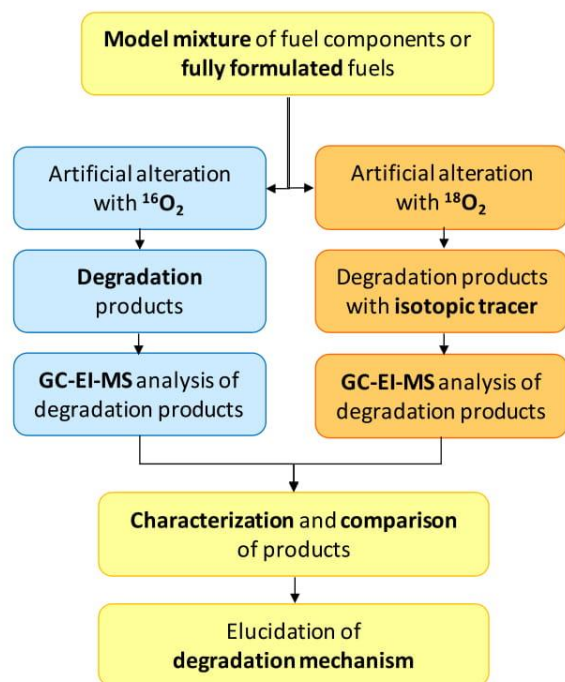


Fig. 1. Strategy comprising artificial alteration, a stable isotopic tracer, and GC-EI-MS.

one of the components where oxidation preferably starts.

### 2.3. Artificial alteration method and conventional analysis

The appropriate alteration method for this specific scope of work was developed in a previous work [10]. Briefly, a modified method utilizing a closed pressurized vessel that relates to the ASTM D 2272 (Rotary Pressure Vessel Oxidation Test, RPVOT) [27] was set up to collect all volatile components produced. The device mentioned in the standard norm is primarily designed for artificial alteration of turbine oil based on pressure drop upon oxidation. For suitable alteration of fuels and fuel components, less severe parameters regarding temperature and pressure were applied, and no catalyst was used. Alteration conditions of the modified RPVOT method as used for this work and the original standard ASTM D 2272 are given in Table 1.

Application of RPVOT for artificial alteration offers not only the possibility to collect the gaseous phase evolved during the degradation process, but also gives the opportunity to record the oxygen pressure curve on-line and, hence, the alteration condition.

The first pressure drop marks the start of oxidation processes. While the main part of the degradation takes place, a rapid pressure drop can be observed. The end of this oxidative process has been reached when there is no further pressure decrease, i.e., all oxygen is consumed by the available compounds. Alterations at this terminal point can be considered so-called lifetime alterations.

In order to achieve a proof of concept of the described approach, a sufficient amount of stable degradation products was necessary. Hence, as a first step, alteration to a defined endpoint was performed. According to the pressure curve at this point, defined by the authors, the main reaction processes had already taken place, and no further significant decrease in pressure was expected. Moreover, attention was paid to reach similar values for the pressure difference between start and endpoint in consecutive experiments. Consequently, the conditions of alteration were applied to the sample until the selected “endpoint” was reached and subsequently the experiment was stopped. Furthermore, if evaluated with appropriate analytical methods, this state provides plenty of information concerning a distinct number of degradation products as well as the end products.

Condition monitoring of the altered fuel aliquots was performed in terms of the following two conventional parameters:

- Neutralisation Number (NN)

The neutralisation number (NN) was determined according to standard DIN 51558 [28] by colour-indicator titration. The NN is defined as the amount of base, which is required to neutralise all acidic components in 1 g of sample aliquot.

- Water content

The water content was measured according to standard DIN 51777-2 [29] by the indirect method after Karl Fischer. Thereby, the water in the sample is evaporated at elevated temperatures, induced in a measuring cell and iodometrically determined.

### 2.4. Stable isotopic tracer

According to ASTM 2272, an oxygen atmosphere of 6.2 bar has to be applied. As the sample amount was reduced from 50 g to 15 g for the modified method, the pressure was reduced from 6.2 to 2.0 bar. For oxygen-containing fuel components and potential lubricant additives, the origin of oxygen can hardly be distinguished. For a clear assignment if the oxygen atoms in a degradation product

**Table 1**  
Comparison of alteration parameters of ASTM D 2272 and modified RPVOT.

|                        | ASTM D 2272 RPVOT             | Modified RPVOT  |
|------------------------|-------------------------------|---|
| System                 | closed pressured vessel       | closed pressured vessel   |
| Sample amount (g)      | 50                            | 15  |
| Temperature (°C)       | 150                           | 95  |
| Oxygen pressure (bar)  | 6.2                           | 2; <sup>16</sup> O <sub>2</sub> or <sup>18</sup> O <sub>2</sub> |
| Catalyst               | Cu coil, water                | none  |
| Endpoint of alteration | pressure decrease of 1.75 bar | constant final pressure   |

derives from the initial component or the oxidative attack by atmosphere, a stable isotopic tracer was applied. Hence, besides conventional <sup>16</sup>O<sub>2</sub> atmosphere, alterations with <sup>18</sup>O<sub>2</sub> atmosphere were performed in order to procure isotope labelled oxidation products. To remove ambient air from the vessel and the inlet system, the container was evacuated with an oil-free stroke piston vacuum pump. Oxygen atmospheres were applied with an appropriate oxygen-tight valve. <sup>16</sup>O<sub>2</sub> and <sup>18</sup>O<sub>2</sub> gases were used in purities of 99.998% and more than 99%, respectively. <sup>16</sup>O<sub>2</sub> was obtained from AirLiquide (Paris, France), and <sup>18</sup>O<sub>2</sub> from Sigma Aldrich (St. Louis, MO, USA).

### 2.5. GC-EI-MS

Qualitative information of the model mixture in fresh (before the start of the accelerated alteration process) as well as altered condition was obtained using an instrumental setup composed of a TriPlus autosampler and a Trace capillary Ultra GC coupled to a TSQ Quantum XLS mass spectrometer, all from Thermo Scientific (Austin, TX, USA).

In order to detect degradation products formed during alteration of the model fuels, fresh mixtures and altered sample were diluted to 5 (w/w) % in dichloromethane (DCM). Samples subjected to artificial alterations as well as the fresh model fuel were silylated due to expected presence of ionic and/or polar degradation products (e.g., containing active hydrogen as in case of acids). The applied silylation reagent N,O-bis(trimethylsilyl)-trifluoroacetamide (BSTFA) was used in mass excess (2:1) compared to sample weight, and reaction proceeded for 1 h at 70 °C. Silylation was applied to enhance volatility and avoid undesired adsorption, both resulting in improved sensitivity.

The injection volume of 1 µL was introduced to a programmable temperature vaporization injector (PTV) kept at 300 °C constant temperature with an applied split ratio of 1:25. Helium (He) carrier gas was set to 2 mL min<sup>-1</sup> constant flow. Chromatographic separation was performed by means of TG-17MS (composed of 50 %-diphenyl/50 %-dimethylpolysiloxane stationary phase) capillary column of 30 m length, 0.25 mm internal diameter (I.D.), and 0.25 µm film thickness obtained from Thermo Fisher Scientific (Waltham, MA, USA). The oven temperature programme started at 50 °C kept for 2 min, subsequently the oven was heated to 300 °C with a 7 °C min<sup>-1</sup> temperature ramp followed by a 10 min final isothermal step.

Transfer line was kept at 250 °C, and the effluent was ionized by electron impact (EI) ionization (70 eV) with the source temperature held at 200 °C, while the mass analyzer operated in full scan mode ranging from 40 to 650 mass-to-charge (*m/z*). For data acquisition and data processing, the Xcalibur v2.0 software was used. NIST library 14 and additional standard substances for hexanoic and octanoic acid, obtained from Sigma Aldrich (St. Louis, MO, USA) in GC grade quality (≥99%), were applied for the final identification of compounds.

## 3. Results and discussion

### 3.1. Fuel alteration

In Table 2, the applied model fuels with the respective alteration durations until complete oxygen consumption as well as water content and neutralisation number (NN) are given. The modified RPVOT experiments were performed according to the parameters listed in Table 1. Both lifetime alterations of C18:2 ME in C12 with the two oxygen isotopes were stopped after 42 and 44 h, respectively, indicating absence of influence of the respective isotope on reactivity. Beyond this point, no remarkable further decrease of the pressure was monitored.

As a reference, C12, the main component of the model mixture, was also subjected to modified RPVOT alteration. In this case, the endpoint of the alteration was reached after a significantly longer alteration duration, which reflects the higher stability of plain C12 against oxidation. As discussed later, regarding the build-up of degradation products as well as the pressure curve of the C18:2 ME alterations under both atmospheres, no influence of the <sup>18</sup>O isotope on the degradation process compared to the <sup>16</sup>O oxygen was observed. Moreover, good reproducibility of the independently performed alterations was obtained. Hence, the determination of water content and neutralisation number was performed only for C18:2 ME alteration with <sup>16</sup>O<sub>2</sub> as a representative. When reviewing the values after alteration for C12 and C18:2 ME, a higher neutralisation number (6.0 mg KOH g<sup>-1</sup>) was determined for C18:2 ME compared to the pure hydrocarbon (1.1 mg KOH g<sup>-1</sup>), which reflects the higher stability of C12. Water content in the fresh model fuels was determined with 70 mg kg<sup>-1</sup> for C18:2 ME and 40 mg kg<sup>-1</sup> for C12. A lower water content (600 mg kg<sup>-1</sup>) for the ME compared to C12 (2 g kg<sup>-1</sup>) was obtained.

Evaluation of the visual appearance after artificial alteration showed no deposit formation for any of the samples. Nevertheless, a slight turbidity for the C18:2 ME aliquots was visible. This may result from the lower solubility of the polar degradation products in the nonpolar main component C12 and can be considered as precursors for sludge and deposit formation. The disability of diesel fuels to dissolve polar products formed during alteration processes was already observed in previous works [10]. Consequently, their precipitation results in turbidity and/or final solid deposits.

Obviously, the model fuel (C12) without any unsaturated components showed much higher stability against oxidative stress

**Table 2**  
Model fuels – Alteration duration till final constant pressure oxygen atmosphere, water content (after alteration), and NN (after alteration).

| Analyte  | Duration (h) | Oxygen                       | Water content (mg/kg) after alteration | NN (mg KOH/g) after alteration |
|----------|--------------|------------------------------|--|--------------------------------|
| C18:2 ME | 42           | <sup>16</sup> O <sub>2</sub> | 600                                    | 6                              |
| C18:2 ME | 44           | <sup>18</sup> O <sub>2</sub> | 575                                    | 5.9                            |
| C12      | 166          | <sup>16</sup> O <sub>2</sub> | 2000                                   | 1.1                            |

compared with the mixture containing the unsaturated C18:2 ME (see Table 2). These observations can be explained by the hypothesis that unsaturated ME such as C18:2 serve as oxidation starters in diesel fuel blends and, hence, these blends exhibit reduced oxidative stability.

Fig. 2 shows the pressure curve over time of alterations of C12 under  $^{16}\text{O}$  atmosphere, and C18:2 ME under  $^{16}\text{O}$  atmosphere and  $^{18}\text{O}$  atmosphere, respectively, also confirming that application of different oxygen isotopes had no consequence on the alteration duration.

At the beginning of the pressure curve plotting of the ME alteration, a slight pressure increase was monitored resulting from heating of the pressurized vessel in the oil bath. After approximately 2 h, the first pressure drop indicates the start of oxidation reactions. The endpoint of the alteration with an almost constant pressure level was reached after 42 and 44 h, respectively. For both ME alterations, pressure curves with very similar progress were obtained. At the endpoint, an almost equal pressure difference ( $\Delta p = 0.52$  bar and  $\Delta p = 0.53$  bar, respectively) and, hence, a similar oxygen consumption was determined. Compared to the model mixture with C18:2 ME, the decline of the pressure curve of C12 was remarkably smoother and more continuous. The pressure decrease at the endpoint was monitored with  $\Delta p = 0.48$  bar. Moreover, the start of oxidation was observed after 7 h, substantially later than in the presence of a ME. These observations corroborate the assumption of unsaturated ME acting as oxidation starters.

### 3.2. Identification of degradation products

Subsequent to alteration, diluted and silylated model fuels – fresh as well as altered – were analyzed using GC-MS with EI in the positive ion mode. Fig. 3 shows the total ion chromatograms (TIC) of the altered C18:2 ME – with and without stable isotopic tracer – and the altered C12.

Comparison of the degradation products of both C18:2 ME alterations exhibit no influence of the oxygen labelling on the formed components, and also good reproducibility of the RPVOT alteration. Although C12 is the main component of the C18:2 ME model mixture, aliquots of both alterations show clearly distinct degradation patterns. Hence, it can be confirmed overall that most degradation products derive from C18:2 ME and not from C12. For the most important and abundant peaks marked in Fig. 3 (a to h), the following parameters are given in Table 3 for artificial alteration

under  $^{16}\text{O}_2$  and  $^{18}\text{O}_2$  atmosphere, respectively: retention time, calculated as well as detected monoisotopic mass of the molecular ion, highest detected  $m/z$  value, and deviation between calculated mass and the highest  $m/z$  value.

Mainly, carboxylic acids from propanoic acid up to dodecanoic acids as well as dicarboxylic acids were formed as degradation products of C18:2 ME. Because Table 3 gives only the main products, the carboxylic acids are listed only up to nonanedioic acid. Due to silylation, they were detected as trimethylsilyl (TMS) esters. It was observed that for none of the carboxylic acid TMS esters a molecular ion was detectable. However, for all these compounds a fragment ion, namely  $[M - 15]^+$  was clearly detectable, which is well known. This loss most probably derives from the removal of one methyl group from the TMS part. These observations were also described in literature for molecules with a TMS derivatization measured with EI-MS [30,31]. Besides, the fragmentation pattern of all carboxylic acids is very similar and only differs in the increasing detectable  $m/z$  value, always representing  $[M - 15]^+$  ions correlating with higher number of C-atoms.

Figure S-1 in the supporting information shows the fragmentation pattern of an analytical standard of C8:0 TMS ester as a representative for all carboxylic acid TMS esters of various chain lengths. As already observed for the degradation products in the C18:2 ME model fuel, the molecular ion was not detectable even for an analytical standard solution. The proposed fragmentation for the most abundant and typical fragments (a to k) are given in Tables S-1.

Identification of selected carboxylic acid TMS esters was not only performed via NIST library comparison, but also corroborated with an additional analytical standard. Figure S-2 shows good correlation with the retention time of C6:0 TMS ester in the C18:2 ME alteration sample (1A) and the analytical standard (1B). Beyond that, fragmentation patterns are similar (2A and 2B), and hence, a confirmation via retention time and fragmentation behaviour was required. This was indeed obtained for the given representative example.

Moreover, alcohols silylated to ethers, esters, ketones (see 1–3 in Fig. 3), and alkanes, branched and linear, were detected as further degradation products of C18:2 ME. Analysis of C12 alteration also revealed the formation of carboxylic acids (C4:0 to C8:0), but in considerably lower amounts than in the model fuels containing C18:2 ME. Additionally, branched and linear alkanes, alcohols, and ketones (e.g., methyl-9-oxododecanoate) are further degradation products of C12, which were only detected in low

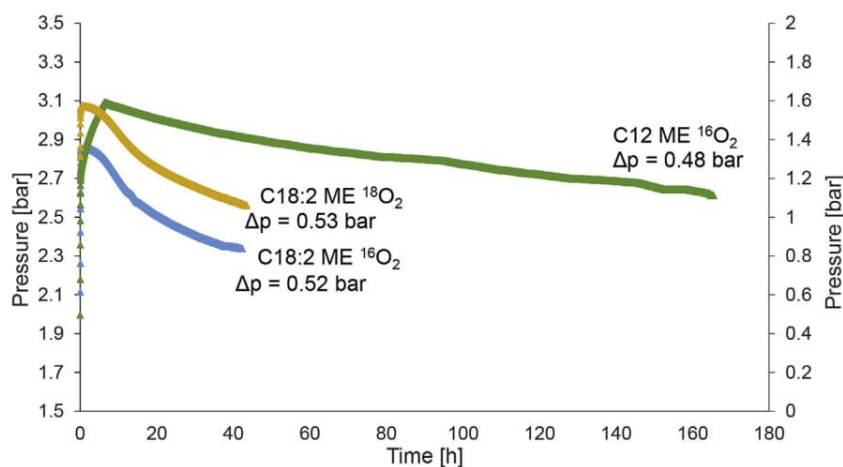
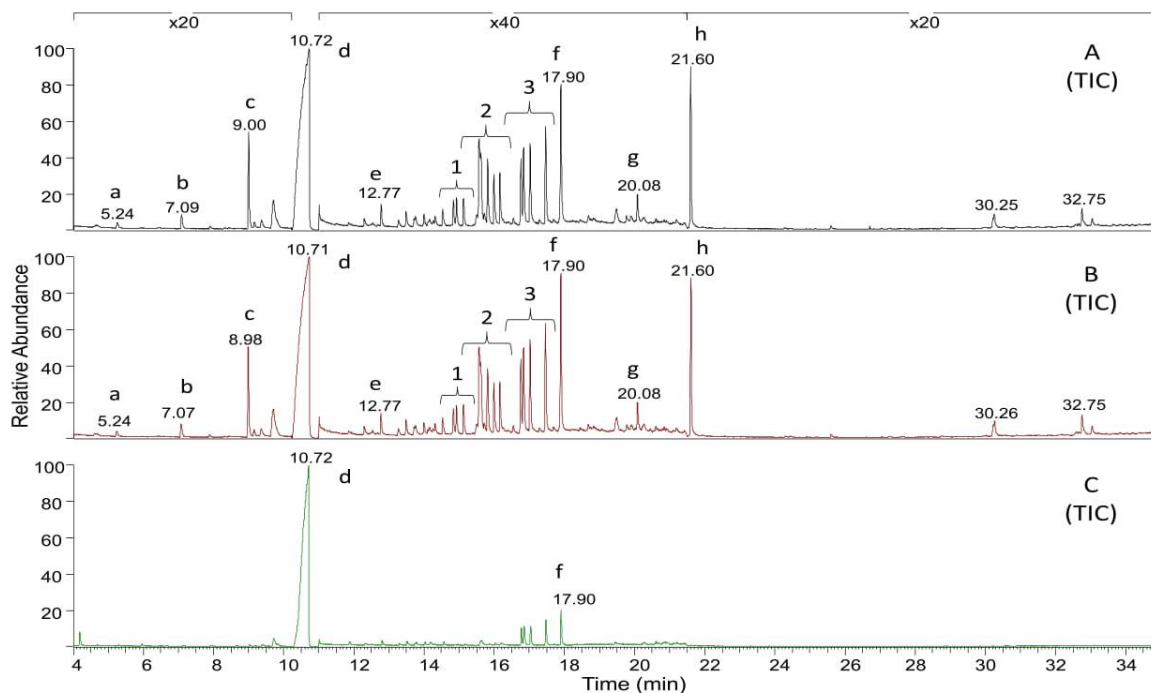


Fig. 2. Pressure curve of C12 alteration as well as C18:2 ME alteration with  $^{16}\text{O}_2$  and  $^{18}\text{O}_2$  atmosphere, respectively, depicting the pressure drop.



**Fig. 3.** Total ion chromatogram (TIC) of C18:2 ME altered under  $^{16}\text{O}_2$  atmosphere (A), C18:2 ME altered under  $^{18}\text{O}_2$  atmosphere (B) and of altered C12 (C). In both alterations of C18:2 ME, the entire amount of target molecule was degraded. Alteration products a to h are given in Table 3, respectively. 1 represents a group of alcohols, 2 a group of ketones, and 3 a group of esters.

**Table 3**

Main degradation products of C18:2 ME altered under  $^{16}\text{O}_2$  and  $^{18}\text{O}_2$  atmosphere, respectively.  $m/z$  value of the monoisotopic molecular ion (calculated and detected), the highest  $m/z$  value of an ion detected and the deviation are given. Molecules in bold letters are main degradation products.

| $^{16}\text{O}_2$ Analyte                              | Retention time (min) | Calculated monoisotopic isotopic $m/z$ value | Detected mono-isotopic $m/z$ value | Highest detected $m/z$ value | Deviation (ppm) |
|--|----------------------|--|------------------------------------|------------------------------|-----------------|
| <b>a</b> Butanoic acid TMS ester                       | 5.24                 | 160.1  | –                                  | 145.2                        | –               |
| <b>b</b> Pentanoic acid TMS ester                      | 7.09                 | 174.1  | –                                  | 159.3                        | –               |
| <b>c</b> <b>Hexanoic acid TMS ester</b>                | 9.00                 | 188.3  | –                                  | 173.3                        | –               |
| <b>d</b> Dodecane                                      | 10.72                | 170.2  | 170.3                              | 170.3                        | +0.1            |
| <b>e</b> Octanoic acid TMS ester                       | 12.77                | 216.2  | –                                  | 201.3                        | –               |
| <b>f</b> <b>Methyl-9-oxodecanoate</b>                  | 17.90                | 200.1  | 199.5                              | 199.5                        | –0.6            |
| <b>g</b> Nonanoic acid bis(TMS)ester                   | 20.08                | 332.2  | –                                  | 245.3                        | –               |
| <b>h</b> <b>9-Methoxy-9-oxononanoic acid TMS ester</b> | 21.60                | 274.2  | –                                  | 259.3                        | –               |

| $^{18}\text{O}_2$                                      | Retention time (min) | Calculated monoisotopic isotopic $m/z$ value | Detected mono-isotopic $m/z$ value | Highest detected $m/z$ value | Deviation (ppm) |
|--|----------------------|--|------------------------------------|------------------------------|-----------------|
| <b>a</b> Butanoic acid TMS ester                       | 5.24                 | 164.1  | –                                  | 149.2                        | –               |
| <b>b</b> Pentanoic acid TMS ester                      | 7.07                 | 178.1  | –                                  | 163.3                        | –               |
| <b>c</b> <b>Hexanoic acid TMS ester</b>                | 8.98                 | 192.3  | –                                  | 177.3                        | –               |
| <b>d</b> Dodecane                                      | 10.71                | 170.2  | 170.3                              | 170.3                        | +0.1            |
| <b>e</b> Octanoic acid TMS ester                       | 12.77                | 220.2  | –                                  | 205.4                        | –               |
| <b>f</b> <b>Methyl-9-oxodecanoate</b>                  | 17.90                | 202.1  | 201.5                              | 201.5                        | –0.6            |
| <b>g</b> Nonanoic acid bis(TMS)ester                   | 20.08                | 336.2  | –                                  | 249.3                        | –               |
| <b>h</b> <b>9-Methoxy-9-oxononanoic acid TMS ester</b> | 21.60                | 278.2  | –                                  | 263.4                        | –               |

abundance even after an alteration period 4 times longer than for the model fuel. However, one has to keep in mind that C18:2 ME is known to promote the initiation step of autoxidation (see introduction). A much lower oxidation stability of branched, aromatic and unsaturated hydrocarbons compared to linear and unbranched hydrocarbons is explained by the difference in reactivity of the respective radicals [32]. Therefore, the presence of an unsaturated compound and its role in autoxidation could influence the stability as well as the amount of products formed of C12. Although alteration of neat C12 was performed and the sparse originating degradation products were analyzed carefully, an effect of the model biodiesel C18:2 ME component on the alteration of the

model diesel component C12, evoking amplified formation of products originating from C12, cannot be determined. For this purpose, an adaption of the target molecules, e.g., by introducing an isotope labelled alkyl moiety, could reveal the origin of the shorter chain oxidation products from C12 or C18:2 ME.

### 3.3. Stable isotopic tracer

A stable oxygen isotopic tracer was applied during alteration to overcome the difficulty of assignment of the oxygen origin in degradation products from oxygen-containing components such as the target molecule C18:2 ME in the model fuel. Subsequent GC-El-

MS analysis clearly revealed the sites of bond cleavage and oxidative attack as well as the degree of oxidation by comparison of mass spectra from samples altered under  $^{16}\text{O}_2$  atmosphere with those from aliquots altered with  $^{18}\text{O}_2$ . Hence, the differentiation of oxygen origin – either from the fuel itself or yielded via oxidation – in degradation products of oxygen-containing fuels and fuel components, e.g. ethers and esters, is possible.

Preferential cleavage of the molecule during oxidative attack at or in the direct neighbourhood of a double bond was confirmed by detailed interpretation of the obtained mass spectra. Exemplarily, Fig. 4 illustrates the derived products of C18:2 ME degradation via oxidation to octanoic acid.

As the active hydrogens of acids were derivatized with a trimethylsilyl group (TMS) in order to improve volatility for the analysis, they were detected as esters. Compared to mass spectra of alterations under  $^{16}\text{O}_2$  atmosphere (A), the peaks of the oxygen-containing fragments of the  $^{18}\text{O}_2$  alteration (B) exhibit an  $m/z$  shift of +2 Dalton (Da) for one O atom and +4 Da for fragments with two O atoms. The shift of the hardly detectable molecular ion  $[\text{M}]^+$  from 216.3 in conventional atmosphere to 220.3 for the molecular ion under  $^{18}\text{O}_2$  atmosphere  $[\text{M}^{18}\text{O}]^+$  clearly reveals the presence of two  $^{18}\text{O}$  atoms in the entire octanoic acid TMS ester molecule. Furthermore, several fragment ions shifting by +4 Da, e.g.,  $m/z$  116.9 to 120.9, 144.9 to 148.9 or 201.1 to 205.1, respectively, are visible in the mass spectra. These fragment ions contain two  $^{18}\text{O}$  atoms, whereas the fragment ions  $m/z$  74.9 and 76.9 contain only one  $^{18}\text{O}$  atom.

The assignment of the respective oxygen isotope was possible by the careful comparison of the fragment pattern of the oxidation products obtained by alteration under  $^{16}\text{O}_2$  and  $^{18}\text{O}_2$  atmosphere, respectively.

Thus, by comparing mass spectra of artificial alterations under

$^{16}\text{O}_2$  and  $^{18}\text{O}_2$  atmospheres, one can elucidate the formation of the degradation product of the target molecule as depicted in Fig. 4. During alteration, cleavage next to the double bond between C9 and C10 takes place resulting in a carboxyl acid ME and the unsaturated alkene. Due to consecutive oxidative attack of the unsaturated alkene, another carboxylic acid, i.e., octanoic acid, can be formed. Moreover, the double bond of the resulting ME between C9 and C10 can undergo further oxidative reactions, resulting in a methyl-9-oxodecanoate.

As the C18:2 molecule contains  $^{16}\text{O}$  atoms almost exclusively, and octanoic acid consists of 2  $^{18}\text{O}$  atoms in contrast, these oxygen atoms derive from oxidation when performed under  $^{18}\text{O}$  isotope atmosphere, and not from the target molecule itself. Hence, by tracking the oxygen isotopes, the formation of degradation products is properly identified.

With the residual ME fragment after cleavage (see Fig. 4 and Figure S-4), further oxidation reactions can take place as mentioned above, which leads to molecules containing both  $^{16}\text{O}$  and  $^{18}\text{O}$  atoms. As example, 9-methoxy-9-oxononanoic acid is shown in Figure S-3. Although four oxygen atoms are present in the molecule in total, the mass shift thereof is only +4 Da. This leads to the finding that two oxygen atoms derive from the ME fragment, while two are from the stable isotopic tracer alteration with  $^{18}\text{O}_2$ . Moreover, and as demonstrated in Figure S-4, the degradation and oxidation of C18:2 ME to hexanoic acid is an example for the cleavage of the molecule within the C-C double bond between C12 and C13. Similar to the formation of octanoic acid, this results in a carboxyl acid ME fragment that can be further oxidized to 9-methoxy-9-oxononanoic acid, and, after oxidative attack of the other fragment, a carboxylic acid. Among the formed carboxylic acids with different chain lengths, the hexanoic acid was detected as the most abundant.

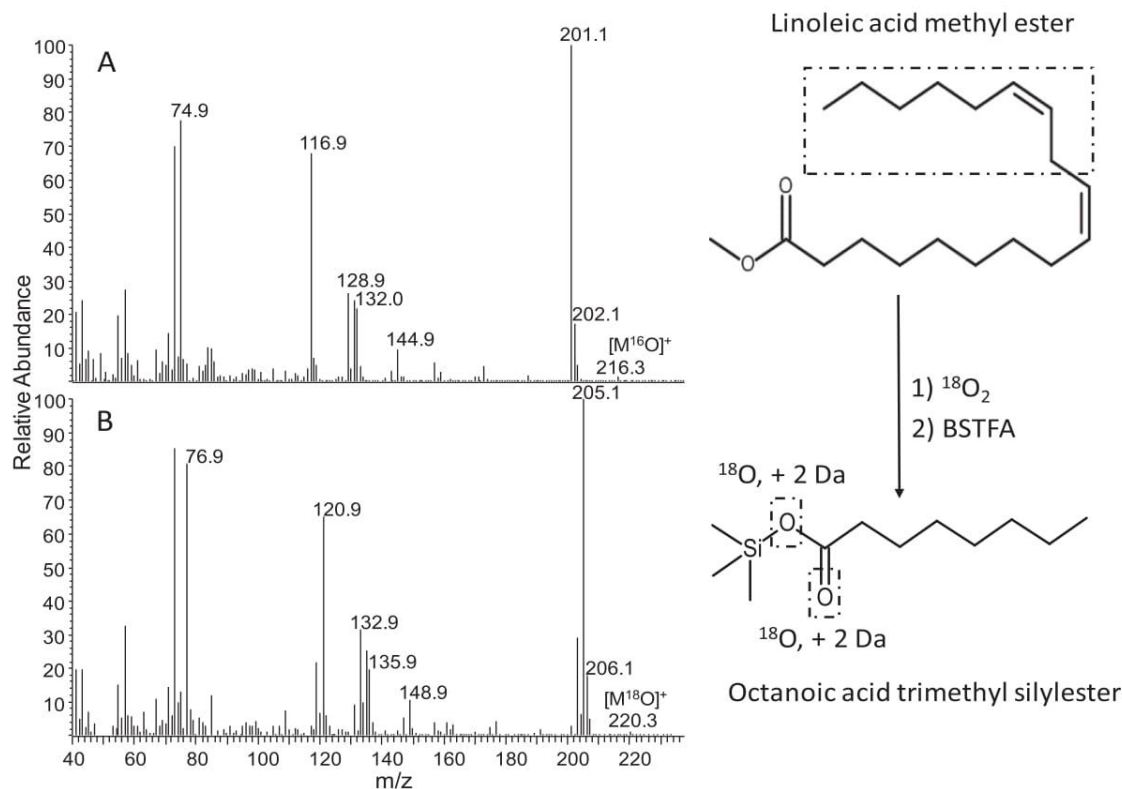


Fig. 4. Mass spectra of octanoic acid TMS ester without (A) and with (B) stable  $^{18}\text{O}$  isotopic tracer. Comparison of the mass spectra reveals the origin of the degradation product.

Based on the examples given, it was shown that one can distinctly assign the oxygen origin by detailed interpretation of the fragments. Carboxylic acids of two different chain lengths as well as esters thereof were presented to provide the proof of concept, due to the fact that they were the most abundant degradation products of C18:2 ME altered under oxygen atmosphere.

In summary, this strategy of a stable oxygen isotopic tracer in combination with GC-EI-MS can be regarded as a general tool of assignment of the oxidative attack during the degradation of various molecules of interest containing oxygen atoms.

Furthermore, various products containing  $^{18}\text{O}$  caused by oxidative attack of the alteration atmosphere were detected. As the focus of this study was put on the introduction and presentation of this novel strategy, degradation products such as alcohols, ethers as well as alkane-fragments are not discussed in detail in this paper. Nevertheless, these molecules and in particular precursors thereof may also contribute to the complex radical oxidation mechanism of the target molecule at some times during the reaction. Therefore, systematic sampling at various times of the reaction to elucidate the products built at distinct states of the degradation process are of high interest. The structural position where oxidation reactions initially started on a target molecule can be determined via detection of particular fragment ions either containing  $^{16}\text{O}$  or  $^{18}\text{O}$  atoms.

#### 4. Conclusions

The proof of concept for a novel strategy for the structure elucidation of formed oxidative degradation products of esters with a representative model fuel was successfully demonstrated by joint use of accelerated artificial alteration, a stable isotopic tracer, and GC-EI-MS. In detail, C12 simulating the diesel fuel matrix was spiked with the C18:2 ME as representative of an important biodiesel component. This model fuel was subjected to artificial alteration in a closed pressurized vessel (RPVOT) under a well-defined oxygen atmosphere to accelerate oxidation processes. Beside the adjustment of tailor-made alteration conditions, the RPVOT method offers the advantage of the collection of all degradation products, finally also including potential volatiles. Artificial alterations were performed under oxygen atmosphere consisting of the most abundant oxygen isotope  $^{16}\text{O}_2$  and also under  $^{18}\text{O}_2$  isotope atmosphere to clearly differentiate between oxygen atoms in the original ester from those incorporated via oxidation.

Comparing the stability of the model fuel containing C18:2 ME with pure hydrocarbon samples (C12), a considerably higher resistance against oxidative stress of pure C12 was observed.

A large number of oxygen containing products such as carboxylic acids of various chain lengths, esters, ethers, ketones, alcohols, but also alkanes and alkenes were identified for the model fuel. C12 showed significantly less degradation products, amongst them small amounts of C4:0 to C8:0 carboxylic acids, esters, ketones, and alcohols. As most of the degradation products contain oxygen, the aim was to identify the origin of the oxygen atoms. The degradation reactions responsible for the main degradation products deriving from the C18:2 ME target molecule could be proven by precise tracking of oxygen origin.

The complexity of reaction pathways such as oxidation also requires the description of intermediate degradation products for a full understanding of the mechanisms. To determine these intermediates, sampling at various time stages during the alteration process – according to the oxygen consumption related to the pressure curve – will be carried out in the future.

Based on these findings, beneficial adaptations of fuels and additives regarding the improvement of stability will allow to reveal

the optimum formulation of lubricants and fuels.

#### Acknowledgements

The work presented was funded by the Austrian COMET Programme (Project XTribology, no. 849109) and carried out at the “Excellence Centre of Tribology” (AC2T research GmbH).

#### Appendix A. Supplementary data

Supplementary data related to this article can be found at <https://doi.org/10.1016/j.aca.2017.09.009>.

#### References

- [1] United Nations Framework Convention On Climate Change. [http://unfccc.int/paris\\_agreement/items/9485.php](http://unfccc.int/paris_agreement/items/9485.php) (2017-05-26; 17:13 pm MEST).
- [2] S.N. Naik, V.V. Goud, P.K. Rout, A.K. Dalai, *Renew. Sustain. Energy Rev.* 14 (2010) 578–597.
- [3] M.A. Oehlschläger, H. Wang, M.N.J. Sexton, *Therm. Sci. Eng. Appl.* 5 (2013), 021006/1-021006/9.
- [4] R. Mythili, P. Venkatchalam, P. Subramanian, D. Uma, *Int. J. Energy Res.* 38 (10) (2014) 1233–1259.
- [5] FCIO Fachverband der chemischen Industrie Österreichs: Biokraftstoffberichte Österreich. <http://www.biokraft-austria.at/> (2017-05-25; 10:40 pm MEST).
- [6] Global Agricultural Information Network (GAIN), EU Biofuels Annual 2016 (EU-28), Report Number NL6021, 2016-06-29. [https://gain.fas.usda.gov/Recent%20GAIN%20Publications/Biofuels%20Annual\\_The%20Hague\\_EU-28\\_6-29-2016.pdf](https://gain.fas.usda.gov/Recent%20GAIN%20Publications/Biofuels%20Annual_The%20Hague_EU-28_6-29-2016.pdf) (2017-08-01, 10:34 am MEST).
- [7] K. Bacha, A. Ben-Amara, A. Vannier, M. Alves-Fortunato, M. Nardin, *Energy Fuel* 29 (2015) 4345–4355.
- [8] H.W.-S. Chan, D.T. Coxor, K.E. Peers, K.R. Price, *Food Chem.* 9 (1–2) (1982) 21–34.
- [9] N.A. Porter, S.E. Caldwell, K.A. Mills, *Lipids* 30 (4) (1995) 277–290.
- [10] Z.A.M. Zielinski, D.A.J. Pratt, *Org. Chem.* 82 (2017) 2817–2825.
- [11] W.Y. Cobb, E.A.J. Day, *Am. Oil Chem. Soc.* 42 (1965) 420–422.
- [12] H.W.-S. Chan, G. Levett, J.A. Matthew, *Chem. Phys. Lipids.* 24 (1979) 245–256.
- [13] C. Besser, L. Pisarova, M. Frauscher, H. Hunger, N. Dörr, U. Litzow, A. Orfanoti, *Fuel* 206C (2017) 524–533.
- [14] M. Serrano, M. Martinez, J. Aracil, *Fuel Process. Technol.* 116 (2013) 135–141.
- [15] G. Karavalakis, S. Stournas, D. Karonis, *Fuel* 89 (2010) 2483–2489.
- [16] DIN EN 15751, Automotive Fuels – Fatty Acid Methyl Ester (FAME) Fuel and Blends with Diesel Fuel – Determination of Oxidation Stability by Accelerated Oxidation Method, Deutsches Institut für Normung, Berlin, Germany, 2014.
- [17] G. Karavalakis, D. Hilari, L. Givalou, D. Karonis, S. Stournas, *Energy* 36 (2011) 369–374.
- [18] E. Farmer, A.J. Sundralingam, *Chem. Soc.* (1942) 121–139.
- [19] J.L.Q. Bolland, *Rev. Chem. Soc.* 3 (1949) 1–21.
- [20] J. Hall, R. Davies, N. Long, S. Marsh, Abstracts of Papers, 241st ACS National Meeting & Exposition, Anaheim, CA, United States, 2011. March 27–31, FUEL-157.
- [21] G. Lercker, M.T. Rodriguez-Estrada, M. Bonoli, *J. Chromatogr. A* 985 (2003) 333–342.
- [22] R.R. Catharino, H.M.S. Milagre, S. Saraiva, C.M. Garcia, U. Schuchardt, M.N. Eberlin, *Energy Fuel* 21 (2007) 3698–3701.
- [23] Commission on isotopic abundances and atomic weights, International Union of pure and applied chemistry (IUPAC). <http://www.ciaaw.org/oxygen.htm> (2016-04-21; 16:50 pm MEST).
- [24] J. Laeter de, J. Böhlke, P. Bièvre de, H. Hidaka, H. Peiser, K. Rosman, P. Taylor, IUPAC technical report, *Pure Appl.* 75 (2003) 683–800.
- [25] O. Charour, D. Cobice, J. Malone, *J. Pharm.* 113 (2015) 2–20.
- [26] L. Pisarova, C. Gabler, N. Dörr, E. Pittenauer, G. Allmaier, *Tribol. Int.* 46 (2012) 73–83.
- [27] ASTM D 2272, Standard Test Method for Oxidation Stability of Steam Turbine Oils by Rotating Pressure Vessel, ASTM International, West Conshohocken (PA, USA), 2014.
- [28] DIN 51558, Testing of Mineral Oils; Determination of Neutralization Number by Color-indicator Titration, Deutsches Institut für Normung, Berlin, Germany, 1979.
- [29] DIN 51777–2, Testing of Mineral Oil Hydrocarbons and Solvents; Determination of Water Content According to Karl Fischer; Indirect Method, Deutsches Institut für Normung, Berlin, Germany, 1974.
- [30] B. Molnár, B. Fodor, I. Boldizsár, I. Molnár-Perl, *J. Chromatogr. A* 1440 (2016) 172–178.
- [31] D. Dejongh, T. Radford, J. Hribar, S. Hanessian, M. Bieber, G. Dawson, C.J. Sweeley, *Am. Chem. Soc.* 91 (1969) 1728–1740.
- [32] T. Mang, W. Dresel, *Lubricants and Lubrication*, WILEY-VCH, Weinheim, Germany, 2001, ISBN 3-527-29536-4, p. 84f.

## Supporting information

### Elucidation of oxidation and degradation products of oxygen containing fuel components by combined use of a stable isotopic tracer and mass spectrometry

Marcella Frauscher<sup>a,b</sup>, Charlotte Besser<sup>a</sup>, Nicole Dörr<sup>a,\*</sup>, Günter Allmaier<sup>b</sup>

<sup>a</sup> ACZT research GmbH, Viktor-Kaplan-Strabe 2C, 2700 Wiener Neustadt, Austria

<sup>b</sup> Institute of Chemical Technologies and Analytics, Vienna University of Technology, Getreidemarkt 9/164, Vienna, Austria

#### Supporting information includes

Figure S-1: Typical EI fragmentation pattern of hexanoic acid trimethylsilyl ester (C6:0 TMS ester) at -70 eV. The molecular ion at  $m/z$  188.1 (i) is hardly visible. The most abundant and relevant fragments are marked (a to j) and described in table S-1.

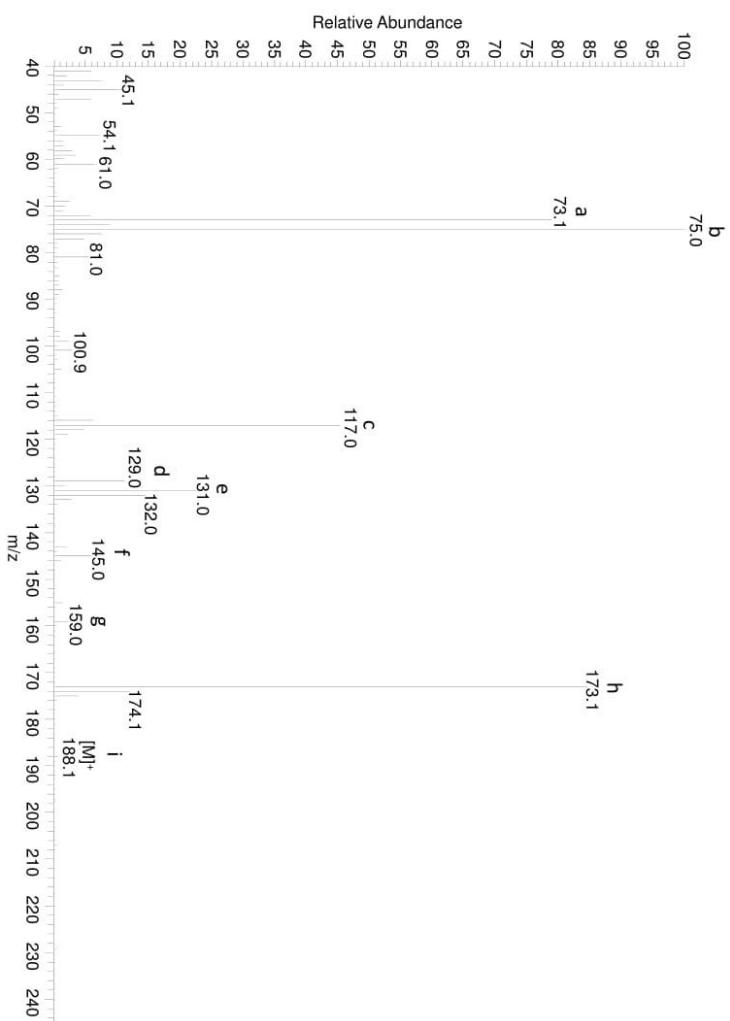
Table S-1: Fragment ions of C6:0 TMS ester with proposed elemental composition of the fragments.

Figure S-2: Total ion chromatogram (TIC) of C18:2 ME alteration depicting the C6:0 TMS ester (1A) and C8:0 TMS ester standard (1B) at a retention time of 8.98 and 8.97 min, respectively.

Fragmentation pattern of the C6:0 TMS ester are given for the alteration (2A) and the standard (2B).

Figure S-3: Mass spectra of 9-methoxy-9-oxononanoic acid TMS ester without (A) and with (B) stable <sup>18</sup>O isotopic tracer obtained due to oxidation under <sup>18</sup>O<sub>2</sub> atmosphere. Comparison of the mass spectra reveals the origin of the degradation product.

Figure S-4: Mass spectra of hexanoic acid TMS ester without (A) and with (B) stable <sup>18</sup>O isotopic tracer obtained due to oxidation under <sup>18</sup>O<sub>2</sub> atmosphere. Comparison of the mass spectra reveals the origin of the degradation product.



**Figure S-1:** Typical EI fragmentation pattern of hexanoic acid trimethylsilyl ester (C6:0 TMS ester) at 70 eV. The molecular ion at m/z 188.1 (i) is hardly visible. The most abundant and relevant fragments are marked (a to i) and described in table S-1.

**Table S-1:** Fragment ions of C<sub>6</sub>:0 TMS ester with proposed elemental composition of the fragments.

| Peak | m/z value | Proposed fragment  |
|------|-----------|--|
| a    | 73.1      | [Si(CH <sub>3</sub> ) <sub>3</sub> ] <sup>+</sup>                |
| b    | 75.0      | [Si(CH <sub>3</sub> ) <sub>2</sub> OH] <sup>+</sup>              |
| c    | 117.0     | [M-CH <sub>3</sub> -C <sub>4</sub> H <sub>8</sub> ] <sup>+</sup> |
| d    | 129.0     | [M-CH <sub>3</sub> -C <sub>3</sub> H <sub>8</sub> ] <sup>+</sup> |
| e    | 131.0     | [M-CH <sub>3</sub> -C <sub>3</sub> H <sub>6</sub> ] <sup>+</sup> |
| f    | 145.0     | [M-CH <sub>3</sub> -C <sub>2</sub> H <sub>4</sub> ] <sup>+</sup> |
| g    | 159.0     | [M-CH <sub>3</sub> -CH <sub>2</sub> ] <sup>+</sup>               |
| h    | 173.1     | [M-CH <sub>3</sub> ] <sup>+</sup>                                |
| i    | 188.1     | [M] <sup>+</sup>   |

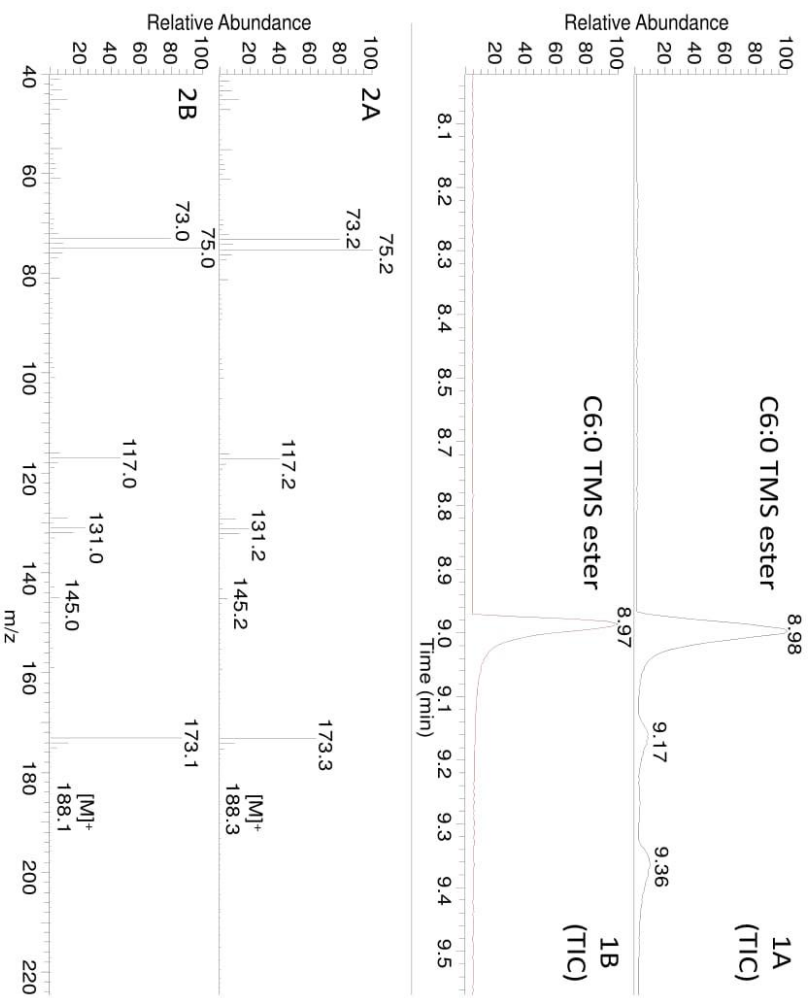


**Figure S-2:** Total ion chromatogram (TIC) of C18:2 ME alteration depicting the C6:0 TMS ester (1A) and C8:0 TMS ester standard (1B) at a retention time of 8.89 and 8.97 min, respectively. Fragmentation pattern of the C6:0 TMS ester are given for the alteration (2A) and the standard (2B).

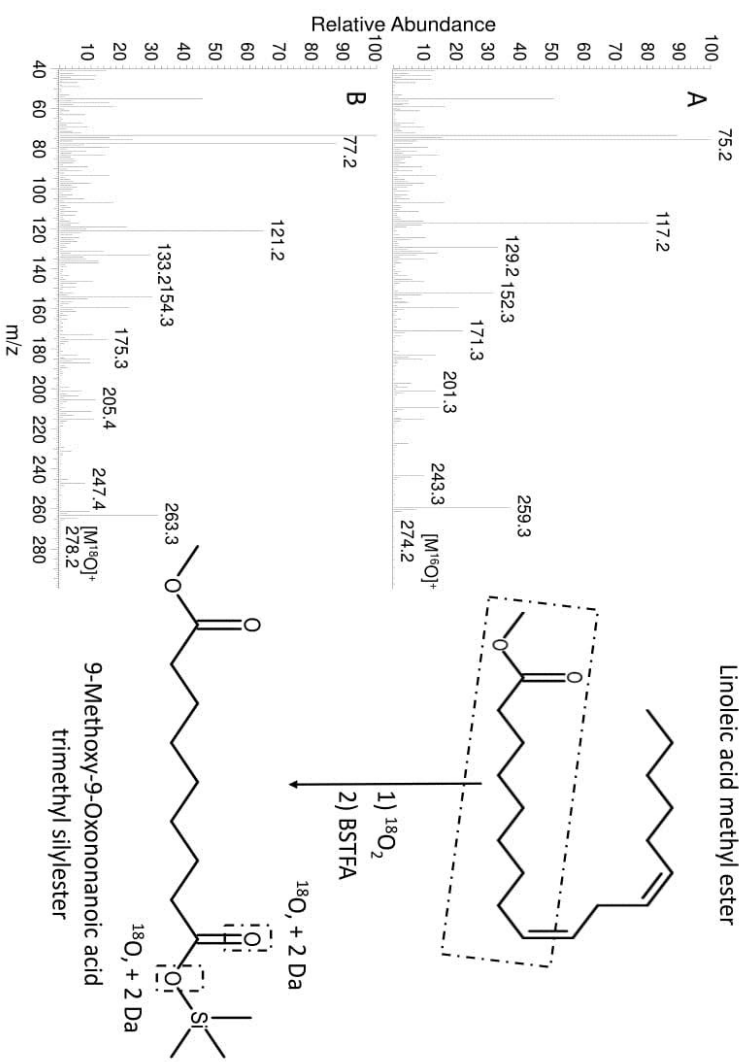


**Figure S-3:** Mass spectra of 9-methoxy-9-oxononanoic acid TMS ester without (A) and with (B) stable  $^{18}\text{O}$  isotopic tracer obtained due to oxidation under  $^{18}\text{O}_2$  atmosphere. Comparison of the mass spectra reveals the origin of the degradation product.

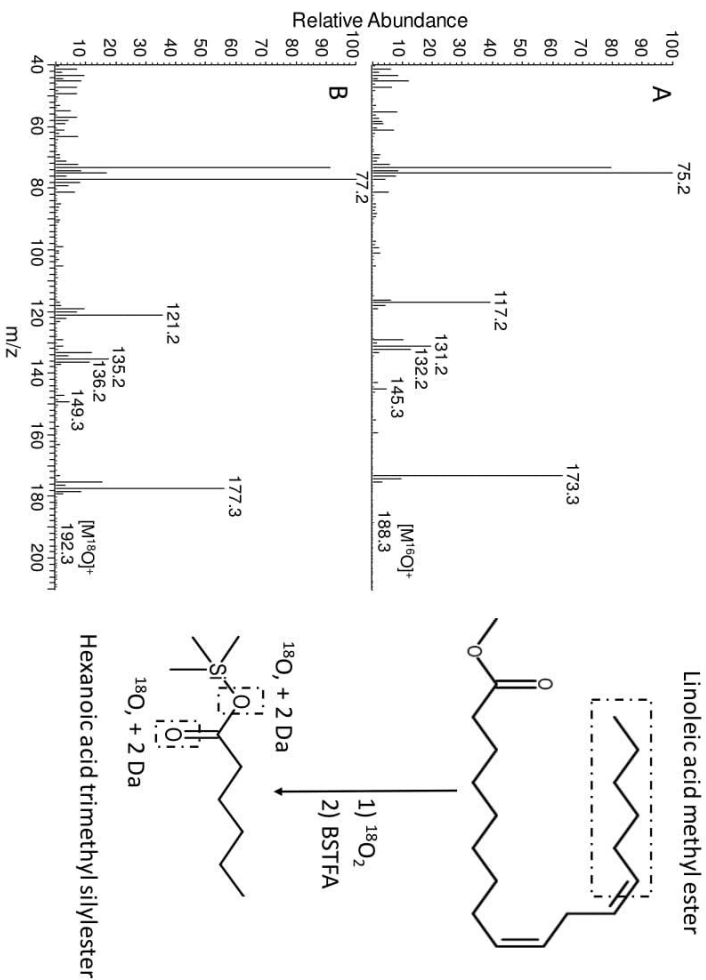


**Figure S-4:** Mass spectra of hexanoic acid TMS ester without (A) and with (B) stable  $^{18}\text{O}$  isotopic tracer obtained due to oxidation under  $^{18}\text{O}_2$  atmosphere. Comparison of the mass spectra reveals the origin of the degradation product.

## **2.3 Publication 3 - Time-resolved quantification of phenolic antioxidants and oxidation products in a model fuel by GC-EI-MS/MS**

In press (Energy & Fuel)

The publication is reprinted on the following pages

# Time-resolved quantification of phenolic antioxidants and oxidation products in a model fuel by GC-EI-MS/MS

Marcella Frauscher<sup>a,c\*</sup>, Adam Agocs<sup>a,c</sup>, Charlotte Besser<sup>a</sup>, Alexandra Rögner<sup>b</sup>, Günter Allmaier<sup>c</sup> and Nicole Dörr<sup>a</sup>

<sup>a</sup> AC2T research GmbH, Viktor-Kaplan-Straße 2C, 2700 Wiener Neustadt, Austria  
[marcella.frauscher@ac2t.at](mailto:marcella.frauscher@ac2t.at), [charlotte.besser@ac2t.at](mailto:charlotte.besser@ac2t.at), [nicole.doerr@ac2t.at](mailto:nicole.doerr@ac2t.at)

<sup>b</sup> OMV Refining & Marketing GmbH, Mannswörtherstraße 28, 2320 Schwechat, Austria  
[alexandra.roegner@omv.com](mailto:alexandra.roegner@omv.com)

<sup>c</sup> Institute of Chemical Technologies and Analytics, TU Wien (Vienna University of Technology), Getreidemarkt 9/164, Vienna, Austria  
[guenter.allmaier@tuwien.ac.at](mailto:guenter.allmaier@tuwien.ac.at)

\* Author to whom correspondence should be addressed

Marcella Frauscher

AC2T research GmbH, Viktor Kaplan-Straße 2, 2700 Wiener Neustadt, Austria

Tel: +43 2622 81600 304

E-mail address: [marcella.frauscher@ac2t.at](mailto:marcella.frauscher@ac2t.at)

## Abstract

Phenol-type components, amongst them butylated hydroxytoluene (BHT) are used as antioxidants (AO) to enhance thermo-oxidative stability in kerosene-type JET A-1 fuels. While the antioxidative effect of BHT is well known and often published, there is far less information regarding degradation products of BHT in fuel and their impact on the stability towards oxidation. In order to provide a time-resolved depletion of BHT in model kerosene, an artificial alteration method adapted for regular sampling was applied. Subsequently, the molecular structure of degradation products of BHT were identified by gas chromatography with electron impact ionisation mass spectrometry (GC-EI-MS). For the quantification of the residual BHT as well as two representatives of degradation products, namely 3,5-di-*tert*-butyl-4-hydroxybenzaldehyde (HBA) and 2,6-di-*tert*-butyl-*p*-benzoquinone (BQ) an analytical technique comprising a GC-EI triple quadrupole mass spectrometer run in the MS/MS mode was developed. BHT, BQ, and HBA were determined with a limit of detection and

quantification (LOQ and LOD) below 1 ppb. The formation of BQ and HBA was observed shortly after the nascent degradation of BHT, while an increase of oxidation products deriving from the fuel ascended remarkably after full depletion of both, the initial AO BHT and the monitored oxidation products BQ and HBA. As the evolution of BQ and HBA followed a characteristic trend, the option is offered to use these compounds as markers to reliably predict the residual time until a total consumption or a predefined threshold of BHT is reached. This way, quality management of in-service or stored kerosene type fuels is enhanced.

## Keywords

kerosene, mass spectrometry, gas chromatography, antioxidant, butylated hydroxytoluene, oxidative stability

## 1. Introduction

In order to increase the thermo-oxidative stability and to provide the required stability during transport and storage, additives are used in fuel formulations. Antioxidants (AOs) are applied to delay the fuel degradation process, also known as auto-oxidation. This free-radical chain reaction comprises four steps: initiation – propagation – branching – termination. Based on their chemical structure, AOs can either inhibit the formation of free radicals or interrupt the propagation process of the free radical by different mechanisms. In presence of an aromatic or phenolic ring donation of a hydrogen atom to the free radicals emerging during oxidation takes place and the AO becomes a radical itself [1-3].

The range of AOs allowed for application in fuel blends is given by specifications, whereas sterically hindered phenols are commonly used. For kerosene type Jet A-1 fuels, the applicable AOs are limited by the specifications for aviation fuel quality requirements for jointly operated systems [4] in chemistries and concentrations. Following additives, all sterically hindered phenols, and mixtures thereof with alkylated butylphenols are applicable: 2,6-di-tert-butylphenol (2,6-DTBP), 2,6 di-tert-butyl-4-methylphenol (also known as butylated hydroxy toluene, BHT), 2,4-dimethyl-6-tert-butylphenol, all together in a total concentration of min. 17 mg/L and max. 24 mg/L in the fuel blend [4-6].

Among the sterically hindered phenolic AOs, the AO activity of BHT is one of the most commonly studied one in different research disciplines [1]. With increasing use of fatty acid methyl ester (FAME) in biodiesel blends and the inherent limitation of this fuel component towards oxidative stability, more emphasis was put on the stabilizing effect of BHT. The

influence on the stability of either pure BHT or in mixture with other synthetic AOs was investigated in various biodiesel fuel blends from B0 (pure diesel without any biodiesel components) to B100 (pure FAME/biodiesel) and by applying different methods of thermo-oxidative stress, ranging from plain oven test via Rancimat to PetroOxy test [7-12]. In these studies, focus is put on the induction period (IP), which is defined as period of time from the start of a stability test until the maximum rate change of oxidation, as well as on the oxidation kinetics and the activation energy of the AO. BHT turned out to be highly efficient regarding AO efficiency. But one has to keep in mind results are depending on oxygen pressure, temperature and oxidation method [9, 10]. Re-addition of AO after the process of oxidation proceeded seems to show only limited success. Via the determination of AO depletion rate and the induction period after adding AO to aged jet fuel samples, no improvement on inhibition of hydroperoxide formation in the aged fuel was observed [13].

When it comes to precise determination and quantification of the AOs, methods for analysis have to overcome the challenge of the very complex matrix of kerosene fuels as well as the low levels of additives. Typically, jet fuels are blended according to the specification, but additional quantification of the AO is not envisaged. However, long transport times or storage periods and variable environmental impacts such as temperature or humidity can cause degradation of the blended fuel additives. In order to ensure quality at purchase, a determination of the type and the concentration of AO may be advisable. For a precise identification of the compound as well as the quantification of AOs, chromatographic methods on-line coupled to mass spectrometry (MS) are the method of choice for quite a number of reasons. Due to the volatile character of sterically hindered phenolic AOs, capillary gas chromatography (GC) with EI-MS in the selected ion monitoring (SIM) mode is widely applied as the method of choice in order to detect low amounts of this additive in the complex matrix and well established for various AOs [14-16].

More recently, the application of a triple quadrupole (QqQ) provided promising results for detection and quantification of phenolic AOs in fresh and in-service middle distillate fuels when applied in GC-EI-QqQ-MS mode. Multiple reaction monitoring (MRM) turned out to be well suitable for analytical challenges requiring improved sensitivity, a minimum of background interference and unambiguous identification of low-level analytes (ranges from 0.1 to 20 mg/L) in complex matrices without intensive previous sample preparation steps [17]. Application of the relative “soft” gas-phase ionization technique chemical ionization (CI) combined with GC-QqQ in MS/MS mode even enabled lower quantification limits (LLOQ) of 0.05 mg/L for 2,6-

di-tert-butyl-4-sec-butylphenol and 0.11 mg/L for BHT in ICP-grade kerosene blended with 10% (v/v) 2-propanol as model jet fuel [18].

Although numerous publications on the antioxidative effect of BHT in fuels are published, the major amount of these works reports mainly the impact of AOs on the IP or analytical methods for determination of AOs. Less attention is spent on the degradation products occurring while depletion of BHT in fuels. As BHT is considered as safe for human health, it is commonly used in cosmetic and polymer industry and, in particular in food products [19]. In life sciences, the aspect of biotransformation into metabolites and their possible toxicological impact is not neglected. Analysis of the oxidation products of BHT is mainly performed with liquid chromatography on-line coupled with MS. However, most attention is paid to degradation products that are under suspicion to be harmful to human health, and their formation in aqueous media [20, 21]. These degradation products are not always consistent with these ones relevant in hydrocarbon matrices such as kerosene, and no quantification or time-resolved progress of AO depletion correlated with the oxidation products is provided.

The paper in hand reports on the development of an artificial alteration method to provide kerosene type fuel samples in a defined degradation condition and the determination of residual BHT. The time-resolved depletion of the AO as well as the formation of oxidation products of BHT and their molecular structures are monitored by GC-MS with electron impact ionization (GC-EI-MS), and the limitations of Fourier-transform infrared spectroscopy (FT-IR) methods for AO quantification are shown. An appropriate analytical method for quantification of BHT and two representative AO oxidation products is elaborated using GC-EI-QqQ in MS/MS mode. Correlation of the time-resolved depletion of the AO and the formation of AO degradation products, acting as markers of the emerging fuel degradation, which was monitored via the amount of fuel oxidation products, is given. This information is crucial, when information regarding residual AO content, additional additive dosage or evaluation of the quality of in-service or stored kerosene type fuels is required.

The presented approach offers multiple advantages compared to conventional antioxidant monitoring techniques, such as linear sweep voltammetry, e.g., Remaining Useful Life Evaluation Routine (RULER) [22]. The RULER technique provides practically no information regarding the chemical structure of the AO and the resulting degradation products. Hence, no better understanding of the chemical degradation of the AO in fuel can be achieved [23]. An absolute quantification is strongly limited, as the RULER technique is primarily used for quantification of the residual amount of AO relative to the fresh product.

## 2. Materials and methods

### 2.1 Model kerosene

With the aim to reduce the tremendous complexity of the applied kerosene blend containing the AO BHT, as well as the formed degradation products, *n*-dodecane (C12) was selected as defined, simplified representative of kerosene-type Jet A-1. In accordance with concentration levels given in the specification for Jet A-1 [2-4], a blend of C12 and BHT with a final concentration of 500 mg BHT/L was prepared without any further additives. As a reference, pure *n*-dodecane was subjected to the same artificial alteration steps and subsequent analysis. Both components were obtained from Sigma Aldrich (St. Louis, MO, USA) in GC grade quality ( $\geq 99\%$ ).

### 2.2 Artificial alteration method and conventional analysis

The artificial alteration, a laboratory-based controlled degradation process, was carried out in a modified RPVOT device corresponding ASTM D2272 – 14a Method B [24]. The QUANTUM® Oxidation Tester device (Tannas Co. & King Refrigeration Inc., Midland, Michigan, USA) was extensively modified in order to meet safety and chemical purity requirements. The magnetic cup with the glass sample beaker was replaced by a custom-made Teflon cup. A gas conduit in the outer wall of the Teflon cup allows gas flow from the gas inlet into the cup. Due to this modification, deposit formation of condensed volatile samples between sample beaker and pressure chamber described in ASTM D2272 was avoided.

For suitable alteration of fuel components, less severe parameters compared to the standard method for turbine oils regarding pressure were applied, and no catalyst was used. 15.0 g sample were tempered in a pressured vessel with a 30 slant. The gas phase of the pressure vessel was flushed 3 times with oxygen to remove residual air, then 2.0 bar initial pressure (corresponding to 200.0 kPa) with O<sub>2</sub> (5.0 corresponding to 99.998 % purity, obtained from AirLiquide, Paris, France) was applied. During the artificial alteration process, the vessel was kept at a temperature of 150 °C. Small sample aliquots were collected at regular intervals. A sampling kit assembly (purchased by Tannas Co. & King Refrigeration Inc., Midland, Michigan, USA) was improved to reduce the dead-volume and, hence, the amount of the sampled aliquot to ensure a minimized impact on the progress of alteration, and to enable the extraction of small sample aliquots without de-pressurizing the alteration device. Sampling was done at up to 10 different points of interest, from 0 to 15 hours for C12 with AO and 0 to 5 hours for neat C12 as reference.

Pressure and temperature were monitored continuously throughout the whole alteration process. The change in pressure can be correlated with the oxygen consumption and hence with oxidation stability and alteration condition of the liquid sample [24].

Condition monitoring of the altered C12 aliquots was performed with FT-IR analysis by a Bruker Tensor 27 device (Bruker, Ettlingen, Germany). Evaluation of the fuel oxidation in A/cm (absorption per path length) at a wavelength of  $1720\text{ cm}^{-1}$  was performed similarly to the method described in [25]. Due to relatively high oxidation of some samples, resulting in total absorption in the characteristic oxidation band, additional dilution in C12 was necessary for the determination of oxidation. The determination of the relative BHT content (at a wavelength of  $3650\text{ cm}^{-1}$ ) was performed with undiluted samples as described in [25] and [26] for residual phenolic antioxidants.

## 2.3 Separation and detection

### 2.3.1 GC-EI-MS

Subsequent to artificial alteration, a GC-EI-MS instrumental setup composed of a TriPlus autosampler and a Trace capillary Ultra GC coupled to a TSQ Quantum XLS mass spectrometer, all from Thermo Scientific (Austin, TX, USA) were used. Fresh and all sampled aliquots of altered C12 without or with BHT were diluted to 4 (w/w) % in dichloromethane ( $\text{CH}_2\text{Cl}_2$ ) in HPLC Plus for HPLC and GC grade obtained by Sigma Aldrich (St. Louis, MO, USA). In order to avoid undesired adsorption and enhance volatility of degradation product for GC the silylation reagent N,O-bis(trimethylsilyl)-trifluoroacetamide (BSTFA) was used in mass excess (2:1) compared to sample weight. The reaction was conducted at  $70^\circ\text{C}$  for one hour. A TG-17MS (composed of 50 %-diphenyl/50 %-dimethylpolysiloxane stationary phase) capillary column of 30 m length, 0.25 mm internal diameter (I.D.), and 0.25  $\mu\text{m}$  film thickness obtained from Thermo Fisher Scientific (Waltham, MA, USA) was used for chromatographic separation.

1  $\mu\text{L}$  of the sample was injected via a programmable temperature vaporization injector (PTV) at  $300^\circ\text{C}$  and a split ratio of 1:25. Separation was performed with a constant helium (He) carrier gas flow of 2 mL/min, starting with an oven temperature of  $50^\circ\text{C}$  kept for 2 min, followed by a ramp of  $7^\circ\text{C}/\text{min}$  up to  $300^\circ\text{C}$ . The final temperature was kept for 5 min.

Temperature of the transfer line was set at  $250^\circ\text{C}$  and the (EI) ion source was held at a temperature of  $200^\circ\text{C}$ . Ionization was done at 70 eV and for detection and partial identification a Q1 full scan mode in a range from m/z (mass-to charge number) 40 to 650 was applied.

Data acquisition and data processing was done with Xcalibur v2.0 software. NIST library 14 and additional standard substances for 3,5-di-*tert*-butyl-4-hydroxybenzaldehyde (HBA) and 2,6-di-*tert*-butyl-*p*-benzoquinone (BQ) obtained from Alfa Aesar (Haverhill, MA, USA) in high purity (98+ %), were applied for the final identification of compounds. For the degradation products without reliable matches from NIST library 14 the identification was supported by structure elucidation with a high resolution LTQ orbitrap XL hybrid tandem mass spectrometer (ThermoFisher Scientific, Bremen, Germany) fitted with an ESI ion source operated in negative ion mode. Additionally, the molecular ion of the respective substances was determined with GC-MS and chemical ionization (CI), using methane (purity 4.5, obtained from Messer Austria, Gumpoldskirchen, Austria) as reaction gas. Chemical ionization gas flow as set to 2.0 mL/min and a Q1 full scan mode in a range from  $m/z$  65 to 650 was applied. Distinct structures of the degradation products of the AO were identified by using the high resolution MS. A high mass resolution along with high mass accuracy gives the ability to determine not only the exact elemental composition of the molecular ion based, but also to obtain the elemental composition of fragment ions that can be clearly assigned to the distinct structures. Subsequently, the identified degradation products obtained from LTQ analysis were compared with the molecular ion data obtained by GC-CI-MS and the fragmentation patterns obtained by GC-EI-MS, and a final comparison with standards, whenever available, was done.

### 2.3.2 GC-EI-MS/MS

In order to quantify the AO BHT as well as two of the identified degradation products, namely HBA and BQ, in correlation with progress of alteration time, a method using GC-EI-MS/MS was developed. Sample preparation was done with a dilution of 8 (w/w) % sample with a mass excess of 2:1 BSTFA in  $\text{CH}_2\text{Cl}_2$ , and 2,5-di-*tert*-butyl-*p*-benzoquinone from Alfa Aesar (Haverhill, MA, USA) was added as an internal standard (IS). Multicomponent standards containing equal amounts of BHT, HBA and BQ in concentrations from 0 to 500 ppm were prepared analogue to the sample aliquots including an IS.

Parameters for sample introduction as well as for chromatographic separation and the transfer line to QqQ were kept the same as described in 2.3.1., except the oven program which was stopped at an end temperature of 250 °C as the entire sample was eluted at this temperature, and kept for 30 seconds (s). As a first step for the development of a quantification method, the most appropriate collision energy for the detection of BHT was determined. In MS/MS product scan mode with parent pass  $m/z$  205 and a scan range from  $m/z$  40 - 300, collision energies

from 0 V up to 200 V in steps of 10 V each were applied. The final method consisted of 5 parallel scan events: Scan 1 was a Q1 full scan with a  $m/z$  range from 40 - 300, scans 2 to 5 were all performed as product ion scans with a mass range from  $m/z$  40 - 300 and a collision energy of 10 V. As parent ions  $m/z$  205, 177, 219 and 234 were selected. Limit of detection (LOD) as well as limit of quantification (LOQ) were determined according to DIN 32645 [27], and quantification of BHT, HBA and BQ was evaluated according to the standard calibration curve.

### 3. Results and discussion

#### 3.1 Oxygen pressure progression and FTIR analysis

Figure 1 shows the pressure progression during alteration as well as the oxidation (dashed line) measured via FT-IR for C12 with (orange) and without BHT (blue). The circular marks indicate the points of sampling as described in 2.2. During the first minutes of alteration, the sample is heated up to 150 °C, and the pressure reaches a maximum in similar time for both fuels. For pure C12, a pressure drop immediately after that occurs, whereas the sample containing BHT maintains at an almost constant pressure for nearly 9 hours. Besides the difference in induction time, the pressure progression after the pressure drop is highly similar for both samples with a very short constant period at approximately 2.6 bar and a close-to-constant final pressure value around 1.8 bar. The antioxidative effect of BHT is demonstrated by the prolonged alteration time while, after depletion of BHT, similar thermo-oxidative reactions seem to take place (based on findings in chapter 3.2). Finally, the oxidation reaches a comparable level of ~ 250 A/cm in both fuels. The comparability of the final oxidation values is further confirmed by the very similar pressure changes in both systems.

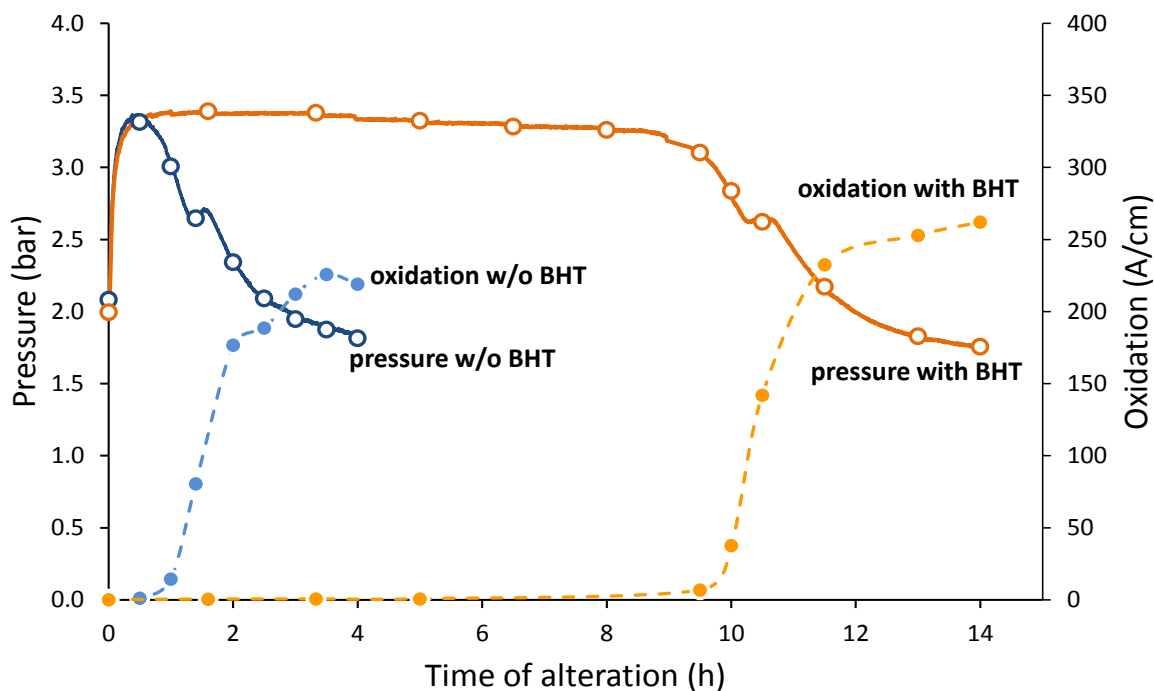


Figure 1: Pressure progression and oxidation (measured via FT-IR; dashed line) for C12 with (orange) and without (blue) BHT. Circular marks indicate the points of sampling. Dashed lines may be used as guide for the eyes and are no measured values.

In Figure 2, the pressure progression in correlation with the evaluated relative BHT (assuming 100 % for the initial BHT concentration) content determined by FT-IR is depicted. The BHT content according to FT-IR decreases in a close-to-linear manner until the distinct pressure drop, then a rapid depletion can be observed. The BHT content reaches a final value around 30 % and stays constant until the end of the selected artificial alteration time scale. However, the FT-IR method is strongly limited in this case due to the very low signal ( $< 1$  A/cm) of the phenol absorption peak compared to the blank samples without any phenolic AO in the selected concentration range as well as the fact that absorption peaks of some degradation and oxidation products overlap with the initial phenol peak. Thus, a remaining content of approximately 30 % of the initial concentration of AO remains in the sample until the end of the artificial alteration seems highly unlikely. Moreover, the FT-IR analysis is not capable of monitoring/identifying exact structures of phenolic AOs or degradation products thereof.

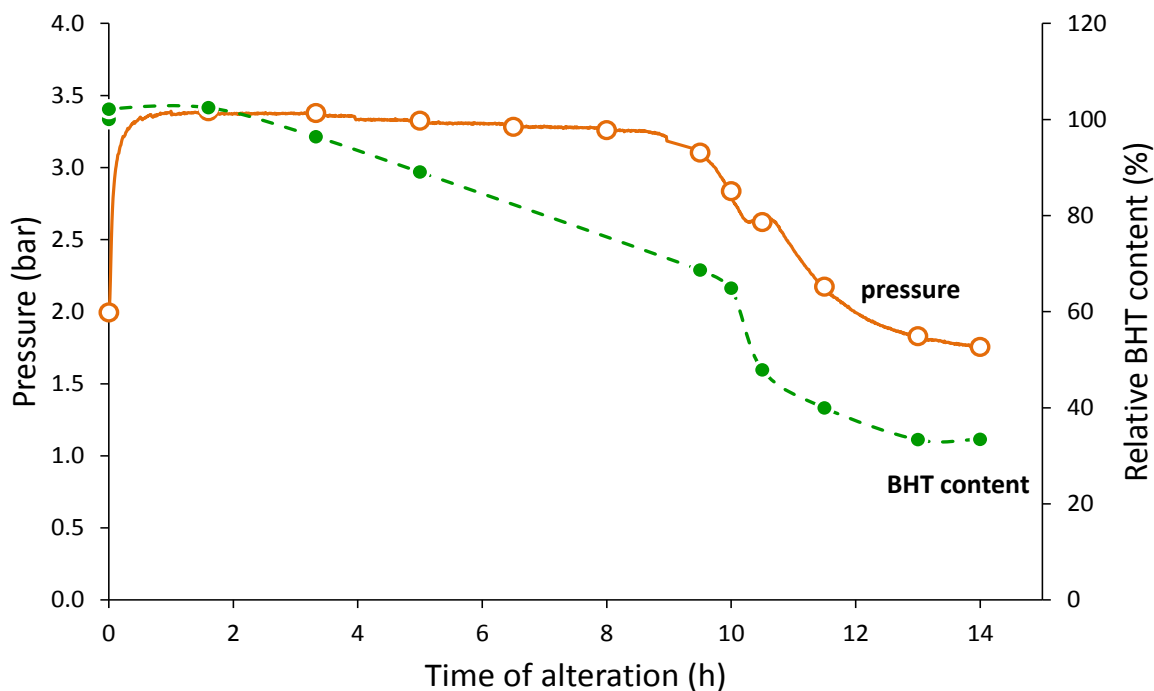


Figure 22: Pressure progression and correlation with residual relative BHT content determined by FT-IR (dashed line), given for C12 with BHT. Circular marks indicate the points of sampling. Dashed lines may be used as guide for the eyes and are no measured values.

### 3.2 Identification of degradation products

All samples from C12 with and without BHT obtained due to sampling during artificial alteration were subjected to sample preparation, separation and detection as described in 2.3. The degradation products of all C12 blends with the time frame 0 to 15 h and without 0 to 4 h BHT were determined. Figure 3 shows chromatograms of the blend with BHT after 8 h (A) and 9.7 h (B) of artificial alteration, as well as pure C12 after 1 h of alteration (C). At a retention time of  $R_t = 18.10$  min the peak of the residual BHT is visible for the sample aliquot with an alteration time of 8 h (E). Degradation products of the phenolic AO are indicated with triangular marks. Peaks marked with an asterisk are obtained from a polysiloxane contamination, most probably derived from the used vial septa. For the aliquot of C12 containing BHT and a time of alteration of 8 h (A), degradation products were detected at following retention times: 16.34 (b, 2-(hydroxymethyl)-4,6-dimethyl-cyclohexa-2,5-diene-1-one), 16.96, 17.05 (c, BQ), 17.26 (d, 2,6-di-*tert*-butyl-4-methylene-2,5-cyclohexadienone), 19.29, 20.47 (f, 2-(5-*tert*-butyl-3-methyl-6-oxo-cyclohexa-1,4-diene-1-yl)-2-methyl-propanal), 21.04, 21.22, 22.03, 23.00 (g, HBA), and 23.48 min. Degradation products of BHT where an accurate structure was identified are labelled with letters and given in Table 1. Besides that, in all three samples (A, B, C)

degradation deriving from C12 in various amounts were found. Representatives thereof are octanoic acid (a) and nonanoic acid (h), both detected as TMS ester due to silylation. Numerous other products were identified by their structures, and for a better depiction and understanding assigned to groups according to their functional groups and labelled with numbers. These groups are: furanes (1), alcohols (2), ketones (3), and esters and ethers (4).

*Table 1: Selected oxidation products of C12 with and without BHT at different states of alteration. Bold, cursive small letters are products deriving from oxidation of BHT, and non-bold letters are degradation products of C12. The initial BHT is marked with a large, bold letter. Numbers indicate groups of degradation products.*

| <b>Code</b> | <b>Analyte</b>  | <b>Retention time (min)</b> |
|-------------|---|-----------------------------|
| a           | Octanoic acid TMS ester   | 11.89                       |
| <b>b</b>    | 2-(hydroxymethyl)-4,6-dimethyl-cyclohexa-2,5-diene-1-one                            | 16.34                       |
| <b>c</b>    | 2,6-di- <i>tert</i> -butylquinone (BQ)  | 17.05                       |
| <b>d</b>    | 2,6-di- <i>tert</i> -butyl-4-methylene-2,5-cyclohexadienone                         | 17.26                       |
| <b>e</b>    | 2,6-di- <i>tert</i> -butyl-4-methylphenol (BHT)                                     | 18.10                       |
| <b>f</b>    | 2-(5- <i>tert</i> -butyl-3-methyl-6-oxo-cyclohexa-1,4-diene-1-yl)-2-methyl-propanal | 20.47                       |
| <b>g</b>    | 3,5-di- <i>tert</i> -butyl-4-hydroxybenzaldehyde (HBA)                              | 23.00                       |
| h           | Nonanoic acid TMS ester   | 13.61                       |
| 1           | Furanes   | -                           |
| 2           | Alcohols  | -                           |
| 3           | Ketones   | -                           |
| 4           | Ethers, esters  | -                           |
| *           | Polysiloxanes   | -                           |
| ▼           | Degradation products of BHT   | -                           |

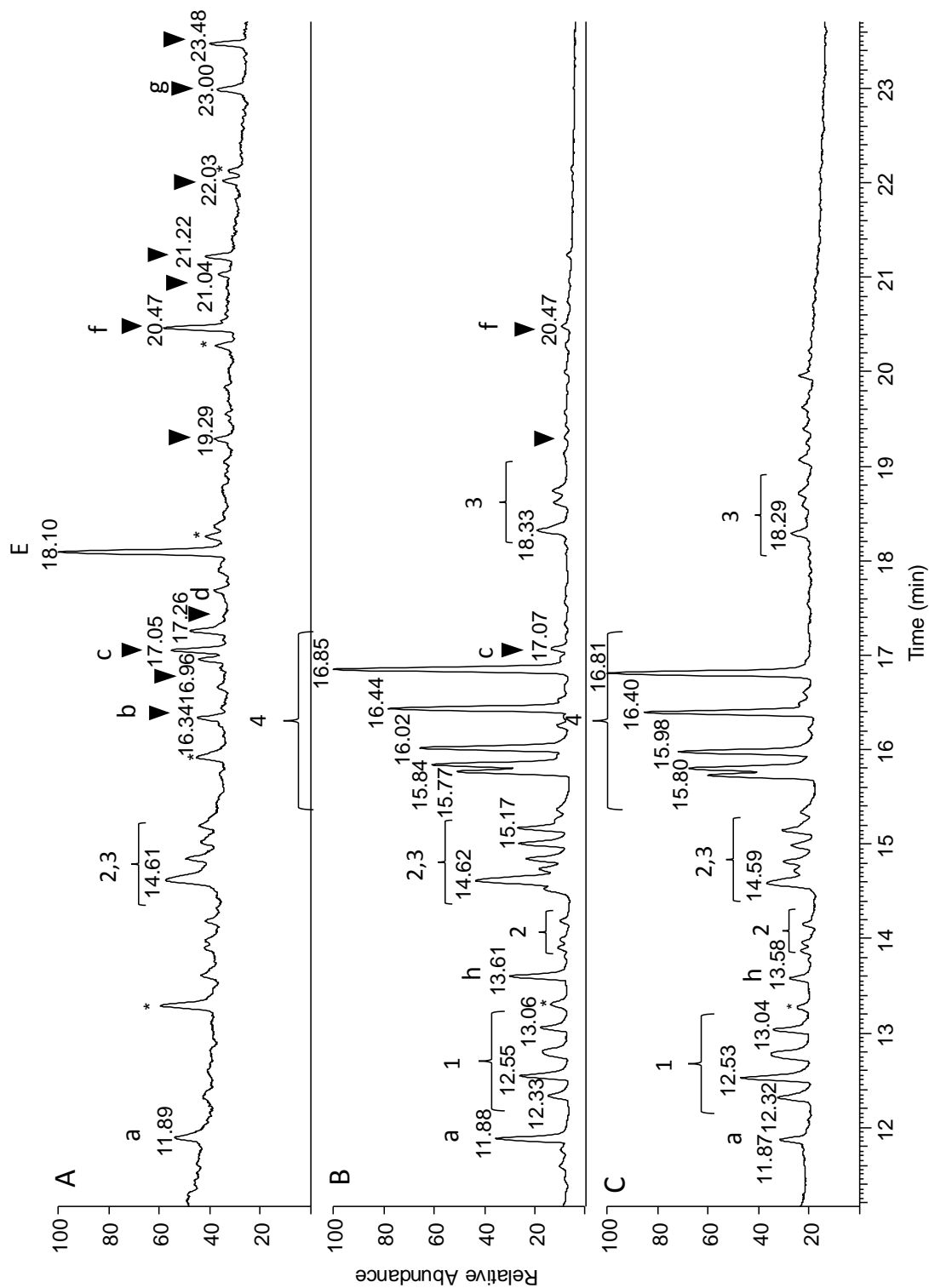


Figure 3: Total Ion Chromatogram of C12 with BHT after 8 h (A) and 9.7 h (B) as well as pure C12 after 1 h (C) time of alteration. Triangular marks indicate oxidation products of BHT (E), selected degradation products are labelled with small letters. Numbers are assigned to groups of degradation products, and peaks from contamination with polysiloxane are marked with an asterisk.

For the sample aliquot artificially altered for 9.7 h (B), no residual BHT was detected with the GC-EI-MS method anymore. Only three degradation products of the AO, among them BQ, were found in this sample, while the others seem to be further depleted. However, not only the number of degradation products deriving from C12 increased, but also their concentration was considerably higher. Additionally to octanoic acid TMS ester at a retention time of 11.88 min (a), degradation products as listed were detected: nonanoic acid TMS ester at 13.61 min (h), furanes (1), alcohols (2), ketones (3), esters, and ethers (4) (see Table 1). Compared to the alteration of pure model kerosene consisting of neat C12 (time of alteration 1 h), the same degradation products excluding these deriving from the AO were detected.

As depicted in Figure 3 C, a similar state of degradation for the blend with BHT after 9.7 h as for the pure C12 after 1 h time of alteration was obtained. The formed degradation products with origin in the oxidation of C12 are highly comparable, while the life time is increased remarkably when blending with BHT.

### 3.3 Quantification with GC-EI-MS/MS

#### 3.3.1 Selection of ions and optimisation of collision energy

In order to ascertain the most suitable collision energy for a quantification of the AO BHT in MS/MS mode, a row of variation with collision energies from 0 to 200 V was performed with the above described parameters (see 2.3.2). In Table 2, the intensities for the ions  $m/z$  205.1, 177.0, and 144.8 are given, as well as the three most intensive ions obtained at the respective collision energy, starting with the highest intensity from the left. In general and starting from 10 V, the higher the selected collision energy is, the smaller are the resulting fragments of BHT. Hence, the intensity of the selected ions 205.1, 177.0, and 144.8 is decreasing, except for  $m/z$  144.8 at 20 V. With a collision energy of 0 (Figure 4, A), 10 (Figure 4, B) and 20 V (Figure 4, C), respectively, all three ions are detectable. From 30 to 80 V only the smallest ( $m/z$  144.8) fragment ion among them is originated with even lower intensity. In respect of detection with a low limit of detection and a good reproducibility, fragments with not only a high intensity, but also a good selectivity were of interest for a MS/MS method in parent ion mode. Therefore, a GC-EI-MS/MS method with a collision energy of 10 V was set up.

Table 2: Intensities of fragment ions of BHT obtained with collision energies from 0 to 200 V.

| Collision energy (V) | Intensity m/z 205.1 | Intensity m/z 177.0 | Intensity m/z 144.8 | Most intensive ions (m/z) |       |       |
|----------------------|---------------------|---------------------|---------------------|---------------------------|-------|-------|
| 0                    | 7.5E+05             | 4.5E+05             | 2.3E+05             | 205.1                     | 177.0 | 144.8 |
| 10                   | 1.7E+07             | 1.4E+07             | 6.0E+06             | 205.1                     | 177.0 | 144.8 |
| 20                   | 2.7E+05             | 2.2E+06             | 1.1E+07             | 144.8                     | 104.9 | 90.9  |
| 30                   | -                   | -                   | 1.8E+06             | 128.9                     | 114.8 | 104.9 |
| 40                   | -                   | -                   | 3.1E+05             | 114.8                     | 127.8 | 90.9  |
| 50                   | -                   | -                   | 1.3E+05             | 114.8                     | 127.8 | 76.9  |
| 60                   | -                   | -                   | 3.8E+04             | 127.8                     | 114.8 | 76.9  |
| 70                   | -                   | -                   | 4.0E+04             | 114.8                     | 76.9  | 51.1  |
| 80                   | -                   | -                   | 1.4E+04             | 114.8                     | 76.9  | 51.1  |
| 90                   | -                   | -                   | -                   | 114.8                     | 63.0  | 51.1  |
| 100                  | -                   | -                   | -                   | 63.1                      | 51.1  | 50.0  |
| 110                  | -                   | -                   | -                   | 62.0                      | 51.1  | 50.1  |
| 120                  | -                   | -                   | -                   | 73.9                      | 51.1  | 50.0  |
| 130                  | -                   | -                   | -                   | 74.0                      | 62.1  | 50.1  |
| 140                  | -                   | -                   | -                   | 62.1                      | 61.2  | 50.1  |
| 150                  | -                   | -                   | -                   | 62.1                      | 61.1  | 50.0  |
| 160                  | -                   | -                   | -                   | 62.0                      | 60.9  | 50.0  |
| 170                  | -                   | -                   | -                   | 74.0                      | 61.0  | 50.1  |
| 180                  | -                   | -                   | -                   | 61.1                      | 50.4  | 49.7  |
| 190                  | -                   | -                   | -                   | 72.8                      | 61.0  | 49.7  |
| 200                  | -                   | -                   | -                   | 60.9                      | 50.2  | 49.1  |

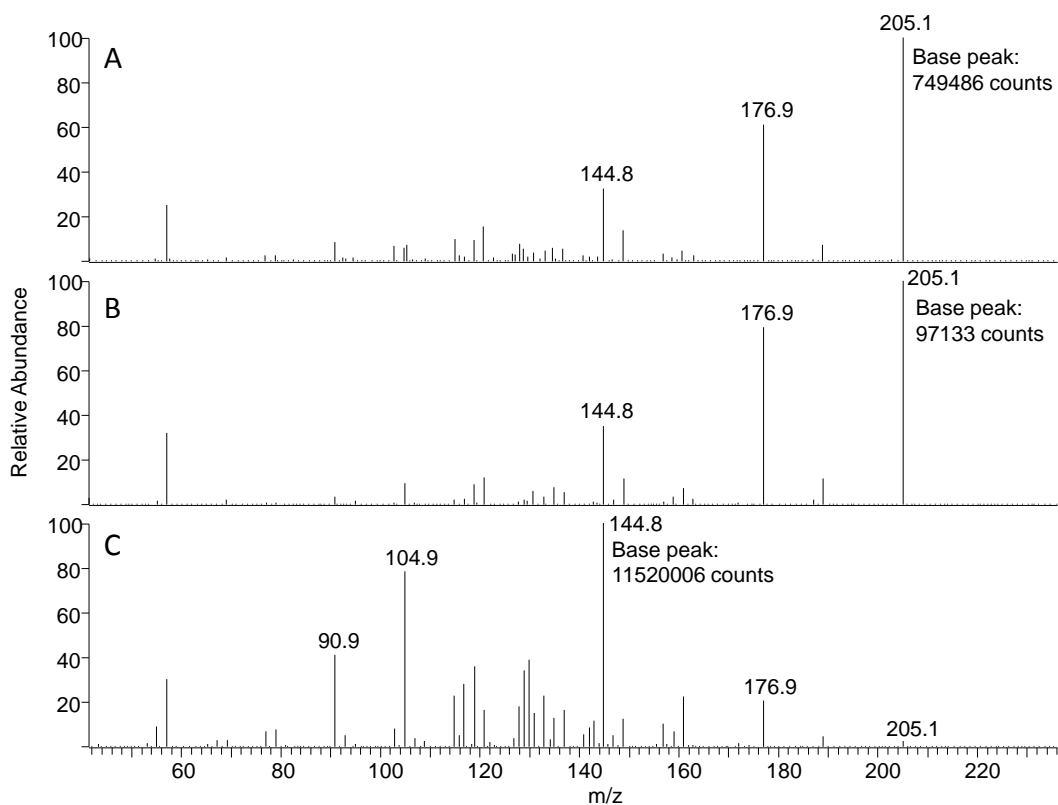
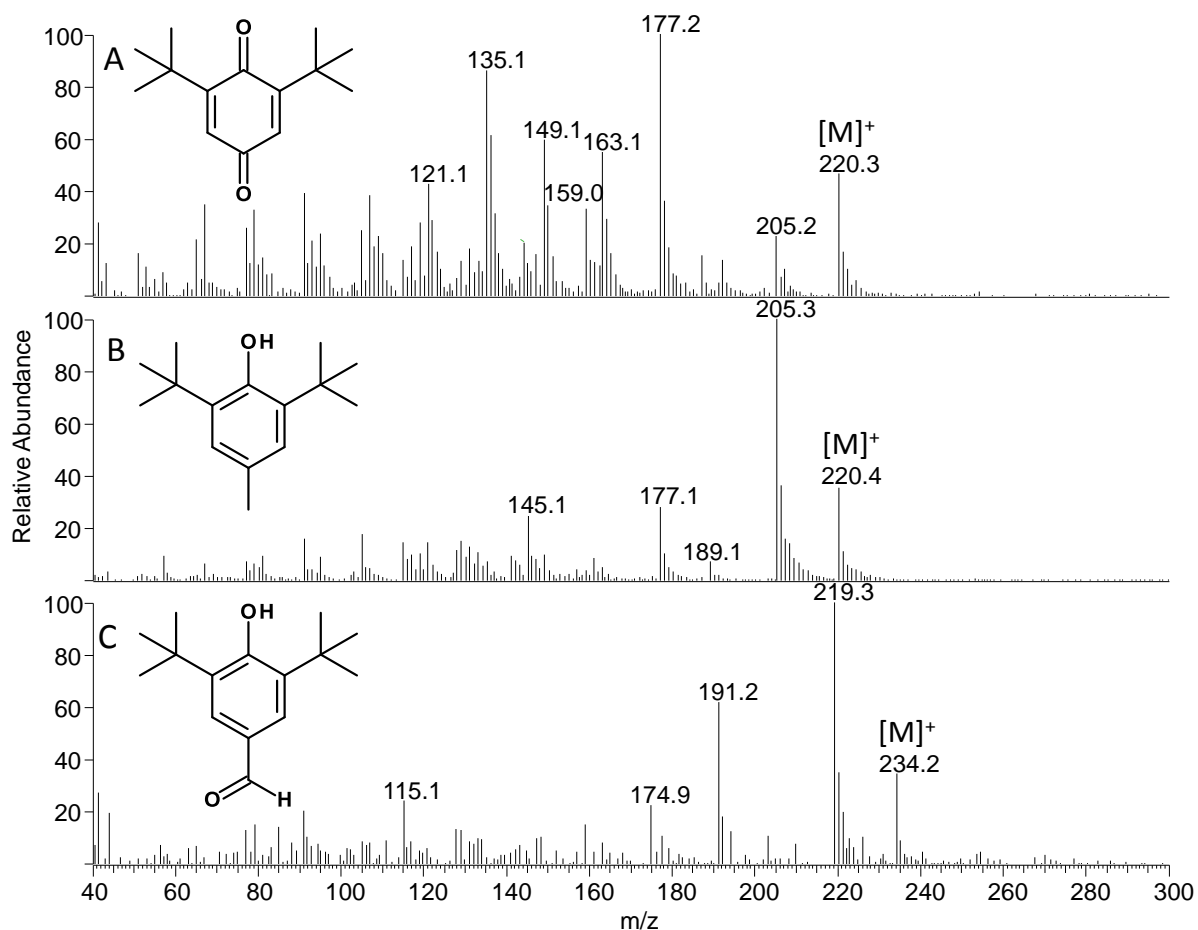


Figure 4: Product ion scan mode of parent ion mass  $m/z$  205.1 of analyte BHT at 0 V (A), 10 V (B) and 20 V (C) collision energy.

Quantification of BHT as well as the degradation products HBA and BQ was done as described in 2.3.2. After determination of the ideal collision energy for BHT, the parent ions for product ion scans of the respective analytes were selected based on their fragmentation pattern. Figure 5 depicts the spectra of BQ (A), BHT (B) and HBA (C) generated by EI at 70 eV.



*Figure 5: Positive ion mass spectra of BQ (A), BHT (B) and HBA (C) obtained by means of GC-EI-MS at 70 eV. The most abundant and selected fragment ions and the molecular ion of each analyte are labelled.*

For all three analytes, the molecular ion is clearly visible, and some of the most abundant fragments are labelled. As Parent ion the fragment ion  $m/z$  177 was chosen for BQ, resulting in the most abundant product ions  $m/z$  159, 149, and 135. For BHT the fragment ion  $m/z$  205 was selected as parent ion, and quantification was done with  $m/z$  189, 177 and 145. In order to obtain three highly reproducible product ions for HBA two parent ions, namely the fragment ion  $m/z$  219 and the molecular ion  $m/z$  234, were applied for the method, and in product ion scan mode  $m/z$  219, 191 and 175 were selected as the most suitable to quantify the analyte (see Table 3).

Table 3: Selected parent ions and the respective product ions used for quantification.

| Analyte | Parent ion (m/z) | Product ions for quantification (m/z) |     |     |
|---------|------------------|---------------------------------------|-----|-----|
| BQ      | 177              | 159                                   | 149 | 135 |
| BHT     | 205              | 189                                   | 177 | 145 |
| HBA     | 219              | 191                                   | 175 | -   |
| HBA     | 234              | 219                                   | -   | -   |

### 3.3.2 Quantification of BHT and its oxidation products

Subsequent to the optimization of collision energy and the determination of appropriate scan modes for quantification, the three analytes BHT, BQ and HBA were quantified as described in 2.3.2. Quantification as well as determination of LOD and LOQ were performed with 3 product ions (m/z values given in Table 3), and the resulting concentration data showed a good consistency. To give some examples, LOQ for BQ ranges from 0.037 to 0.039 ppb for the ions m/z 135, 149 and 159 and for HBA from 0.05 to 0.08 ppb for the ions m/z 175, 191, 219. The discussed results in this section were obtained with following product ions, as these showed the highest intensity: BHT m/z 177, BQ m/z 135 and HBA m/z 191.

LOD and LOQ for the AO and the two degradation products were determined with following values: For BHT LOD was according to DIN 32645 [27] defined with 0.005 ppb and lower LOQ 0.008 ppb. For BQ a LOD of 0.03 ppb and a lower LOQ of 0.05 ppb was observed. LOD for HBA was determined with 0.21 ppb, and lower LOQ with 0.37 ppb. For all three analytes a linear range up to at least 500 ppm was determined, and a satisfying reproducibility according to DIN 32645 [27] was obtained.

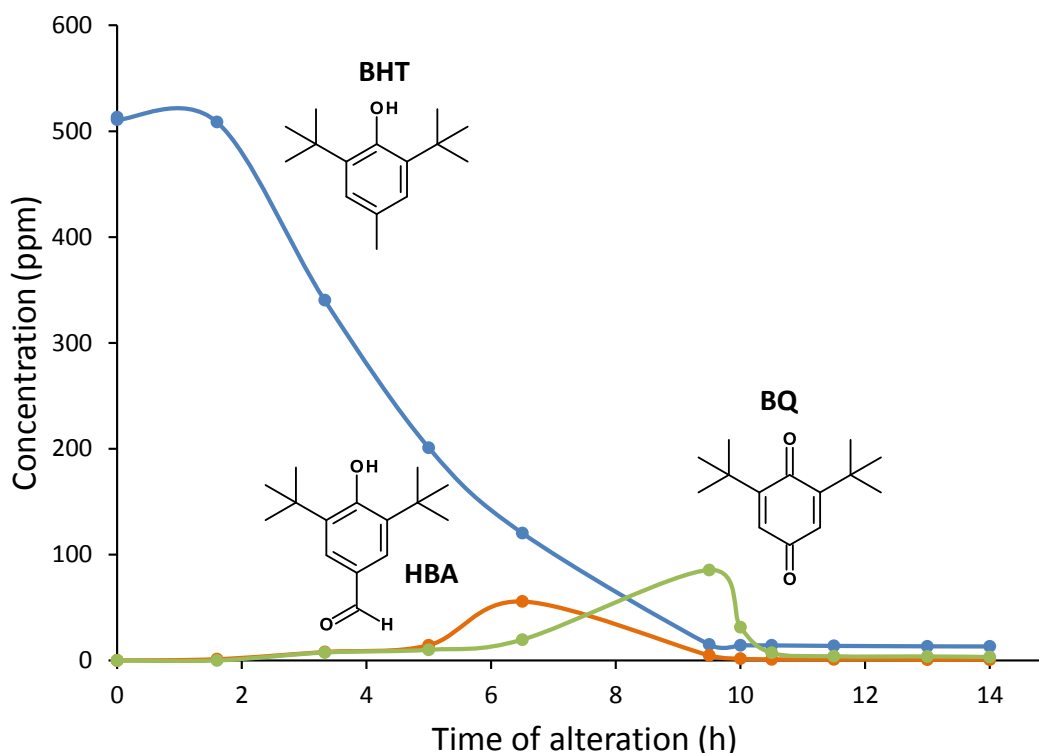


*Figure 6: Concentration of BHT (blue) and the two oxidation products BQ (green) and HBA (orange) in ppm during the alteration progress in hours. Determined ppm values are given at the circular marks. The lines may be seen as guide for the eye and are no measured values.*

For the initial C12 containing BHT as well as for all 10 aliquots obtained from artificial alteration the concentration in ppm was evaluated, which is depicted in Figure 6. For BHT, a continuous decrease from the initial concentration of 500 ppm starting after 1.6 h of alteration was detected, resulting in a minimum of about 10 ppm after 9.7 h. This value stays constant until the end of the artificial alteration at 14 h. The formation of HBA in very low levels (around 1 ppm) starts at 1.6 h, as soon as BHT starts to degrade. A maximum of 55 ppm HBA was detected after 6.5 h of alteration, followed by a decrease to less than 1 ppm after 10.5 h. For BQ, a slightly delayed formation was observed. In the sample aliquot at 3.3. h duration of alteration a value around 10 ppm was detected. At 9.7 h the BQ content reaches a maximum of 85 ppm, followed by a sharp decrease to 3 ppm. To sum up, while the initial BHT decreases quite consistent over the duration of alteration, ending in a low residual amount, the two representatives of the degradation products are formed at different states of alteration. At first, HBA is formed and at the same time a simultaneous formation of BQ was detected, but the concentration of both diminished almost completely after 14 h. However, the formation of other degradation products, in particular larger and non-volatile degradation products might be formed, but were not able to be monitored via GC-EI-MS analysis.

When comparing these results with the temporal progress of the pressure curve in Figure 1 and 2, respectively, the remarkable drop of pressure coincides with the almost complete consumption of BHT as well as the deterioration of the degradation products HBA and BQ. Moreover, a distinct difference between the residual amount of AO measured with FT-IR (30% of initial concentration) and the substantially more precise GC-EI-MS/MS method (10 ppm) has to be pointed out. As the FT-IR value is a relative value compared with the initial concentration of BHT, 30% would account for 150 ppm. Quantification in ppm level reveals a residual amount of only 2 %.

The almost complete depletion of BHT (10 ppm at 9.5 h) leads to an amplified formation of degradation products of C12, which is depicted in Figure 3 B (alteration after 9.5 h). This increase of formed oxidation products is accompanied by an elevated consumption of oxygen. Therefore, based on the results obtained with GC-EI-MS the time of the pressure drop monitored during alteration (Figures 1 and 2) can be explained. Without any AO, there is no delay of the degradation, and the oxidation process accompanied by a sharp pressure drop starts almost immediately after heating up of the system.

#### 4. Conclusions

The used pressurized vessel oxidation device was modified to fulfil the requirements when working with volatile samples at elevated temperatures and elaborating trends based on regular sampling. As expected, alteration of C12 containing 500 ppm of BHT showed a three times prolonged alteration time until a constant monitored pressure at 1.8 bar compared with pure C12. Determination of the residual amount of BHT revealed clear limitations of the FT-IR method. While the determination via FT-IR provides residual amounts of approximately 30 % of the initial AO content, GC-EI-MS/MS quantification revealed a residual concentration of only 10 ppm. Hence, when working with additives dispensed or remaining in a very low level, conventional methods in fuel analytics such as FT-IR are very limited. These methods can be used for a time and cost-efficient overview, and to reveal general trends. However, with the gained knowledge of more precise analytical methods such as MS and MS/MS techniques to further improve conventional methods such as FT-IR, the reliable application of routine lab equipment can be enhanced.

Identification of degradation products of AO in model kerosene shows a variety of oxidation products of the AO formed during degradation of BHT. After almost complete consumption of BHT, the oxidation of C12 shows similar progress as without BHT, and a broad range of

degradation products such as acids, ketones or alcohols are formed. While the stability towards oxidation is enhanced by addition of BHT, the formed oxidation products deriving from C12 do not differ.

As representatives for oxidation products of BHT two molecules were quantified with an appropriate GC-EI-MS/MS method. It was observed, that some degradation products of BHT are formed earlier in the alteration process than others. This fact together with the achieved low LOD and LOQ despite the complex matrix of altered C12 introduces the possibility to use these compounds as intermediate molecules before a total consumption or a predefined threshold of the AO is reached. Appropriate thresholds of these intermediate compounds and characteristic ratios can be defined to ensure a high fuel quality in terms of sufficient oxidation stability of kerosene even after transport and storage. The initial concentration of BHT is 500 ppm in the model kerosene blend, HBA was detected with a maximum of 55 ppm and BQ with a maximum of 85 ppm. However, vanishing of these oxidation products can be observed with temporal progress of the alteration going along with the depletion of BHT. It cannot be excluded the formation of larger as well as more polar oxidation products characterized by low volatility. Hence, GC-EI-MS and -MS/MS may not be the only detection method to gain comprehensive knowledge in the molecular structures and the mechanisms of their formation. For the determination of distinct structures of further oxidation products of BHT a reverse-phase liquid chromatography separation coupled to a high-resolution MS as well as MS/MS with ESI or APCI (atmospheric pressure chemical ionization) ion source could be applied. Moreover, the limited availability of appropriate analytical standards for oxidation products requires considerable efforts, as for example the synthesis of desired reference compounds. When a quantification for all main degradation products of the AO during the entire alteration process is envisioned, a new design-quality of kerosene fuels seems to be feasible.

## 5. Acknowledgements

The work presented was funded by the Austrian COMET Programme (Project XTribology, no. 849109) and carried out at the “Excellence Centre of Tribology” (AC2T research GmbH).

## 6. References

[1] Yehye WA, Rahman NA, Ariffin A, Hamid SBA, Alhadi AA, Kadir FA, et al. Understanding the chemistry behind the antioxidant activities of butylated hydroxytoluene

(BHT): A review. *Eur J Med Chem* 2015;101:295-312

[2] Ramalingam S, Rajendran S, Ganesan P, Govindasamy M. Effect of operating parameters and antioxidant additives with biodiesels to improve the performance and reducing the emissions in a compression ignition engine – A review. *Renew Sust Energ Rev* 2018;81:775–788

[3] Varatharajana K, Pushparanib DS. Screening of antioxidant additives for biodiesel fuels. *Renew Sust Energ Rev* 2018;82:2017-2028

[4] JIG Joint Inspection Group. Aviation fuel quality requirements for jointly operated systems (AFQJOS). Product Specifications 2015, Issue 28, Bulletin No. 76

[5] British Ministry of Defence Standard. Defence Standard 91-9. Turbine Fuel, Kerosene Type, Jet A-1. NATO Code F-35. Joint Service Designation: AVTUR. Issue 7, 2001; Amendment 3 2015

[6] ASTM D 1655. Standard specification for aviation turbine fuels. ASTM International; West Conshohocken, PA, USA; 2017

[7] Maia ECR, Borsato D, Moreira I, Spacino KR, Rodrigues PRP, Gallin AL. Study of the biodiesel B100 oxidative stability in mixture with antioxidants. *Fuel Proc Technol* 2011;92(9):1750-55

[8] Borsato D, Cini JR, Silva HC, Coppo RL, Angilelli KG, Moreira I, et al. Oxidation kinetics of biodiesel from soybean mixed with synthetic antioxidants BHA, BHT and TBHQ: Determination of activation energy. *Fuel Proc Technol* 2014;127:111-16

[9] Zhou J, Xiong Y, Shi Y. Antioxidant consumption kinetics and shelf-life prediction for biodiesel stabilized with antioxidants using the Rancimat method. *Energ Fuel* 2016;30:10534-42

[10] Zhou J, Xiong Y, Shihai X. Evaluation of the oxidation stability of biodiesel stabilized with antioxidants using the PetroOXY method. *Fuel* 2016;184:808-14

- [11] DIN EN 15751: Automotive fuels – Fatty acid methyl ester (FAME) fuel and blends with diesel fuel –Determination of oxidation stability by accelerated oxidation method; German version EN 15751:2014. Deutsches Institut für Normung; Berlin, Germany; 2014
- [12] DIN EN 16091: Liquid petroleum products – Middle distillates and fatty acid methyl ester (FAME) fuels and blends – Determination of oxidation stability by rapid small scale oxidation method; German version EN 16091:2011. Deutsches Institut für Normung; Berlin, Germany; 2012
- [13] Rawson PM, Stansfield C, Webster RL, Evans D. Re-addition of antioxidant to aged MEROX and hydroprocessed jet fuels. *Fuel* 2015;139:652-58
- [14] Bernabei M, Bocchinfuso G, Carrozzo P, De Angelis C. Determination of phenolic antioxidants in aviation jet fuel. *J Chromatogr A* 2000;871:235-41
- [15] Shin H, Ahn, H, Jung D. Determination of phenolic antioxidants in spilled aviation fuels by gas chromatography-mass spectrometry. *Chromatographia* 2003;58:495-99
- [16] Shin H. GC-MS determination of antioxidants in ground water contaminated with JP-8. *Chromatographia* 2007;66:893-97
- [17] Webster RL, Rawson PM, Evans DJ, Marriot PJ. Synthetic phenolic antioxidants in middle distillate fuels analyzed by gas chromatography with triple quadrupole and quadrupole time-of-flight mass spectrometry. *Energ Fuel* 2014;28:1097-102
- [18] Loegel TN, Morris RE, Myers KM, Katilie CJ. Analysis of phenolic antioxidants in navy mobility fuels by gas chromatography-mass spectrometry. *Energ Fuel* 2014;28:6267-74
- [19] Regulation (EC) No 1333/2008 of the European parliament and of the council of 16 December 2008 on food additives <https://eur-lex.europa.eu/legal-content/EN/TXT/?uri=celex%3A32008R1333> [accessed January 11, 2019]
- [20] Nieve-Echevarria B, Manzanos MJ, Goicoechea E, Guillen MD. 2,6-Di-tert-butyl-hydroxytoluene and its metabolites in foods. *Compr Rev Food Sci F* 2015;14:67-80

- [21] Antolovich M, Bedgood DR, Bishop AG, Jardine D, Prenzler PD, Robards K. LC-MS investigation of oxidation products of phenolic antioxidants. *J Agr Food Chem* 2004;52:962-71
- [22] ASTM D6810-13, Standard Test Method for Measurement of Hindered Phenolic Antioxidant Content in Non-Zinc Turbine Oils by Linear Sweep Voltammetry. ASTM International; West Conshohocken, PA, USA; 2013
- [23] Andrews NL, Fan JZ, Omrani H, Dudelzak A, Looock HP. Comparison of lubricant oil antioxidant analysis by fluorescence spectroscopy and linear sweep voltammetry. *Tribol Int* 2016;94:279-87
- [24] ASTM D 2272. Standard test method for oxidation stability of steam turbine oils by rotating pressure vessel. ASTM International; West Conshohocken, PA, USA; 2016
- [25] Besser C, Agocs A, Ronai B, Ristic A, Repka M, Jankes E, McAleese C, Dörr N. Generation of engine oils with defined degree of degradation by means of a large scale artificial alteration method. *Tribol Int* 2019;132:39-49
- [26] Dörr N, Agocs A, Besser C, Ristic A, Frauscher M. Engine oils in the field – A comprehensive chemical assessment of engine oil degradation in a passenger car. *Tribol Lett* 2019;67:1-21
- [27] DIN 32645: Chemical analysis – Decision limit, detection limit and determination limit under repeatability conditions – Terms, methods, evaluation. Deutsches Institut für Normung; Berlin, Germany; 2008

## List of figures

Figure 1: Pressure progression and oxidation (measured via FT-IR; dashed line) for C12 with (orange) and without (blue) BHT. Circular marks indicate the points of sampling. Dashed lines may be used as guide for the eyes and are no measured values.

Figure 2: Pressure progression and correlation with residual relative BHT content determined by FT-IR (dashed line), given for C12 with BHT. Circular marks indicate the points of sampling. Dashed lines may be used as guide for the eyes and are no measured values.

Figure 3: Total Ion Chromatogram of C12 with BHT after 8 h (A) and 9.7 h (B) as well as pure C12 after 1 h (C) time of alteration. Triangular marks indicate oxidation products of BHT (E), selected degradation products are labelled with small letters. Numbers are assigned to groups of degradation products, and peaks from contamination with polysiloxane are marked with an asterisk.

Figure 4: Product ion scan mode of parent ion mass  $m/z$  205.1 of analyte BHT at 0 V (A), 10 V (B) and 20 V (C) collision energy.

Figure 5: Positive ion mass spectra of BQ (A), BHT (B) and HBA (C) obtained by means of GC-EI-MS at 70 eV. The most abundant and selected fragment ions and the molecular ion of each analyte are labelled.

Figure 6: Concentration of BHT (blue) and the two oxidation products BQ (green) and HBA (orange) in ppm during the alteration progress in hours. Determined ppm values are given at the circular marks. The lines may be seen as guide for the eye and are no measured values.

## List of tables

Table 1: Selected oxidation products of C12 with and without BHT at different states of alteration. Bold, cursive small letters are products deriving from oxidation of BHT, and non-bold letters are degradation products of C12. The initial BHT is marked with a large, bold letter. Numbers indicate groups of degradation products.

Table 2: Intensities of fragment ions of BHT obtained with collision energies from 0 to 200 V.

Table 3: Selected parent ions and the respective product ions used for quantification.

### 3 Conclusions

The comprehensive elucidation of oxidation products and oxidation processes in lubricants and fuels was achieved based on a combined approach as described in chapter 0. Regarding artificial alteration, a method based on a RPVOT device was modified to account for the needs of lubricant as well as fuel alterations. Thermo-oxidative stress was applied to various, mostly eco-friendly components such as ester-based oils, FAME components and phenolic additives. Sampling during the entire stability assessment or at points of interest, e.g., during phases of distinct pressure changes in combination with appropriate analytical techniques enabled a time-resolved mapping of degradation products. Consequently, artificial alterations were performed under conventional  $^{16}\text{O}_2$  and under  $^{18}\text{O}_2$  atmosphere. When the oxygen from the atmosphere participates in the oxidation reaction, the resulting degradation products are carrying a stable isotopic tracer, either  $^{16}\text{O}$  or  $^{18}\text{O}$ . In contrary, when the reactions take place with an oxygen from a lubricant molecule, no isotope labelling occurs. Compared to the more conventional approach, where the target molecule is labelled with an isotopic moiety, the application of a gas-phase stable isotopic tracer to monitor the oxidation process during alteration is a novel approach in lubricant and fuel research. One cannot only identify the reactions involving the target molecule, but also reactions involving oxygen attack from atmosphere.

Capillary GC-EI-MS (Q) was used to separate the complex samples and identify the resulting degradation products. This analytical method enables structure elucidation of both individual chemical structures and quantification of components in low concentrations. In order to identify degradation products of the sterically hindered phenol BHT used as antioxidant in kerosene-type fuels, a tandem-MS method was elaborated. The time-resolved sampling during alteration revealed oxidation products formed before a considerable degradation of the other fuel components took place. These products, determined by GC-EI-MS/MS in single-digit ppm ranges, can be used as indicator for the beginning of an oxidative process. Hence, countermeasures can be implemented before remarkable changes of the fuel quality or performance occur due to oxidation.

To sum up, it can be stated that a unique approach comprising artificial alteration, isotopic tracers, separation techniques and MS was introduced to investigate lubricant and fuel stability. The aim of unambiguous identification of oxidative degradation products and their origin in fuels and lubricants was fully achieved for components of interest. Moreover, time-resolved mapping of additive degradation products turned out to be a helpful tool for the prediction of oxidative deterioration not detectable by conventional analysis used in lubricant and fuel

industry. The information gained by the described approach leads to an in-depth understanding of degradation processes and provides the required knowledge for modifications (tailoring) of lubricant, fuel components and compositions.

## 4 Curriculum vitae

### Personal data

Name: Marcella Frauscher  
Address: Schindlergasse 4/2  
1180 Wien  
Telephone: 0699 / 12904988  
E-mail: marcella.eder@gmx.at; marcella.frauscher@ac2t.at  
Date/place of birth: 29<sup>th</sup> of April, 1988, Vienna  
Nationality: Austria  
Languages: German (mother tongue), English (fluently), Italian (basic)



### Education

Since 10/2014 PhD studies (Dr. rer. nat.)  
at Vienna University of Technology, Austria  
Faculty of Technical Chemistry, Institute of Chemical  
Technologies and Analytics  
04/2011 – 08/2013 Master of Science (MSc)  
at the University of Vienna, Austria  
Faculty of Chemistry, Institute of Analytical Chemistry  
10/2006 – 04/2011 Bachelor of Science (BSc)  
at the University of Vienna, Austria  
Faculty of Chemistry, Department of Food Chemistry and  
Toxicology

### Professional experience

Since 09/2017 Area leader – Lubricants & interface mechanisms  
at the Austrian Excellence Center of Tribology,  
AC<sup>2</sup>T research GmbH, Wiener Neustadt, Austria  
03/2015 – 09/2018 Project leader – Lubricants & interface mechanisms  
at the Austrian Excellence Center of Tribology,  
AC<sup>2</sup>T research GmbH, Wiener Neustadt, Austria  
Since 04/2014 Scientist – Advanced Chemical Analysis  
at the Austrian Excellence Center of Tribology,  
AC<sup>2</sup>T research GmbH, Wiener Neustadt, Austria

- 10/2013 – 03/2014      Scientific assistant – Laboratory  
at the Vienna University of Technology, Vienna, Austria  
Faculty of Civil Engineering, Institute für Water Quality,  
Resource and Waste Management
- 03/2012 – 10/2012      Master thesis „*Development and Evaluation of Enzyme  
Immobilized Gold Nanoparticles*“  
at the University of Vienna, Vienna, Austria  
Faculty of Chemistry, Institute of Analytical Chemistry
- 09/2013                  Summer school Seggau – Participation  
„*Chromatographie und Kopplung mit Massenspektrometrie*“
- 01/2010 – 02/2010      Bachelor thesis „*Modulation des Phosphorylierungsstatus des  
Signalelements ERK durch Silicananopartikel*“  
at the University of Vienna, Vienna, Austria  
Faculty of Chemistry, Department of Food Chemistry and  
Toxicology
- 08/2009, 08/2010,  
08/2011, 06/2013,      Project assistant – Laboratory  
at the Vienna University of Technology, Vienna, Austria  
Faculty of Civil Engineering, Institute für Water Quality,  
Resource and Waste Management

## Publications

### Peer reviewed publications

Dörr N., Merstallinger A., Holzbauer R., Pejakovic V., Brenner J., Pizarova L., Stelzl J., **Frauscher M.** Five-stage selection procedure of ionic liquids for lubrication of steel-steel contacts in space mechanisms, *Tribology Letters* 2019;67:73

Dörr N., Agocs A., Besser C., Ristic A., **Frauscher M.** Engine oils in the field – comprehensive chemical assessment of engine oil degradation in a passenger car. *Tribology Letters* 2019;67:68

Dörr N., Brenner J., Ristic A., Ronai B., Besser C., Pejakovic V., **Frauscher M.** Correlation between engine oil degradation, tribochemistry, and tribological behavior with focus on ZDDP deterioration. *Tribology Letters* 2019;67:62

**Frauscher M.**, Besser C., Allmaier G., Dörr N. Elucidation of oxidation and degradation products of oxygen containing fuel components by combined use of a stable isotopic tracer and mass spectrometry. *Analytica Chimica Acta* 2017;993:47-54

Besser C., Pizarova L., **Frauscher M.**, Hunger H., Litzow U., Orfaniotis A., Dörr N. Oxidation products of biodiesel in diesel fuel generated by artificial alteration and identified by mass spectrometry. *Fuel* 2017;206:524-533

**Frauscher M.**, Besser C., Dörr N., Allmaier G. Oxidation products of ester-based oils with and without antioxidant identified by stable isotope labelling and mass spectrometry. *Applied Science* 2017;7:396

## Conference proceedings and oral presentations

**Frauscher M.**, Dörr N., Besser C., Rögner A. Quantification of antioxidant degradation products as indicator for Jet A-1 fuel degradation by gas chromatography mass spectrometry (GC-MS/MS). 17<sup>th</sup> IASH 2019, September 8<sup>th</sup> to 12<sup>th</sup> proceedings, Long Beach, CA (US), 2019

**Frauscher M.**, Besser C., Dörr N., Rögner A. Quantification of phenolic antioxidants and oxidation products thereof in kerosene type fuels by gas chromatography coupled with mass spectrometry (GC-MS). 12<sup>th</sup> International Colloquium Fuels, June 25<sup>th</sup> to 27<sup>th</sup> 2019, Ostfildern, Germany

**Frauscher M.**, Ristic A., Agocs A., Dörr N. Identification of oxidation products of biodegradable ester-based hydraulic oils by use of mass spectrometry and stable isotopic tracers. 7<sup>th</sup> European Conference on Tribology ECOTRIB, June 12<sup>th</sup> to 14<sup>th</sup> 2019, Vienna, Austria

Dörr N., Budnyk S., Ristic A., **Frauscher M.**, Agocs A. Impact of ZDDP degradation - influence of engine oil condition on friction and wear, program guide. 74<sup>th</sup> STLE Annual Meeting & Exhibition, May 19<sup>th</sup> to 23<sup>th</sup> 2019, Nashville, USA

Dörr N., **Frauscher M.**, Ristic A., Besser C., Allmaier G. Time-resolved oxidative degradation of ester-based lubricants identified by mass spectrometry, program guide. 74<sup>th</sup> STLE Annual Meeting & Exhibition, May 19<sup>th</sup> to 23<sup>th</sup> 2019, Nashville, USA

Ronai B., **Frauscher M.**, Ristic A., Besser C., Dörr N. Engine tribology influenced by ZDDP degradation – understanding on molecular level. 3rd Young Tribological Researcher Symposium, May 9<sup>th</sup> to 10<sup>th</sup> 2019, Wiener Neustadt, Austria

**Frauscher M.**, Ristic A., Besser C., Dörr N. Understanding ZDDP degradation in engine oils on the molecular level – comparison between lab and field. OilDoc Conference and Exhibition, January 29<sup>th</sup> to 31<sup>th</sup> 2019, Rosenheim, Germany

Agocs A., Ronai B., Besser C., **Frauscher M.**, Dörr N. The challenge of pre-defined oil degradation – correlation between lab-scale method, large scale artificial alteration and the field. ÖTG Symposium, November 22<sup>th</sup> 2018, Vienna, Austria

Kronberger M., Dörr N., Rodriguez Ripoll M., **Frauscher M.**, Linhardt P. Selective tribochemistry: a potentiodynamic study of a lubricated metal-ceramic contact. ÖTG Symposium, November 22<sup>th</sup> 2018, Vienna, Austria

Dörr N., **Frauscher M.**, Besser C., Allmaier G. Oxidative degradation of ester-based oils identified by isotope labelling and mass spectrometry, program guide. 73<sup>th</sup> STLE Annual Meeting & Exhibition, May 20<sup>th</sup> to 24<sup>th</sup> 2018, Minneapolis, USA

**Frauscher M.**, Ristic A., Besser C., Dörr N. Correlation of engine oil degradation products with friction and wear properties. 21<sup>th</sup> International Colloquium Tribology Industrial and Automotive Lubrication, January 9<sup>th</sup> to 11<sup>th</sup> 2018, Ostfildern, Germany

**Frauscher M.**, Dörr N., Besser C., Rögner A. Identification and quantification of oxidation products of fuel components analysed by mass spectrometry. 16<sup>th</sup> IASH 2017, September 10<sup>th</sup>

to 14<sup>th</sup> 2017, Rom, Italy.

Gabler C., Brenner J., **Frauscher M.**, Grafl A., Dörr N.. ZDDP degradation and tribochemistry revealed by mass spectrometry. 44th Leeds-Lyon Symposium, September 4<sup>th</sup> to 6<sup>th</sup> 2017, Lyon, France

**Frauscher M.**, Dörr N., Besser C., Rögner A., Koliander W. Oxidation characteristics of fuels and fuel components identified by mass spectrometry. 11<sup>th</sup> International Colloquium Fuels, June 27<sup>th</sup> to 29<sup>th</sup> 2017, Ostfildern, Germany

**Frauscher M.**, Besser C., Ronai B., Dörr N., Allmaier G. Oxidation mechanisms of ester oils identified by isotope labelling and mass spectroscopy. 6<sup>th</sup> European Conference on Tribology ECOTRIB, June 7<sup>th</sup> to 9<sup>th</sup> 2017, Ljubljana, Slovenia

Dörr N., Gabler, C., Ristic A., **Frauscher M.** ZDDP tribochemistry influenced by oxidative degradation. 72<sup>th</sup> STLE Annual Meeting & Exhibition, May 21<sup>th</sup> to 25<sup>th</sup> 2017, Atlanta, USA

**Frauscher M.**, Besser C., Dörr N., Allmaier G. Identification of oxidation products of lubricant and fuel components by combination of gas-phase isotope labelling combined with capillary gas chromatography mass spectrometry (GC-MS). 13<sup>th</sup> ASAC JunganalytikerInnen-Forum, May 12<sup>th</sup> to 13<sup>th</sup> 2017, Vienna, Austria

Dörr N., **Frauscher M.**, Gabler, C., Aswath P.B. How oxidative degradation can influence tribolayer chemistry of model oils containing ionic liquid additives. 71<sup>th</sup> STLE Annual Meeting & Exhibition, May 15<sup>th</sup> to 19<sup>th</sup> 2016, Las Vegas, USA

Dörr N., **Frauscher M.**, Gabler, C., Aswath P.B. Tribological performance of model oils containing ionic liquid additives influenced by oxidative degradation. 71<sup>th</sup> STLE Annual Meeting & Exhibition, May 15<sup>th</sup> to 19<sup>th</sup> 2015, Las Vegas, USA

Dörr N., **Frauscher M.**, Gabler, C., Aswath P.B. Long-term behaviour of oils containing ionic liquid additives. 20<sup>th</sup> International Colloquium Tribology Industrial and Automotive Lubrication, January 12<sup>th</sup> to 14<sup>th</sup> 2016, Ostfildern, Germany

**Frauscher M.**, Besser C., Dörr N., Allmaier G. Oxidative degradation products of fuel components identified by mass spectrometry and isotope labelling. 20<sup>th</sup> International Colloquium Tribology Industrial and Automotive Lubrication, January 12<sup>th</sup> to 14<sup>th</sup> 2016, Ostfildern, Germany

**Frauscher M.**, Besser C., Dörr N., Allmaier G. Identification of oxidative degradation mechanisms of esters by joint use of mass spectroscopy and isotope labelling. 5<sup>th</sup> European Conference on Tribology ECOTRIB, June 3<sup>th</sup> to 5<sup>th</sup> 2015, Lugano, Switzerland

Dörr N., **Frauscher M.**, Besser C. Degradation mechanisms of esters by joint use of mass spectroscopy and isotope labelling. 70<sup>th</sup> STLE Annual Meeting & Exhibition, May 17<sup>th</sup> to 21<sup>th</sup> 2015, Dallas, USA

## References

- [1] T. Mang, Ed., *Lubricants and lubrication*, 2nd edition. Wiley-VCH, 2007.
- [2] R. F. Haycock, A. J. Caines, and J. E. Hillier, *Automotive lubricants reference book*, 2nd edition. John Wiley & Sons, 2004.
- [3] P. K. B. Hodges, *Hydraulic fluids*, 1st edition. John Wiley & Sons, 1996.
- [4] American Petroleum Institute, “API 1509, APPENDIX E - API base oil interchangeability guidelines for passenger car motor oils and diesel engine oils,” 2004.
- [5] American Petroleum Institute, “API 1509, Engine oil licensing and certification system,” 2019.
- [6] Noria Corporation, “Understanding the differences in base oil groups,” [www.machinerylubrication.com](http://www.machinerylubrication.com). [Online]. Available: <https://www.machinerylubrication.com/Read/29113/base-oil-groups>. [Accessed: 20-Mar-2019].
- [7] L. R. Rudnick, *Synthetics, mineral oils, and bio-based lubricants: Chemistry and technology*, 1st edition. CRC Press, 2005.
- [8] ASTM D2786-91(2016), “Test method for hydrocarbon types analysis of gas-oil saturates fractions by high ionizing voltage mass spectrometry,” ASTM International, 2016.
- [9] ASTM D3239-91(2016), “Test method for aromatic types analysis of gas-oil aromatic fractions by high ionizing voltage mass spectrometry,” ASTM International, 2016.
- [10] R. Gunderson and A. Hart, *Synthetic lubricants*, 1st edition. Chapman & Hall, 1962.
- [11] L. R. Rudnick and R. L. Shubkin, *Synthetic lubricants and high-performance functional fluids*, 1st edition. CRC Press, 1999.
- [12] A. R. Lansdown, *High temperature lubrication*, 1st edition. Mechanical Engineering Publications, 1994.
- [13] J. Eastwood, “Esters-The most versatile of base stock technologies,” *Lube Mag.*, no. 129, pp. 32–37, 2015.
- [14] B. Elvers, *Ullmann’s encyclopedia of industrial chemistry*, 1st edition. Wiley-VCH, 2000.
- [15] Noria Corporation, “Lubricant additives - A practical guide,” [www.machinerylubrication.com](http://www.machinerylubrication.com). [Online]. Available: <https://www.machinerylubrication.com/Read/31107/oil-lubricant-additives>. [Accessed: 08-Mar-2019].
- [16] L. R. Rudnick, *Lubricant additives: Chemistry and applications*, 3rd edition. CRC Press, 2017.
- [17] N. Canter, “STLE special report - Use of antioxidants in automotive lubricants,” 2008.
- [18] M. Soleimani, L. Dehabadi, L. D. Wilson, and L. G. Tabil, “Antioxidants classification and applications in lubricants,” in *Lubrication - Tribology, lubricants and additives*, 1st edition., IntechOpen, 2018.
- [19] W. Bartz, *Additive für Schmierstoffe*, 1st edition. Expert-Verlag, 1994.
- [20] D. Scholz, J. Kuclick, and R. Pond, “A Decision-maker’s guide to dispersants: A review of the theory and operational requirements,” American Petroleum Institute Health & Environmental Sciences Department, 1999.
- [21] S. Q. A. Rizvi, Ed., *A comprehensive review of lubricant chemistry, technology, selection, and design*, 1st edition. ASTM International, 2009.
- [22] H. Spikes, “The history and mechanisms of ZDDP,” *Tribol. Lett.*, vol. 17, no. 3, pp. 469–489, 2004.
- [23] R. L. Stambaugh and B. G. Kinker, “Viscosity index improvers and thickeners,” in *chemistry and technology of lubricants*, 2nd edition., Springer US, 2010.

- [24] W. L. Van Horne, "Polymethacrylates as viscosity index improvers and pour point depressants," *Ind. Eng. Chem.*, vol. 41, no. 5, pp. 952–959, 1949.
- [25] T. W. Selby, "The non-Newtonian characteristics of lubricating oils," *A S L E Transactions*, vol. 1, no. 1, pp. 68–81, 1958.
- [26] M. J. Covitch and K. J. Trickett, "How polymers behave as viscosity index improvers in lubricating oils," *Adv. Chem. Eng. Sci.*, vol. 5, no. 2, pp. 134–151, 2015.
- [27] Lubrizol, "Pour point depressants," *www.lubrizol.com*, 16-Mar-2019. [Online]. Available: <https://www.lubrizol.com/Lubricant-and-Fuel-Additives/Viscosity-Modifiers/Technologies/PPD>. [Accessed: 16-Mar-2019].
- [28] M. Duncanson, "Controlling oil aeration and foam," *www.machinerylubrication.com*, 11-Mar-2019. [Online]. Available: <https://www.machinerylubrication.com/Read/255/oil-foam>. [Accessed: 11-Mar-2019].
- [29] L. Maugeri, *The age of oil: The mythology, history, and future of the world's most controversial resource*, 3rd edition. Praeger, 2006.
- [30] S. P. Srivastava and J. Hancsók, *Fuels and fuel-additives*, 1st edition. John Wiley & Sons, 2013.
- [31] A. Pandey, C. Larroche, S. C. Ricke, C.-G. Dussap, and E. Gnansounou, *Biofuels - alternative feedstocks and conversion processes*, 1st edition. Academic Press, 2011.
- [32] A. P. Singh, *Prospects of alternative transportation fuels*, 1st edition. Springer Berlin Heidelberg, 2018.
- [33] B. Niethammer, S. Wodarz, M. Betz, P. Haltenort, D. Oestreich, K. Hackbarth, U. Arnold, T. Otto, J. Sauer, "Alternative liquid fuels from renewable resources," *Chem. Ing. Tech.*, vol. 90, no. 1–2, pp. 99–112, 2018.
- [34] M. A. Oehlschlaeger, H. Wang, and M. N. Sexton, "Prospects for biofuels: A review," *J. Therm. Sci. Eng. Appl.*, vol. 5, no. 2, p. 021006, 2013.
- [35] I. Gerasimchuk, "Biofuel policies and feedstock in the EU," Chatham House, 2013.
- [36] OENORM EN 228:2017-07-15, "Unleaded petrol - Requirements and test methods," Beuth Verlag GmbH, 2017.
- [37] K. Kohse-Höinghaus, P. Oßwald, T. Cool, T. Kasper, N. Hansen, F. Qi, C. Westbrook, P. Westmoreland, "Biofuel combustion chemistry: From ethanol to biodiesel," *Angew. Chem. Int. Ed.*, vol. 49, no. 21, pp. 3572–3597, 2010.
- [38] K. Reif, Ed., *Dieselmotor-Management im Überblick: einschließlich Abgastechnik*, 1st edition. Springer Vieweg, 2014.
- [39] OENORM EN 590:2019-08-01, "Automotive fuels - Diesel - Requirements and test methods," Beuth Verlag GmbH, 2019.
- [40] C. Besser, L. Pisarova, M. Frauscher, H. Hunger, U. Litzow, A. Orfanoti, N. Dörr, "Oxidation products of biodiesel in diesel fuel generated by artificial alteration and identified by mass spectrometry," *Fuel*, vol. 206, pp. 524–533, 2017.
- [41] ASTM D1655-19(2019), "Standard specification for aviation turbine fuels," ASTM International, 2019.
- [42] DEF STAN 91-91(Issue 7; Amd 3), "Turbine fuel, kerosine type, Jet A-1; NATO Code: F-35," AVTUR, 2015.
- [43] M. Kaltschmitt and U. Neuling, *Biokerosene: status and prospects*, 1st edition. Springer Berlin Heidelberg, 2018.
- [44] ASTM D7566-19(2019), "Standard specification for aviation turbine fuel containing synthesized hydrocarbons," ASTM International, 2019.
- [45] T. N. Loegel, R. E. Morris, K. M. Myers, and C. J. Katalie, "Analysis of phenolic antioxidants in Navy mobility fuels by gas chromatography-mass spectrometry," presented at the IASH 2013, the 13th International Symposium on Stability, Handling and Use of Liquid Fuels, Rhodes, Greece, 2013, p. 23.

- [46] D. J. Abdallah, L. Kreno, F.P. DiSanzo, R.G. Gaughan, M.W. Genowitz, P.P. Wells, D.H. Hoskin, K.M. Penn, B. Brown, D. Wiseman, “Understanding phenol levels in Jet fuels,” presented at the IASH 2013, the 13th International Symposium on Stability, Handling and Use of Liquid Fuels, Rhodes, Greece, 2013, p. 10.
- [47] European Parliament, “Regulation (EC) No 1907/2006 - Registration, evaluation, authorization and restriction of chemicals (REACH),” European Union, 2019.
- [48] ATC, “Fuel additives: Use and benefits,” The Technical Committee of Petroleum Additive Manufacturer, 2013.
- [49] A. M. Danilov, “Research on fuel additives during 2011-2015,” *Springer US*, vol. 53, no. 5, pp. 705–721, 2017.
- [50] S. Schober and M. Mittelbach, “The impact of antioxidants on biodiesel oxidation stability,” *Eur. J. Lipid Sci. Technol.*, vol. 106, no. 6, pp. 382–389, 2004.
- [51] J. Pullen and K. Saeed, “An overview of biodiesel oxidation stability,” *Renew. Sustain. Energy Rev.*, vol. 16, no. 8, pp. 5924–5950, 2012.
- [52] Z. Yaakob, B. N. Narayanan, S. Padikkaparambil, S. Unni K., and M. Akbar P., “A review on the oxidation stability of biodiesel,” *Renew. Sustain. Energy Rev.*, vol. 35, pp. 136–153, 2014.
- [53] V. D. Kancheva, “Phenolic antioxidants – radical-scavenging and chain-breaking activity: A comparative study,” *Eur. J. Lipid Sci. Technol.*, vol. 111, no. 11, pp. 1072–1089, 2009.
- [54] T. G. Denisova and E. T. Denisov, “Dissociation energies of O-H bonds in natural antioxidants,” *Russ. Chem. Bull.*, vol. 57, no. 9, pp. 1858–1866, 2008.
- [55] S. McAllister, J.-Y. Chen, and A. C. Fernandez-Pello, *Fundamentals of combustion processes*, 1st edition. Springer US, 2011.
- [56] D. Splitter, A. Pawlowski, and R. Wagner, “A historical analysis of the co-evolution of gasoline octane number and spark-ignition engines,” *Front. Mech. Eng.*, vol. 1, pp. 1–22, 2016.
- [57] A. M. Danilov, T. N. Mitusova, V. A. Kovalev, and A. N. Churzin, “Organic peroxides - Cetane-Increasing Additives for Diesel Fuels,” *Chem. Technol. Fuels Oils*, vol. 39, no. 6, pp. 330–333, 2003.
- [58] J. L. Burger, T. M. Lovestead, R. V. Gough, and T. J. Bruno, “Characterization of the effects of cetane number improvers on diesel fuel volatility by use of the advanced distillation curve method,” *Energy Fuels*, vol. 28, no. 4, pp. 2437–2445, 2014.
- [59] G. J. Suppes and M. A. Dasari, “Synthesis and evaluation of alkyl nitrates from triglycerides as cetane improvers,” *Ind. Eng. Chem. Res.*, vol. 42, no. 21, pp. 5042–5053, 2003.
- [60] H. Kuszewski, “Effect of adding 2-ethylhexyl nitrate cetane improver on the autoignition properties of ethanol–diesel fuel blend – Investigation at various ambient gas temperatures,” *Fuel*, vol. 224, pp. 57–67, 2018.
- [61] M. Ciniviz, İ. Örs, and B. Sayın, “The effect of adding EHN (2-ethylhexyl nitrate) to diesel-ethanol blends on performance and exhaust emissions,” *Int. Journal Automot. Sci. Technol.*, vol. 1, pp. 16–21, 2017.
- [62] M. Matzke, U. Litzow, A. Jess, R. Caprotti, and G. Balfour, “Diesel lubricity requirements of future fuel injection equipment,” *SAE Int. J. Fuels Lubr.*, vol. 2, no. 1, pp. 273–286, 2009.
- [63] CEC L-48-A-00, “Oxidation stability of lubricating oils used in automotive transmissions by artificial ageing,” Coordinating European Council (CEC), 2014.
- [64] ASTM D7214-07a(2012), “Standard test method for determination of the oxidation of used lubricants by FT-IR using peak area increase calculation,” ASTM International, 2012.

- [65] ASTM D6186-08(2013), “Oxidation induction time of lubricating oils by pressure differential scanning calorimetry (PDSC),” ASTM International, 2013.
- [66] OENORM EN ISO 4263-1:2005-04-01, “Petroleum and related products - Determination of the ageing behaviour of inhibited oils and fluids - TOST test - Part 1: Procedure for mineral oils,” Beuth Verlag GmbH, 2005.
- [67] OENORM EN ISO 4263-2:2003-10-01, “Petroleum and related products - Determination of the ageing behaviour of inhibited oils and fluids - TOST test - Part 2: Procedure for category HFC hydraulic fluids,” Beuth Verlag GmbH, 2003.
- [68] OENORM EN ISO 4263-3:2016-04-01, “Petroleum and related products - Determination of the ageing behaviour of inhibited oils and fluids using the TOST test - Part 3: Anhydrous procedure for synthetic hydraulic fluids,” Beuth Verlag GmbH, 2016.
- [69] OENORM EN ISO 4263-4:2006-09-01, “Petroleum and related products - Determination of the ageing behaviour of inhibited oils and fluids - TOST test - Part 4: Procedure for industrial gear oils,” Beuth Verlag GmbH, 2006.
- [70] ASTM D2272-14a(2014), “Test method for oxidation stability of steam turbine oils by rotating pressure vessel,” ASTM International, 2014.
- [71] M. Frauscher, C. Besser, G. Allmaier, and N. Dörr, “Oxidation products of ester-based oils with and without antioxidants identified by stable isotope labelling and mass spectrometry,” *Appl. Sci.*, vol. 7, no. 4, pp. 396–414, 2017.
- [72] OENORM EN ISO 7536:1996-07-01, “Petroleum products - Determination of oxidation stability of gasoline - Induction period method,” Beuth Verlag GmbH, 1996.
- [73] OENORM EN ISO 12205:1997-05-01, “Petroleum products - Determination of the oxidation stability of middle-distillate fuels,” Beuth Verlag GmbH, 1997.
- [74] OENORM EN 15751:2014-05-01, “Automotive fuels - Fatty acid methyl ester (FAME) fuel and blends with diesel fuel - Determination of oxidation stability by accelerated oxidation method,” Beuth Verlag GmbH, 2014.
- [75] OENORM EN 14112:2016-12-01, “Fat and oil derivatives - Fatty acid methyl esters (FAME) - Determination of oxidation stability (accelerated oxidation test),” Beuth Verlag GmbH, 2016.
- [76] E. H. Farmer and A. Sundralingam, “The course of autoxidation reactions in polyisoprenes and allied compounds. Part I. The structure and reactive tendencies of the peroxides of simple olefins,” *J. Chem. Soc. Resumed*, vol. 0, no. 0, pp. 121–139, 1942.
- [77] J. L. Bolland, “Kinetics of olefin oxidation,” *Q. Rev. Chem. Soc.*, vol. 3, no. 1, pp. 1–21, 1949.
- [78] M. Rasberger, “Oxidative degradation and stabilisation of mineral oil based lubricants,” in *Chemistry and Technology of Lubricants*, Dordrecht: Springer Netherlands, 1997.
- [79] Y. Felkel, “Frisch- und Gebrauchtölanalyse von Gasmotorenölen mittels Infrarotspektroskopie,” Dissertation an der Technischen Universität Wien, 2008.
- [80] C. Besser, “Impact of bio-ethanol as oxygenated fuel component in gasoline on the engine oil performance,” Dissertation an der Technischen Universität Wien, 2015.
- [81] DIN 51399-1:2017-02, “Testing of lubricants - Determination of elements content in additives, wear and other contaminations - Part 1: Direct determination by optical emission spectral analysis with inductively coupled plasma (ICP OES),” Beuth Verlag GmbH, 2017.
- [82] ASTM E2412-10(2018), “Standard practice for condition monitoring of in-service lubricants by trend analysis using fourier transform infrared (FT-IR) spectrometry,” ASTM International, 2018.
- [83] DIN 53019-1:2008-09, “Viskosimetrie - Messung von Viskositäten und Fließkurven mit Rotationsviskosimetern - Teil 1: Grundlagen und Messgeometrie,” Beuth Verlag GmbH, 2008.

- [84] ASTM D7042-16e3(2016), “Test method for dynamic viscosity and density of liquids by stabinger viscometer (and the calculation of kinematic viscosity),” ASTM International, 2016.
- [85] DIN 51558-2:2017-07, “Testing of mineral oils - Determination of neutralization number - Part 2: Color-indicator titration, insulating oils,” Beuth Verlag GmbH, 2017.
- [86] ASTM D664-18e2(2018), “Standard test method for acid number of petroleum products by potentiometric titration,” ASTM International, 2018.
- [87] OENORM EN 12634:1999-01-01, “Petroleum products and lubricants - Determination of acid number - Non-aqueous potentiometric titration method,” Beuth Verlag GmbH, 1999.
- [88] N. Dörr, A. Agocs, C. Besser, A. Ristic, and M. Frauscher, “Engine oils in the field: A comprehensive chemical assessment of engine oil degradation in a passenger car,” *Tribol. Lett.*, vol. 67, 2019.
- [89] M. Soleimani, M. Sophocleous, M. Glanc-Gostkiewicz, J. Atkinson, L. Wang, R. Wood, R.I. Taylor, “Engine oil acidity detection using solid state ion selective electrodes,” *Tribol. Int.*, vol. 65, pp. 48–56, 2013.
- [90] DIN 51777-1:1983-03, “Testing of mineraloil hydrocarbons and solvents; determination of water content according to Karl Fischer; direct method,” Beuth Verlag GmbH, 1983.
- [91] DIN 51777-2:1974-09, “Testing of mineral oil hydrocarbons and solvents; determination of water content according to Karl Fischer; Indirect Method,” Beuth Verlag GmbH, 1974.
- [92] DIN 51777:2016-08, “Petroleum products - Determination of water content using titration according to Karl Fischer,” Beuth Verlag GmbH, 2016.
- [93] F. Cadet, S. Garrigues, and M. de la Guardia, “Quantitative Analysis, Infrared,” in *Encyclopedia of analytical chemistry: Applications, theory and instrumentation*, 1st edition., John Wiley & Sons, 2012.
- [94] Z. Pawlak, *Tribochemistry of lubricating oils*, 1st edition. Elsevier Science, 2003.
- [95] D. J. Smolenski and S. E. Schwartz, “Automotive engine-oil condition monitoring,” *Lubr. Eng.*, vol. 50, no. 9, pp. 17–24, 1994.
- [96] J. P. Coates, L. C. Setti, and B. B. McCaa, “The analytical and statistical evaluation of infrared spectroscopic data from used diesel lubricants,” SAE International, SAE Technical Paper, 1984.
- [97] J. P. Coates and L. C. Setti, “Condition monitoring of crankcase oils using computer aided infrared spectroscopy,” SAE International, SAE Technical Paper, 1983.
- [98] R. Nyquist, *Interpreting infrared, raman, and nuclear magnetic resonance spectra - 1st Edition*, 1st edition. Academic Press, 2001.
- [99] S. P. Davis, M. C. Abrams, and J. W. Brault, *Fourier-Transform spectrometry*, 1st edition. Academic Press, 2001.
- [100] DIN 51451:2004-09, “Testing of petroleum products and related products - Analysis by infrared spectrometry - General working principles,” Beuth Verlag GmbH, 2004.
- [101] N. Dörr, J. Brenner, A. Ristic, B. Ronai, C. Besser, V. Pejakovic, M. Frauscher, “Correlation between engine oil degradation, tribochemistry, and tribological behavior with focus on ZDDP deterioration,” *Tribol. Lett.*, vol. 67, 2019.
- [102] L. S. Ettre, “M.S. Tswett and the invention of chromatography,” *LCGC North America*, vol. 21, no. 5, pp. 458–467, 2003.
- [103] IUPAC, *Compendium of chemical terminology - The gold book*, 2nd edition. Blackwell Scientific Publications, 1997.
- [104] A. T. James and A. J. Martin, “Gas-liquid chromatography: A technique for the analysis and identification of volatile materials,” *British Medical Bulletin*, vol. 10, no. 3, pp. 170–176, 1954.

- [105] H. M. McNair and J. M. Miller, *Basic gas chromatography*, 2nd edition. John Wiley & Sons, 2009.
- [106] A. Braithwaite and F. Smith, *Chromatographic methods*, 5th edition. Kluwer Academic Publishers, 1996.
- [107] Emerson Process Management, “Fundamentals of gas chromatography - Oil&gas,” Rosemount Analytical, 2010.
- [108] S. C. Moldoveanu and V. David, “Derivatization methods in GC and GC/MS,” in *Gas chromatography - Derivatization, sample preparation, application*, 1st edition., IntechOpen, 2018.
- [109] F. Orata, “Derivatization reactions and reagents for gas chromatography analysis,” in *Advanced gas chromatography - Progress in agricultural, biomedical and industrial applications*, 1st edition., IntechOpen, 2012.
- [110] Daniel R. Knapp, *Handbook of analytical derivatization reactions*, 1st edition. John Wiley & Sons, 1980.
- [111] W. Engewald and K. Dettmer-Wilde, “Theory of gas chromatography,” in *Practical gas chromatography*, 1st edition., Springer Berlin Heidelberg, 2014.
- [112] R. L. Grob and E. F. Barry, *Modern practice of gas chromatography*, 4th edition. Wiley-Interscience, 2004.
- [113] K. Grob, *Split and splitless injection for quantitative gas chromatography*, 1st edition. Wiley-VCH, 2001.
- [114] R. Salzer, S. Thiele, and A. Zuern, “Probeaufgabetechniken in der Gaschromatographie - Chemgapedia,” [www.chemgapedia.de](http://www.chemgapedia.de), 20-Apr-2019. [Online]. Available: [http://www.chemgapedia.de/vsengine/vlu/vsc/de/ch/3/anc/croma/gc/direkt/split/splitinjgcm66ht0600.vscml.html](http://www.chemgapedia.de/vsengine/vlu/vsc/de/ch/3/anc/croma/gc_probenaufgabe.vlu/Page/vsc/de/ch/3/anc/croma/gc/direkt/split/splitinjgcm66ht0600.vscml.html). [Accessed: 20-Apr-2019].
- [115] T. G. Chasteen, “Split/splitless gas chromatography injection,” Sam Houston State University, 2017.
- [116] L. Waclaski, “Optimizing splitless GC injections,” *The Column*, vol. 14, no. 8, pp. 11–15, 2018.
- [117] E. F. Barry and R. L. Grob, *Columns for gas chromatography: Performance and selection*, 1st edition. John Wiley & Sons, 2007.
- [118] L. S. Ettre, “M.J.E. Golay and the invention of open-tubular (capillary) columns,” *J. High Resolut. Chromatogr.*, vol. 10, no. 5, pp. 221–230, 1987.
- [119] L. S. Ettre, “The development of gas chromatography,” *J. Chromatogr. A*, vol. 112, pp. 1–26, 1975.
- [120] R. D. Dandeneau and E. H. Zerenner, “An investigation of glasses for capillary chromatography,” *J. High Resolut. Chromatogr.*, vol. 2, no. 6, pp. 351–356, 1979.
- [121] Agilent J&W, “GC column selection guide,” Agilent Technologies Inc., 2007.
- [122] Supelco, “GC column selection guide,” Sigma Aldrich, 2015.
- [123] R. Salzer, S. Thiele, and A. Zuern, “Gaschromatographie im Detail - Chemgapedia,” [www.chemgapedia.de](http://www.chemgapedia.de), 20-Apr-2019. [Online]. Available: [http://www.chemgapedia.de/vsengine/vlu/vsc/de/ch/3/anc/croma/gc/stat\\_phase/kapillarsaeule/kapillarsaeule2.vscml.html](http://www.chemgapedia.de/vsengine/vlu/vsc/de/ch/3/anc/croma/gc_detail1.vlu/Page/vsc/de/ch/3/anc/croma/gc/stat_phase/kapillarsaeule/kapillarsaeule2.vscml.html). [Accessed: 20-Apr-2019].
- [124] R. Salzer, S. Thiele, and A. Zuern, “Detektoren in der Gaschromatographie - Chemgapedia,” [www.chemgapedia.de](http://www.chemgapedia.de), 20-Apr-2019. [Online]. Available: [http://www.chemgapedia.de/vsengine/vlu/vsc/de/ch/3/anc/croma/gc\\_detektoren.vlu.html](http://www.chemgapedia.de/vsengine/vlu/vsc/de/ch/3/anc/croma/gc_detektoren.vlu.html). [Accessed: 20-Apr-2019].
- [125] R. P. Rhodes, “US Patent - Thermal conductivity detector,” 24-Dec-1996.

- [126] J. E. Lovelock, "The electron capture detector: Theory and practice," *J. Chromatogr. A*, vol. 99, pp. 3–12, 1974.
- [127] J. E. Lovelock, "A sensitive detector for gas chromatography," *J. Chromatogr. A*, vol. 1, pp. 35–46, 1958.
- [128] A. Karmen and L. Giuffrida, "Enhancement of the response of the hydrogen flame ionization detector to compounds containing halogens and phosphorus," *Nature*, vol. 201, pp. 1204–1205, 1964.
- [129] C. A. Burgett, D. H. Smith, and H. B. Bente, "The nitrogen-phosphorus detector and its applications in gas chromatography," *J. Chromatogr. A*, vol. 134, no. 1, pp. 57–64, 1977.
- [130] I. G. McWilliam and R. A. Dewar, "Flame ionization detector for gas chromatography," *Nature*, vol. 181, no. 4611, p. 760, 1958.
- [131] E. Zachowski and S. Paleologos, "Flame ionization detectors: Applications and operations," *Speciality Gas Report*, 2009.
- [132] J. Sevcik, *Detectors in gas chromatography*. Elsevier, 2011.
- [133] H. Budzikiewicz and M. Schäfer, *Massenspektrometrie: Eine Einführung*, 6th edition. John Wiley & Sons, 2012.
- [134] J. H. Gross, *Mass spectrometry: a textbook*, 2nd edition. Springer, 2011.
- [135] R. Salzer, S. Thiele, A. Zuern, and S. Machill, "Massenspektrometrie - Prinzipieller Geräteaufbau - Chemgapedia," [www.chemgapedia.de](http://www.chemgapedia.de), 23-Apr-2019. [Online]. Available: [http://www.chemgapedia.de/vsengine/vlu/vsc/de/ch/3/anc/masse/masse\\_basic.vlu.html](http://www.chemgapedia.de/vsengine/vlu/vsc/de/ch/3/anc/masse/masse_basic.vlu.html). [Accessed: 23-Apr-2019].
- [136] E. de Hoffmann and V. Stroobant, *Mass spectrometry: principles and applications*, 3rd edition. John Wiley & Sons, 2007.
- [137] R. Salzer, S. Thiele, A. Zuern, and S. Machill, "Massenspektrometer - Die Ionenquelle - Elektronenstoß-Ionisation - Chemgapedia," [www.chemgapedia.de](http://www.chemgapedia.de), 23-Apr-2019. [Online]. Available: [http://www.chemgapedia.de/vsengine/vlu/vsc/de/ch/3/anc/masse/ms\\_ionenquelle\\_ei.vlu/Page/vsc/de/ch/3/anc/masse/2\\_massenspektrometer/2\\_3\\_ionenquelle/2\\_3\\_1\\_elek\\_stoss/2\\_3\\_1\\_3\\_fragmentierung/vertief/fragmentierg\\_vert\\_910ht0202.vscml.html](http://www.chemgapedia.de/vsengine/vlu/vsc/de/ch/3/anc/masse/ms_ionenquelle_ei.vlu/Page/vsc/de/ch/3/anc/masse/2_massenspektrometer/2_3_ionenquelle/2_3_1_elek_stoss/2_3_1_3_fragmentierung/vertief/fragmentierg_vert_910ht0202.vscml.html). [Accessed: 23-Apr-2019].
- [138] T. D. Märk and G. H. Dunn, *Electron impact ionization*, 1st edition. Springer-Verlag Wien, 1985.
- [139] Masspect, "Principle of electron ionization," <http://mass-spectro.com>, 08-Jul-2016. [Online]. Available: <http://mass-spectro.com/electron-ionization>. [Accessed: 23-Apr-2019].
- [140] T. Taylor, "Electron ionization for GC–MS," *LCGC North America*, vol. 30, no. 4, p. 358, 2012.
- [141] A. Harrison, *Chemical ionization mass spectrometry*, 2nd edition. CRC Press, 1992.
- [142] R. Salzer, S. Thiele, A. Zuern, and S. Machill, "Massenspektrometer - Die Ionenquelle - Chemische Ionisation - Chemgapedia," [www.chemgapedia.de](http://www.chemgapedia.de), 23-Apr-2019. [Online]. Available: [http://www.chemgapedia.de/vsengine/vlu/vsc/de/ch/3/anc/masse/ms\\_ionenquelle\\_ci.vlu/Page/vsc/de/ch/3/anc/masse/2\\_massenspektrometer/2\\_3\\_ionenquelle/2\\_3\\_2\\_chem\\_ionisation/2\\_3\\_2\\_6\\_negativ\\_ci/ci\\_neg\\_22ht1101.vscml.html](http://www.chemgapedia.de/vsengine/vlu/vsc/de/ch/3/anc/masse/ms_ionenquelle_ci.vlu/Page/vsc/de/ch/3/anc/masse/2_massenspektrometer/2_3_ionenquelle/2_3_2_chem_ionisation/2_3_2_6_negativ_ci/ci_neg_22ht1101.vscml.html). [Accessed: 23-Apr-2019].
- [143] D. F. Hunt, "Selective reagents for chemical ionization mass spectrometry," in *Applications of the newer techniques of analysis*, Springer US, 1973.

- [144] R. Salzer, S. Thiele, A. Zuern, and S. Machill, “Massenspektrometer - Der Massenanalysator - Chemgapedia,” *www.chemgapedia.de*, 24-Apr-2019. [Online]. Available:  
[http://www.chemgapedia.de/vsengine/vlu/vsc/de/ch/3/anc/masse/ms\\_massenanalysator.vlu.html](http://www.chemgapedia.de/vsengine/vlu/vsc/de/ch/3/anc/masse/ms_massenanalysator.vlu.html). [Accessed: 24-Apr-2019].
- [145] D. J. Douglas, A. J. Frank, and D. Mao, “Linear ion traps in mass spectrometry,” *Mass Spectrom. Rev.*, vol. 24, no. 1, pp. 1–29, 2005.
- [146] R. A. Zubarev and A. Makarov, “Orbitrap mass spectrometry,” *Anal. Chem.*, vol. 85, no. 11, pp. 5288–5296, 2013.
- [147] S. Eliuk and A. Makarov, “Evolution of Orbitrap mass spectrometry instrumentation,” *Annu. Rev. Anal. Chem. Palo Alto Calif*, vol. 8, pp. 61–80, 2015.
- [148] W. Paul and H. Steinwedel, “Ein neues Massenspektrometer ohne Magnetfeld,” *Z. Naturforschung Teil A*, vol. 8, p. 448, 1953.
- [149] R. E. March and J. F. Todd, *Quadrupole ion trap mass spectrometry*, 2nd edition. John Wiley & Sons, 2005.
- [150] R. E. March and J. F. J. Todd, *Practical aspects of ion trap mass spectrometry*, 1st edition. CRC Press, 1995.
- [151] R. A. Yost and C. G. Enke, “Selected ion fragmentation with a tandem quadrupole mass spectrometer,” *J. Am. Chem. Soc.*, vol. 100, no. 7, pp. 2274–2275, 1978.
- [152] R. A. Yost, C. G. Enke, D. C. McGilvery, D. Smith, and J. D. Morrison, “High efficiency collision-induced dissociation in an RF-only quadrupole,” *Int. J. Mass Spectrom. Ion Phys.*, vol. 30, no. 2, pp. 127–136, 1979.
- [153] E. de Hoffmann, “Tandem mass spectrometry: A primer,” *Journal of Mass Spectrometry*, vol. 31, no. 2, pp. 129–137, 2019.
- [154] J. L. Holmes, “Metastable ions,” in *Encyclopedia of spectroscopy and spectrometry*, 3rd edition., Academic Press, 2017.
- [155] S. A. McLuckey, “Principles of collisional activation in analytical mass spectrometry,” *J. Am. Soc. Mass Spectrom.*, vol. 3, no. 6, pp. 599–614, Sep. 1992.
- [156] J. L. Holmes, “Assigning structures to ions in the gas phase,” *Journal of Mass Spectrometry*, vol. 20, no. 3, pp. 169–183, 1985.